Department of Companion Animals and Horses
University of Veterinary Medicine, Vienna
Diagnostic Imaging
(Head: Univ.-Prof. Dr.med.vet. Eberhard Ludewig, Dipl.ECVDI)

# Equine and feline oronasal papillomavirus-positive and -negative squamous cell carcinoma – A comparative study based on diagnostic imaging, pathomorphologic and molecular methods

PhD thesis submitted for the fulfilment of the requirements for the degree of

**DOCTOR OF PHILOSOPHY (PhD)**

University of Veterinary Medicine Vienna

Submitted by

**Dr.med.vet. Carina Strohmayer DipECVDI**

**Vienna, March 2024**

First supervisor

**Sibylle Kneissl, Ao.Univ.-Prof in Dr in med.vet.**

Diagnostic Imaging

Department for Companion Animals and Horses

University of Veterinary Medicine, Vienna

Second supervisor

**Sabine Brandt, Dipl.-Ing in Dr in nat.techn. Priv.-Doz in**

Research Group Oncology (RGO), Equine Surgery

Department for Companion Animals and Horses

University of Veterinary Medicine, Vienna

Third supervisor

**Miriam Kleiter, Ao.Univ.-Prof in Dr in med.vet. Dipl.ACVR-RO Dipl.ECVIM-CA**

Platform Radiooncology and Nuclear Medicine Platform

Department for Companion Animals and Horses

1. **Strohmayer C**, Klang A, Kneissl S (2020): **Computed Tomographic and Histopathological Characteristics of 13 Equine and 10 Feline Oral and Sinonasal Squamous Cell Carcinomas.** Front Vet Sci. 2020; 7:591437 (Impact factor: 3.12)

2. **Strohmayer C**, Klang A, Kummer S, Walter I, Jindra C, Weissenbacher-Lang C, Redmer T, Kneissl S, Brandt S (2022): **Tumor Cell Plasticity in Equine Papillomavirus-Positive Versus-Negative Squamous Cell Carcinoma of the Head and Neck**. Pathogens. 2022; 11(2):266 (Impact factor: 4.531)

This thesis is dedicated to my family and to all researchers and their dedication for science.

First of all, I want to like to thank my supervisor, Ao.Univ.-Prof. Dr.med.vet. Sibylle Kneissl wholeheartedly. From the very beginning of my professional life, she was always there with good advices, challenged me, believed in me and helped me grow as a person and as a researcher. I am enjoying the scientific dialogs as well as conversations about new didactic methods, new efficiency applications, presentation ideas and work-life-balance. She dreams big and has ideas before other think in these directions. I have learned so much from her and am still learning! I hope this mentoring never stops! I owe her everything that I have become! Dankeschön!
Moreover, I would deeply like to thank Dipl.ECVDI Univ.-Prof. Dr.med.vet. Eberhard Ludewig very much for supporting my PhD project and my academic goals with lots of efforts. Above that his dedication for the residency program is inspiring and motivating.
I am very grateful for the opportunity to work on the topic of oral squamous cell carcinoma, which allowed me to enjoy and cherish working interdisciplinary and getting to know and learn from excellent researchers. Dipl.-Ing. Dr.nat.techn. Priv.-Doz. Sabine Brandt and Dr.rer.nat. Christoph Jindra are part of the core of squamous cell carcinoma research. It was a pleasure to work with them. Sabine is an impressive researcher and I learned so many things about squamous cell carcinoma from her. I admire her for her writing style, and she is a great role model on writing submissions for calls. Christoph patiently answered all my hundreds of questions in the lab and without him I would have been lost.
Dearly I also want to thank Dr.med.vet. Andrea Klang, who always responded immediately to my questions, patiently explained and always had an open ear for everything when I was in doubt. She became an indispensable companion and friend during the last years.
An enormous thank you to Ao.Univ.-Prof. Mag.rer.nat. Dr.rer.nat. Ingrid Walter and Mag.rer.nat. Stefan Kummer. Without the tremendous efforts of Stevie (who I know and appreciate for over 10 years now) it would have been half of the fun and outcome.
I want to thank as well Dr.rer.nat Torben Redmer and Mag.rer.nat. Dr.rer.nat. Barbara Pratscher for their expertise and commitment for this project. Barbara patiently introduced me to working with cell cultures and made it a lot fun.

Through the help of Ass. Prof. Irena Pashkunova-Martic, PhD I experienced a more interdisciplinary point of view outside veterinary medicine and was introduced to the fascinating world of theranostics. She always supported me the best possible way. Thank you for broadening my horizon!
Moreover, I want to thank Ao.Univ.-Prof. Dr.med.vet. Dipl.ACVR-RO Dipl.ECVIM-CA Miriam Kleiter for her expertise and support.
I also want to thank all my colleagues from the Clinical Unit of Diagnostic Imaging at the Vetmeduni, who have stood by my side throughout my journey. All these people have become my second family! Thank you for each and every day!

My friends and friends abroad but close to my heart, patiently listened to every obstacle of mine during this project and heroically encouraged me throughout.
Aus tiefstem Herzen: Danke! Thank you! Muchas gracias:)

Nothing of this could be possible without my loving family. They have cheered for me all the way, believed in me, dried my tears, encouraged me and kept me positive. And this for unbelievable 10 years from my doctoral thesis to the residency and now the PhD. I cannot thank you enough for your support! In the middle of my journey my boyfriend has joined me bravely. He was always encouraging, even if I had to spend long hours in front of the computer. He cooked dinner, exercised with me and brought me healthy snacks to my desk to have a fresh mind and keep me motivated. I love you all so much!!

## First publication

**Strohmayer C**, Klang A, Kneissl S (2020): **Computed Tomographic and Histopathological Characteristics of 13 Equine and 10 Feline Oral and Sinonasal Squamous Cell Carcinomas.** Front Vet Sci. 2020; 7:591437 (Impact factor: 3.12)

Contribution:

- Conceptualization
- Investigation
- Data curation
- Writing—original draft preparation, review and editing.

## Second publication

**Strohmayer C**, Klang A, Kummer S, Walter I, Jindra C, Weissenbacher-Lang C, Redmer T, Kneissl S, Brandt S (2022): **Tumor Cell Plasticity in Equine Papillomavirus-Positive Versus-Negative Squamous Cell Carcinoma of the Head and Neck**. Pathogens. 2022; 11(2):266 (Impact factor: 4.531)

Contribution:

- Conceptualization
- Formal analysis
- Investigation
- Data curation
- Writing—original draft preparation, review and editing.

# Declaration

I confirm that the rules of good Scientific Practice have been followed in all aspects.

## Summary

Oral or head and neck squamous cell carcinoma (OSCC, HNSCC) are highly local aggressive neoplasms, most commonly affecting cats and horses among companion animals. At the time of diagnosis this tumor is challenging for owners and veterinarians as the prognosis is poor. Little is known about risk factors, pathogenesis and morphological characteristics of this tumor in veterinary medicine. Therefore, the main goal of this PhD project is to better characterize OSCC and HNSCC in cats and horses with diagnostic imaging, pathomorphologic and molecular methods to improve diagnosis and potentially reveal biomarkers that can act as future targets for therapeutic methods. Thus, we first investigated the morphological character of OSCC in cats and HNSCC in horses by computed tomography and histopathology. To gain insights in the molecular characteristics of this tumor as a second goal all feline OSCC and equine HNSCC samples were analyzed for the presence of species-specific papillomavirus types. To further investigate molecular characteristics papillomavirus positive and negative samples of horses were compared for the expression of selected epithelial, mesenchymal, endothelial and stem-cell markers. As a last step we conducted a pilot project to evaluate the use of cell culture lines of feline OSCC and equine HNSCC for future theranostic approaches by combining a magnetic resonance imaging contrast agent (Gadolinium) with a potential therapeutic agent (Salinomycin) and monitoring the effects on cells. Our results in terms of computed tomographic images displayed different osseous phenotypic tendencies, with more osseous aggressive features in cats. Histopathology showed variable features of keratinization and number of mitotic cells as well as extensive and deep osseous invasion in both cats and horses, which fits to the known infiltrative nature of this tumor. Regarding concurrent papillomavirus infection, 22 % of all equine sample screened positive for equine papillomavirus type 2 and less than 10 % for feline papillomaviruses distributed throughout feline papillomavirus type 1-3. The findings of the immunohistochemical analyzes suggest partial epithelial mesenchymal transition by expression of vimentin, a mesenchymal marker and cytokeratin, an epithelial marker in all papillomavirus-positive and negative equine HNSCC as well as cancer stem-cell markers, CD44 and CD271 as possible malignancy markers. As a result of the cell culture experiments, a dose-dependent response of the theranostic agent (Salinomycin and Gadolinium) on the cell viability could be detected and indicate further investigations.

In conclusion, the findings of this work add diagnostic imaging, pathomorphologic and molecular features of feline OSCC and equine HNSCC to the knowledge of this little investigated tumor to contribute to the advancement of forthcoming diagnosis and treatment.

## Zusammenfassung

Orale bzw. Kopf-Hals-Plattenepithelkarzinome (PEK) sind lokal aggressive Tumore, welche bei Haustieren vorwiegend Katzen und Pferde betreffen. Zum Zeitpunkt der Diagnose ist dieser Tumor aufgrund der schlechten Prognose gleichermaßen herausfordernd für Besitzer und Tierärzt:innen. In der Veterinärmedizin ist wenig zu Risikofaktoren, Pathogenese und morphologische Charakteristika dieses Tumors bekannt. Somit ist das übergeordnete Ziel dieser PhD-Arbeit orale bzw. Kopf-Hals-PEK bei Katzen und Pferden mittels radiologischen, pathomorphologischen und molekularen Methoden besser zu charakterisieren, um die Diagnose zu verbessern und potenzielle Biomarker zu identifizieren, welche für zukünftige Therapieformen verwendet werden könnten. Zu Beginn untersuchten wir die morphologischen Merkmale von oralen PEK bei Katzen und Kopf-Hals-PEK bei Pferden mittels Computertomographie (CT) und Pathohistologie. Um weitere Erkenntnisse über molekulare Merkmale zu erlangen, war ein weiteres Ziel alle verfügbaren pathothistologischen Proben von oralen PEK bei Katzen bzw. Kopf-Hals-PEK bei Pferden auf das Vorhandensein spezies-spezifischer Papillomvirus-Typen zu untersuchen. Um die Plastizität der Tumorzellen in Virus-positiven und -negativen Proben zu untersuchen, wurden immunhistochemische Analysen zur Expression ausgewählter endothelialer, epithelialer, mesenchymaler sowie Stammzell-Marker durchgeführt. Als letzten Schritt führten wir ein Pilotprojekt durch bei dem Zelllinien für zukünftige theranostische Anwendungen untersucht wurden. Hierbei wird ein magnetresonanztomographisches Kontrastmittel mit einem potenziellen Therapeutikum kombiniert und der Effekt auf die Zellen beobachtet. Unsere Ergebnisse im Bezug auf die CT-Untersuchungen zeigten Tendenzen zu verschiedenen ossären Phänotypen, jedoch waren aggressivere Merkmale bei Katzen zu beobachten. Pathohistologisch wurden unterschiedliche Grade an Keratinisierung und eine variable Anzahl an Mitosen in den betroffenen Zellen sowie eine ausgedehnte und tiefe Knocheninfiltration bei beiden Spezies festgestellt. Im Hinblick auf eine gleichzeitige Infektion mit Papillomviren, waren 22 % aller Pferde-Proben positiv auf den equinen Papillomvirus Typ 2 und weniger als 10 % auf die felinen Papillomvirus-Typen 1-3. Die Ergebnisse der immunhistochemischen Analysen deuten auf eine partielle epitheliale-mesenchymale Transition in Form der Expression des mesenchymalen Markers Vimentin und des epithelialen Markers Zytokeratin sowohl bei Papillomvirus-positiven als auch bei -negativen Pferde-Plattenepithelkarzinome

sowie auf das Vorhandensein der Stammzellmarker, CD44 und CD271 als mögliche Malignitätsmarker hin. Abschließend konnte in unseren Zellkultur-Experimenten eine dosisabhängige Reaktion auf die Lebensfähigkeit der PEK-Zellen festgestellt werden, wodurch weitere Untersuchungen vielversprechend erscheinen.

Zusammenfassend, ergänzen die Ergebnisse dieser Arbeit die bisher wenigen radiologischen, pathomorphologischen und molekularen Merkmale von felinen oralen PEK und equinen Kopf-Hals-PEK und leisten einen Beitrag für eine mögliche Verbesserung der Diagnose und Behandlung dieses Tumors.

# Table of Content

**Abbreviations**

| | |
|---|---|
| CSC | cancer stem-cells |
| CT | computed tomography |
| EMT | epithelial-mesenchymal-transition |
| HNSCC | head and neck squamous cell carcinoma |
| MRI | magnetic resonance imaging |
| OSCC | oral squamous cell carcinoma |
| PV | papillomavirus |
| SAL-Gd | salinomycin-gadolinium |
| SCC | squamous cell carcinoma |

# 1 Introduction/Background

## 1.1 General introduction and Epidemiology

Among domestic animals, oral neoplasia is commonly observed in cats, dogs and less frequent in horses (60). In a recent study, the incidence of oral neoplasia was considered similar between cats and dogs with 4.9 per 1,000 cases and said to be increased in comparison to previous studies (17). In cats, squamous cell carcinoma (SCC) is seen in 60-69 % of oral malignancies (17, 60, 90, 109). In dogs, oral melanoma is the most common tumor of this region and SCC is only seen in 17-25 % (17, 60). Although oral neoplasia is less frequent in horses, SCC is diagnosed in more than half of the cases accounting for the most common oral malignancy (60). Oral squamous cell carcinoma (OSCC) is additionally observed in farm animals, rats, hamsters, rabbits, ferrets, hedgehogs, and various other veterinary species, such as reptiles (67).

Since cats and horses are the most common affected animals, these two species were selected as study population of this thesis. In the following sections the current knowledge of this tumor in these two species is reviewed. While there is more information available for cats, less data is existing for horses.

## 1.2 Pathology

OSCC is a malignant neoplasia originating from keratinocytes that are derived from the stratified squamous epithelium of the oral mucosa (67). This tumor is known for its heterogenous macro- and microscopic appearance. Macroscopically, they often initially present as pale plaques or irregular roughened areas of the mucosa of the oral cavity. As they grow they can present as mass lesion with varying underlying infiltrated tissues or as ulcerative lesions. Since they are often diagnosed at a late stage, OSCC present as ulcerated mass that have infiltrated the surrounded tissues. Depending on the appearance of the proliferated cells, the tumor can be further sub-classified (60). Unlike in human medicine, where different subtypes, the amount of tumor-associated inflammation, perineural or lymphovascular invasion reflect certain clinical behavior and are important for prognosis (38, 48, 67), no information exist about the prognosis

of tumor subtypes in domestic animals (60). There have been various classifications proposed. Meuten (60) subtypes SCCs in carcinoma in situ, conventional, verrucous, papillary, basiloid and spindle SCCs. The most frequent OSCC in all domestic animals are classified as conventional. Those are described as trabeculae and nests of epithelial cells, which extend into the submucosa. Commonly solid islets of neoplastic cells, which can be also separate from the primary tumor are observed and represent the infiltrative behavior. Additionally, a disorganized maturation of neoplastic squamous cells can be seen with keratinized cells in between or agglomerated to keratin pearls. Ulcerations of masses with necrosis and secondary infection indicated by neutrophils and bacteria can be seen frequently as well. If the inflammatory component predominates, such as in superficial samples, it can be challenging to diagnose a SCC confidently. Carcinoma in situ presents as oral epithelium with preserved basement membrane, that is thickened secondary to dysplastic cells. Verrucous SCCs have a less infiltrative character since the squamous epithelium proliferates as a whole towards the underlying tissue rather than infiltrating it. In human medicine this subtype shows a better prognosis. Papillary, basiloid and spindle SCCs have been reported especially in dogs (60). Another classification subdivides OSCC in well or poorly differentiated, spindloid or anaplastic types. For all types except the well differentiated type, it is said to be challenging to identify the cells as epithelial in origin (67). Due to its infiltrative nature and the close proximity of osseous structures in the oral cavity, bone involvement is a common finding. A study evaluated bone-invasive OSCC in cats. They found apart from osteolysis also osseous metaplasia of tumor stroma, periosteal new bone formation and direct contact of neoplastic cells to eroded osseous structures. The authors observed in cats with OSCC an increased tumor expression of parathyroid hormone related protein (PTHrP) in those cases with osteolysis and suggested a potential role of PTHrP in bone resorption and tumor infiltration (59). In horses, information about a specific pathologic grading is sparse. Only for the more common penile SCC, a classification system from van den Top *et al*. (103) is reported, which graded malignancies in well, moderately or poorly differentiated tumors.

## 1.3 Risk factors

### *1.3.1 Environmental*

Besides these pathological features, risk factors have been discussed to have an influencing role in the pathogenesis of OSCC. Studies assessing environmental risk factors in cats are sparse with one study almost two decades ago. In this study it has been suggested that diet, flea control products and potentially environmental tobacco smoke could be associated with an increased risk of OSCC (10). To address the lack of information a recent study evaluated demographic, environmental and lifestyle data in a large population of cats. An increased risk of having OSCC included rural environment, outdoor access, environmental tobacco smoke and pet food containing chemical additives. Although in this study based on questionnaires preceding oral inflammatory disease was not significantly higher in cats with OSCC in comparison to a control group, more investigation of this suspected multifactorial disease is warranted (115).

Even less information exists in horses. So the only proposed environmental risk factor is chronic periodontal disease, however data are lacking (68).

### *1.3.2 Papillomavirus*

While environmental risk factors are of little interest so far and also multifactorial and more difficult to study, papillomavirus infection as a risk factor for developing SCC is an area of progressing interest. Generally, papillomavirus (PV) virions are nonenveloped, spherical, 55 nm in diameter and have double-stranded DNA genomes. The genome encodes 8-10 proteins. The capsid is formed by two proteins, namely L1 and L2. The main viral proteins (E1-E8) include replicative and regulatory properties. The replication has a tropism for keratinocytes of the stratified squamous epithelium of the skin and some mucous membranes. Through external abrasions, the virus enters the organism and infect first dividing basal cells in the stratum germinativum. The virus needs the infected cell to undergo differentiation in order to complete its life cycle. Due to exfoliation of keratinized cells of the stratum corneum or non-keratinized cells of the mucosal membranes the virus is finally shed. Papillomaviruses are usually species-

and site-specific. Papillomaviruses can lead to the formation of papillomas, which are seen for example in ruminants, dogs, horses. Also, malignancies have been reported in conjunction with this virus, namely SCC of the mucocutaneous regions (54, 64, 65). In human medicine a scientific focus of SCC is centered on the pathogenesis associated human papillomavirus (HPV) and the related immunology (14, 79). Despite other processes, the integration of the E6 and E7 genes in the host DNA is described responsible for excessive cell growth and inhibiting apoptosis in PV-induced cancer (21). Although the pathogenesis is a flourishing research field, the exact mechanisms are only partly understood (65).

In the domestic cat *(Felis catus)*, six papilloma types (FcaPV-1 to 6) are known (64). Recently it has been proposed that PV-types may have a regional different prevalence as has been seen between Italy and Austria (5). Among the various PV-types, which are mainly asymptomatic, *felis catus* papillomavirus type 2 (FcaPV-2) is the most common clinically relevant agent being associated with cutaneous SCC and OSCC (63, 64). However, the role of FcaPV-2 in OSCC is still controversial. The reported prevalence is quite variable ranging from 7.5-30 % (2, 5), possibly attributing to regional differences or different technical methodologies such as the use of species-specific primers for PCR (5, 112). Amongst others a large research group around Gennaro Altamura studies on possible mechanisms of the pathogenesis of PV and SCC (3, 4). The authors showed that FcaPV-2 oncogene E6 improves the activation of mitogen-activated protein kinase (MAPK) involved in cellular proliferation and inhibition of apoptosis mediated by serine-threonin kinase, AKT (3). However in a more recent study, Altamura *et al*. (6) demonstrated differences in human and feline PV associated oral SCC. They found that the oncogene E6 in cats unlike in humans is not involved in processes of cancer progression via increased expression of telomerase reverse transcriptase and matrix metalloproteinases. Also, Chu *et al*. (15) stated a supplementary or uncommon role of PVs in the pathogenesis of OSCC in cats. Regarding the route of infection, a possible hypothesis proposes that through direct contact, likely during the grooming process, FcaPV-2 reaches the oral cavity since this virus is mainly detected cutaneously (2). A study about repeated cutaneous swabs from kittens and queens detected FcaPV-2 DNA in almost all sample with various

quantities. The mean viral DNA load was similar for kittens and queen of the same household suggesting that kittens get in contact with FcaPV-2 early in life presumably from close contact to the queen (100). A later study also detected mRNA, indicating infection, in few cutaneous samples of kittens, suggesting that some kittens can also get infected by FcaPV-2 (102). The reason why FcaPV-2 infection results in clinical disease is still not completely resolved but is considered multifactorial including immunologic factors (2, 6, 64). Although the exact mechanisms of infection and pathogenesis are not resolved, ongoing scientific efforts pave the way to elucidate those processes.

In the last decade there has been also a growing scientific interest of *Equus caballus* papillomavirus types (EcPV) in the pathogenesis of SCC in general (30, 69, 96, 99). Although seven EcPV-types (1-7) are described, the most frequent virus type is EcPV-2 (7, 30, 41, 43, 47, 85). Routes of transmission have been hypothesized to include direct contact through insects or contaminated fomites as well as sexual contact (96). Besides, EcPV-2 could be also detected in subset of oral and pharyngeal samples of asymptomatic horses, highlighting the importance to further elucidate the role of PV in the pathogenesis of developing SCC (1, 43).

## 1.4 Clinical presentation

Despite the pathogenesis, the time of presentation and diagnosis is crucial for the further work-up and prognosis. Overall, animals seem to cope for a longer time with mass lesions until clinical signs develop or the mass is observed adding to the late onset of presentation. Usually, feline patients with OSCC are seen by the veterinarian at a progressed stage of the disease when the tumor reaches a certain size or a skull deformity is noted by the owners. Above noticing the mass itself, cats with OSCC can present first due secondary clinical signs, such as dysphagia, anorexia, ptyalism, foetor ex ore, tooth loss, pain (51, 67). Common locations are gingiva, mandible (22) and sublingual/lingual (66). Regarding the age at presentation, in a study, cats with lingual OSCC were seen with a mean age of 11.9 years, while cats diagnosed with gingival OSCC were slightly older with a mean age of 13.6 years (59).

Regarding horses, reports of oral, oropharyngeal and sinonasal location of SCC are described (7, 40, 62, 88, 104, 110). Thus the general term head and neck SCC (HNSCC), which comprises tumors of the paranasal sinuses, nasal cavity, oral, laryngeal or pharyngeal region has been used (41). Horse are usually reported to be older than 10 years at presentation (68). The reason for presentation thus varies according to the anatomical location and size of the mass and include loosening of teeth, dysphagia and dyspnea (68). Concerning the oropharyngeal region, the affected locations include gingiva, palate, tongue, larynx, pharynx (68). The maxillary sinus however is reported to be the most affected paranasal sinus (19). For tumors that are large in size it has been proposed that it might not be easily determined whether the mass originated from the paranasal or oral cavity (36). Mass lesions tend to be extensive in size, locally aggressive in terms of infiltration of the surrounding soft tissue or osseous structures thus contributing to the poor prognosis.

## 1.5 Diagnosis and Staging

Once the clinical examination directly identifies a mass, a further diagnostic work-up depends on the owner's aspirations including ethical considerations. After a clinical examination, assessing the extent of the mass and sampling of the mass to classify it as benign or malignant is crucial. If the mass is not directly accessible for sampling, computed tomography (CT) as a cross-sectional diagnostic imaging technique can identify the anatomical location and therefore guide the approach to acquire the sample. Biopsies are preferred over fine needle aspirations since oral tumors are often secondary infected thus results can be misled by necrosis and inflammation (50). Once the oral tumor is confirmed, clinical staging is performed. According to the World Health Organization (WHO) the clinical staging called TNM staging system include assessing local tumor (T), regional lymph nodes (N) characteristics and evaluation for distant metastasis (M) (77). CT is most used to describe the extent of the mass in terms of size, bone involvement and infiltrative nature. Additionally, the regional lymph nodes including mandibular, parotid and medial retropharyngeal lymph nodes are important to evaluate for signs of abnormalities such as enlargement or altered contrast enhancement that could indicate metastasis and warrant sampling. Besides palpation

as a clinical tool, CT can accurately describe the size and contrast pattern of even non-accessible lymph nodes such as the parotid and medial retropharyngeal lymph nodes. In cats, CT is not only used for diagnostic imaging but also crucial for radiation therapy planning (50).

However, in horses, once there is a clinical suspicion of a mass that is supported by a thorough oral examination, upper airway endoscopy and/or skull radiographs, cross-sectional imaging can be used to further evaluate the extent of the mass in the head region. With CT being more and more available also in clinical equine practice it has become the imaging modality of choice to further work-up the cause of a clinical noticed mass or nasal discharge (44, 91).

## 1.6 Management, Treatment options

Since this tumor is often diagnosed at a progressed disease stage, therapeutic options are often limited. In cats, the main goal in the management of feline OSCC is therefore local tumor control, since these tumors are locally aggressive with an infiltrative nature and thus can be rarely completely excised. The most common treatment options are surgery and radiation therapy (50). Despite multimodal approaches the prognosis is poor and thus facing clinicians with major therapeutic challenges, similar to human medicine (37). Conservative treatment with nonsteroidal anti-inflammatory drugs alone seem frustrating showing a median survival time of 44 days (35). Unfortunately, OSCC is known to be poorly responsive to radiation therapy with reported median survival times between two to six months (24, 81, 84, 113). Only few reports of various multimodal protocols including surgery, chemotherapy, medical treatment achieved longer survival times (23, 57). Recently, Marconato *et al*. (58) added data to the current knowledge that OSCC is poorly responding to radiation therapy. The authors noted tumor progression after accelerated hypofractionated radiation therapy and medical anti-angiogenic treatment at a median of 4.8 months. On the other hand, a study of eight cats with radical mandibulectomy through which 75 % to 90 % of the mandible was removed, suggested this approach to consider for treatment. The authors described an overall estimated mean survival time of 712 days. After aggressive supportive care 6/8 cats achieved an independent food intake and 4/8 cats lived more

than one year (11). Research effort on investigating various approaches of tumor control will continue in the search for providing better care and improve and refine prognosis.

Similar to feline patients, horses often present late in the disease course. At this disease stage due to the size of the mass and the infiltrative nature of the tumor, treatment options are unfortunately even more limited and often end in euthanasia (110). Surgical reports are sparse potentially due to complexity of the tumor location associated with the anatomical area (75). In a recent study, evaluating the outcome of external beam radiotherapy of non-cutaneous head and neck tumors, the overall survival for SCC was noted between 2 to 48 months with a median of six months. In eight out of 11 horses there was tumor recurrence leading to euthanasia in six horses. Maxillary and nasal cavity tumors showed a shorter median survival time in comparison to other locations. Potentially these locations were clinically more significant leading to a shorter survival time. In conclusion, the authors suggest external beam radiotherapy as a potential treatment of a variety of non-cutaneous tumors of the head of horses (27).

## 1.7 Objectives and Hypotheses

The background given highlights that little is known about OSCC and HNSCC of the main affected companion animal species, namely cats and horses.
Therefore, the main goal of the PhD project is to broaden the knowledge on feline OSCC and equine HNSCC in order to add to the refinement of future diagnosis, prognosis and treatment. To accomplish this we use diagnostic imaging, pathomorphologic and molecular methods defined in three milestones.

**Objective milestone 1**

- Describing morphological features of OSCC in cats and HNSCC in horses by means of computed tomography and histopathology.

**Hypotheses milestone 1**

- All feline OSCC and equine HNSCC can be detected with CT and most CT cases of cats and horses show similar aggressive osseous features, in terms of irregular osteolysis and periosteal reactions.
- The majority of feline OSCC and equine HNSCC samples show aggressive cellular features validated by histopathology.

**Objectives milestone 2**

- Analyzing OSCC and HNSCC samples of cats and horses respectively, for an infection of species-specific papillomavirus types.
- Identifying tumor-type-specific proteins as biomarkers using immunohistochemistry.

**Hypotheses milestone 2**

- The prevalence of papillomavirus infection of the present feline OSCC and equine HNSCC samples is equivalent between these two species.
- Biomarkers for OSCC established in human medicine can be detected in the majority of equine HNSCC samples.
- The identified biomarkers help in elucidating the pathogenesis of equine HNSCC.

**Objective milestone 3**

- Performing preliminary cell culture experiments to help in establishing a tumor-

specific MRI marker in terms of a theranostic approach.

**Hypothesis milestone 3**

- The cell viability of feline OSCC cells and equine HNSCC cells will be equivalent when incubated with the theranostic agent, SAL-Gd.

## 2 Milestones/Results

Veterinarians and researchers are faced with challenges when it comes to OSCC and HNSCC. So, our aims are focused on the clinical diagnosis, molecular background and future treatment options. From an everyday clinical perspective, it is interesting to know more about morphologic features of this tumor that might be applicable to improve clinical diagnosis. Therefore, we evaluated CT images and tissue samples histopathologically of 13 horses and 10 cats. Although the small sample size precluded us from achieving statistical significance, we described morphological patterns in these two species. The range of morphological features are published in the paper of **milestone 1**: **Strohmayer C**, Klang A, Kneissl S (2020): **Computed Tomographic and Histopathological Characteristics of 13 Equine and 10 Feline Oral and Sinonasal Squamous Cell Carcinomas**. Front Vet Sci. 2020; 7:591437.

After gaining morphologic information about this tumor from a clinical perspective, we went a step further by focusing on the molecular level of the tumor in milestone 2. As there is better prognosis reported for tumors with papillomavirus infection in human medicine, we sought to analyze this relationship further in horses and cats. We analyzed 49 horses and 81 cats for the presence of *Equus caballus* papillomavirus type 2 and 3 and *Felis catus* papillomavirus types 1-3 respectively. The findings showed a prevalence of 22 % in horses and less than 10 % in cats. Due to the higher prevalence in horses we decided to investigate tumors in horses on a larger scale for a variety of cell markers. We analyzed endothelial, epithelial, mesenchymal and stem-cell markers in samples with and without papillomavirus infection. Although no difference between papillomavirus positive and negative tumors were found, we detected partial epithelial-mesenchymal transition events and for the first time promising stem-cell marker (CD44 and CD271). Findings of these results of **milestone 2** were published in the article: **Strohmayer C**, Klang A, Kummer S, Walter I, Jindra C, Weissenbacher-Lang C, Redmer T, Kneissl S, Brandt S (2022): **Tumor Cell Plasticity in Equine Papillomavirus-Positive Versus-Negative Squamous Cell Carcinoma of the Head and Neck**. Pathogens. 2022; 11(2):266.

Having attained more insight in the molecular background of this tumor our next step intended investigations focused on a theranostic approach, namely diagnosis and therapy at the same time. In veterinary medicine SCC has not been researched on in this field at all. Consequently, we conducted cell culture experiments to test the feasibility of such a concept. We started a cooperation with cell culture experts at the vetmeduni and a chemist of the Medical University of Vienna. We cultured feline OSCC and equine HNSCC cells and treated them with a compound of a diagnostic (MRI contrast medium Gadolinium) and therapeutic agent (Salinomycin). The preliminary data of these experiments are shown in **milestone 3**.

The papers of milestone 1 and 2 as well as the results from milestone 3 are subsequently displayed in the following section.

frontiers in Veterinary Science

ORIGINAL RESEARCH
published: 23 November 2020
doi: 10.3389/fvets.2020.591437

# Computed Tomographic and Histopathological Characteristics of 13 Equine and 10 Feline Oral and Sinonasal Squamous Cell Carcinomas

*Carina Strohmayer [1]*, Andrea Klang [2] and Sibylle Kneissl [1]*

*[1] Diagnostic Imaging, University of Veterinary Medicine, Vienna, Austria, [2] Department of Pathobiology, Institute of Pathology, University of Veterinary Medicine, Vienna, Austria*

OPEN ACCESS

*Edited by:*
*Tommaso Banzato, University of Padua, Italy*

*Reviewed by:*
*Takehiko Kakizaki, Kitasato University, Japan*
*Christopher Ober, University of Minnesota, United States*

**Correspondence:*
*Carina Strohmayer*
*carina.strohmayer@vetmeduni.ac.at*

*Specialty section:*
*This article was submitted to Veterinary Imaging, a section of the journal Frontiers in Veterinary Science*

*Received: 04 August 2020*
*Accepted: 29 October 2020*
*Published: 23 November 2020*

*Citation:*
*Strohmayer C, Klang A and Kneissl S (2020) Computed Tomographic and Histopathological Characteristics of 13 Equine and 10 Feline Oral and Sinonasal Squamous Cell Carcinomas. Front. Vet. Sci. 7:591437. doi: 10.3389/fvets.2020.591437*

Squamous cell carcinoma (SCC) is the most common equine sinonasal and feline oral tumour. This study aimed to describe the computed tomographic and histopathological characteristics of equine and feline SCC. Thirteen horses and 10 cats that had been histopathologically diagnosed with oral or sinonasal SCC and had undergone computed tomography (CT) of the head were retrospectively included in the study. CT characteristics of the mass and involved structures were noted. Histological examinations were evaluated according to a human malignancy grading system for oral SCC, which considered four grades of increasing aggressiveness. In horses, the masses were at the levels of the paranasal sinuses ($n = 8$), mandible ($n = 3$), tongue ($n = 1$), and nasal cavity ($n = 1$). In cats, the masses were at the levels of the maxilla ($n = 4$), mandible ($n = 3$), tongue ($n = 1$), and buccal region ($n = 1$) and were diffusely distributed (facial and cranial bones; $n = 1$). Masses in the equine paranasal sinuses showed only mild, solid/laminar, periosteal reactions with variable cortical destruction. However, maxillary lesions in cats showed severe cortical destruction and irregular, amorphous/pumice stone-like, periosteal reactions. CT revealed different SCC phenotypes that were unrelated to the histological grade. For morphologic parameters of the tumour cell population, a variability for the degree of keratinization and number of mitotic cells was noted in horses and cats. Concerning the tumour-host relationship a marked, extensive and deep invasion into the bone in the majority of horses and cats was seen. Most cases in both the horses and cats were categorized as histological grade III ($n = 8$); four horses and one cat were categorized as grade IV, and one horse and one cat were categorized as grade II. In this study, we examined the diagnostic images and corresponding applied human histopathological grading of SCC to further elucidate the correlations between pathology and oral and sinonasal SCC imaging in horses and cats.

Keywords: cat, computed tomography, histology, horse, malignancy grading, oral and sinonasal squamous cell carcinoma

## INTRODUCTION

Oral and sinonasal squamous cell carcinomas (SCCs) are keratinocyte tumours derived from the stratified squamous epithelium of the mucosa (1). SCCs are thought to be the most common nasal and paranasal tumour in horses (2, 3) and the most common malignant oral tumour in cats, accounting for 60–70% of all feline malignant oral tumours (4, 5). In horses, ~7% of SCCs are oral (6), and in cats, ~85% of SCCs occur in the head region (7). SCCs are aggressive, infiltrative tumours with predilection for the gingiva and mucosa of the maxillary, mandibular, lingual, tonsillar, lip, and buccal regions (5). Because of their location and infiltrative nature, complete excision is often impossible; thus, current oncologic protocols focus on controlling the primary tumour (8).

Computed tomography (CT) is commonly used in human medicine to assess the local extent and regional lymph nodes in head and neck squamous cell carcinoma (HNSCC) (9). However, few case reports have described the CT characteristics of SCC in the equine head and neck region (10, 11). Kowalczyk et al.(10) provided the most detailed imaging description of two horses with SCC in the paranasal sinuses showing a lobulated heterogeneous soft tissue mass with osteolysis and irregular periosteal new bone formation. Several studies have described oral SCC in cats (12–14). Common imaging features in cats include a mass lesion with marked heterogeneous contrast enhancement and osteolysis (12).

Histologically, SCCs are described according to cellular appearance and can be further subclassified (15). In human medicine, detailed grading schemes focus on different aspects of oral SCC (16). Animals and humans share some aspects of the pathogenesis in certain tumours, such as squamous cell carcinoma, and thus the term "one health" has been introduced and discussed recently (17). Better understanding SCC on a cellular level could support better tumour characterization and consequently better individual treatment and prognosis. Evaluating these two most commonly affected companion animal species relative to SCC could determine a wide range of characteristics related to equine and feline HNSCC.

TABLE 1 | Information on patients and relevant time points of an equine and feline population diagnosed with oral or sinonasal squamous cell carcinoma.

| | Breed | Sex | Age at diagnosis (years) | Time between computed tomography and histological sampling (days) | Mode of sample collection |
|---|---|---|---|---|---|
| Horse 1 | Haflinger | f | 22 | 7 | N |
| Horse 2 | Warmblood mix | mc | 22 | 3 | B |
| Horse 3 | Trakehner | mc | 19 | 12 | B |
| Horse 4 | Connemara pony | f | 16 | 6 | N |
| Horse 5 | Haflinger | mc | 7 | 1 | N |
| Horse 6 | Icelandic horse | f | 18 | 3 | N |
| Horse 7 | Trotter | f | 8 | 0 | N |
| Horse 8 | Icelandic horse | mc | 16 | 0 | N |
| Horse 9 | Shetland pony | f | 26 | 0 | N |
| Horse 10 | Warmblood | f | 20 | 0 | N |
| Horse 11 | Noric horse | mc | 17 | 4 | B |
| Horse 12 | Pony | mc | 27 | 0 | N |
| Horse 13 | Trotter | mc | 12 | 6 | B |
| Cat 1 | European Shorthair | mc | 10 | 1 | B |
| Cat 2 | European Shorthair | fs | 5 | 0 | B |
| Cat 3 | Persian cat | fs | 14 | 0 | B |
| Cat 4 | European Shorthair | fs | 15 | 0 | B |
| Cat 5 | European Shorthair | mc | 13 | 58 | N |
| Cat 6 | European Shorthair | mc | 15 | 0 | B |
| Cat 7 | European Shorthair | mc | 11 | 0 | B |
| Cat 8 | European Shorthair | fs | 15 | 0 | N |
| Cat 9 | European Shorthair | fs | 13 | 0 | B |
| Cat 10 | European Shorthair | fs | 14 | 15 | B |

*mc, male castrated; fs, female spayed; f, female; N, necropsy; B, biopsy.*

## MATERIALS AND METHODS

### Specimens

Medical records of horses and cats from 2002 to 2019 were reviewed and were included in the study if the animal had undergone a CT examination of the head region and if histopathology of the oral or sinonasal SCC was available. **Table 1** lists the breed, sex, age at time of diagnosis, days between CT and histological sampling, and mode of sample collection. Additionally, the survival times (amount of days between histopathological diagnosis and last day of follow up or euthanasia) for all horses and cats were retrieved from the medical records.

### Computed Tomography

CT scans of the head from 2002 to 2008 were performed using a single-slice CT scanner (Pace™, General Electric, Milwaukee, WI, USA), and those from 2009 to 2019 were performed using a 16-slice CT scanner (SOMATOM® Emotion 16, Siemens Healthcare, Erlangen, Germany). Under general anaesthesia, all horses except one were positioned in dorsal recumbency, and cats were positioned in ventral recumbency. Images were acquired after euthanasia for three horses the same or the following day. For contrast studies, iodinated non-ionic contrast medium (iopamidol, 370 mgI/ml) was administered intravenously at 200–300 mgI/kg in horses and 600 mgI/kg in cats. Three contrast phases were available in two horse and six cats; two contrast phases were available in two cats. The CT images were reviewed with an image analysis programme (JiveX, VISUS Health IT GmbH, Germany, Version 5.2.1.). Two radiologists blinded to the histopathological grading but aware of the diagnosis of

squamous cell carcinoma evaluated the following parameters in consensus in a bone window and soft tissue window pre- and post-intravenous contrast medium (when available): the centre of the mass, margination (poor or well-defined), attenuation of the mass (in hounsfield units (HU); a circular region of interest as large as practicable was placed on pre- and post-contrast images), contrast enhancement (homogeneous, heterogeneous, or rim enhancement), size of the mass (Cats: maximum length of the mass in mm on post-contrast images; Horses: sinonasal masses classified as small (less than a third of the size of the maxillary sinus), medium (not extending approximately the size of the maxillary sinus), large (extending the maxillary sinus), oral masses: maximum length of the mass in mm on pre- contrast or if available post-contrast images), number of involved bones, number of involved tissue types (bone, soft tissues, fat, skin), number of involved compartments (oral cavity, pharynx, nasal cavity, nasopharynx, paranasal sinus, orbital region, cranial cavity, or soft tissues), pattern of new bone formation (mild or severe; solid/lamellar, irregular, spiculated, Codman's triangle, or amorphous/pumice stone-like), cortical destruction (mild or severe; permeative and/ or gross), and regional lymph node evaluation. Evaluation of the lymph nodes was performed on CT images in a soft tissue window pre- or, if available, post-administration of contrast medium. Moderate asymmetry to the contralateral side was subjectively assessed. For measurement of the lymph nodes the maximum long axis dimension of the biggest mandibular and medial retropharyngeal lymph node of each side and the maximum perpendicular short axis dimension was noted on transverse CT images. The maximum length of each lymph node was measured on sagittal CT images along the long axis of the lymph nodes. The respective shape of these lymph nodes was described as fusiform, irregular, oval, or round. The number of lymph nodes was noted as: not seen, 1, 2, 3, $\leq$10, $\geq$10, $\geq$20.

## Histopathology

Formalin-fixed, paraffin-embedded tissue samples were retrieved from the archive, prepared on slides and stained with haematoxylin and eosin. One pathologist, who was unaware of the CT findings, reviewed the slides. The samples were evaluated according to a human malignancy grading system by Anneroth et al. (18) for oral SCC considering morphological parameters of the tumour cells and the tumour- host relationship. For all animals, the degree of keratinization, nuclear polymorphism and the average number of mitotic cells per high-power field (HPF) analyzed in 10 HPFs were evaluated as morphologic parameters and hallmarks of malignancy in tumour cell populations. Additionally, tumour-host interactions were considered, including the pattern and stage of invasion and lymphoplasmocytic infiltration. Each of these six parameters were graded from 1 to 4 points (**Table 2**). The total score was allocated to four grades.

# RESULTS

## Specimens

Twenty-three patients (13 horses and 10 cats) met the inclusion criteria. No animal underwent chemotherapy or radiation therapy. Survival times in horses ranged from 0 to 306 days. Patient owners decided for euthanasia in five horses within the 1st day after CT examination due to extensive involvement of the mass. One horse was euthanized due to poor clinical presentation

TABLE 2 | Malignancy grading system of oral squamous cell carcinoma according to Anneroth et al. (18).

| Histologic grading of malignancy of tumour cell population | | | | |
|---|---|---|---|---|
| | Points | | | |
| Morphologic parameter | 1 | 2 | 3 | 4 |
| Degree of keratinization | Highly (>50% of the cells) | Moderate (20–50% of cells) | Minimal (5–20% of cells) | None (0–5% of cells) |
| Nuclear polymorphism | Little (>75% mature cells) | Moderately abundant (50–75% mature cells) | Abundant (25–50% mature cells) | Extreme (0–25% mature cells) |
| Number of mitotic cells/high-power field | 0–1 | 2–3 | 4–5 | >5 |
| **Histologic grading of malignancy of tumour-host relationship** | | | | |
| Pattern of invasion | Pushing, well-delineated infiltrating borders | Infiltrating, solid cords, bands and/or strands | Small groups or cords of infiltrating cells ($n > 15$) | Marked and wide-spread cellular dissociation in small groups of cells ($n < 15$) and/or in single cells |
| Stage of invasion (depth) | Carcinoma *in situ* and/or questionable invasion | Distinct invasion, but involving lamina propria only | Invasion below lamina propria adjacent to muscles, salivary gland tissues and periosteum | Extensive and deep invasion replacing most of the stromal tissue and infiltrating jawbone |
| Lympho-plasmocytic infiltration | Marked | Moderate | Slight | None |

and cytological diagnosis of squamous cell carcinoma, which was confirmed post mortem by histopathology. Five horses were euthanized 5–10 days after histopathological diagnosis with additional pain medication. Two horses underwent surgical debulking with additional pain medication. One horse was euthanized 70 days and one horse 306 days after histopathological diagnosis. The survival times in cats ranged from 0 to 67 days. Four out of 10 cats were euthanized on the same day of CT or histopathological diagnosis. One cat was euthanized after 4 days following histopathology. The remaining five cats were treated conservatively with antibiotics, anti-inflammatory medication, pain control medication, or a range of combination of those. Of those, two cats were lost to follow on days 0, and one cat each 16 days and 32 days after the histopathological diagnosis. One cat was euthanized due to clinical deterioration 67 days after diagnosis. **Table 3** summarizes the differences in CT findings.

## Computed Tomography

### Tumour Characteristics

In horses, the centre of the masses occurred at the paranasal sinus, mandible, tongue, and nasal cavity levels, with the centre at the paranasal sinus in eight out of 13 cases. Of these eight cases, six had soft tissue attenuation filling almost the complete ipsilateral rostral and caudal maxillary sinus, dorsal conchal sinus, ventral conchal sinus, while the conchofrontal and sphenopalatine sinus showed different amount of filling. In one case, the soft tissue mass also affected the contralateral side. In two of the eight horses, one showed nodular masses involving a third of the ipsilateral rostral maxillary sinus and less than a third of the conchofrontal sinus adjacent to the rostral maxillary sinus. In the second horse, the complete rostral maxillary sinus and less than one third of the conchofrontal sinus were affected. In three of the 13 horses, masses were localized at the mandible with varying soft tissue mass extensions. One equine lingual SCC had concurrent involvement of the ipsilateral stylohyoid bone. The fewest changes were noted in one horse with mild unilateral narrowing of the common and ventral nasal meatus by small nodular soft tissue lesions along the nasal septum. In two horses contrast medium was applied and heterogeneous contrast enhancement could be detected, however the masses were poorly defined. The margination of the masses could not be evaluated in 11/13 horses due to lack of contrast medium application. Six out of eight masses in the paranasal sinus were classified as large and mean maximum length of oral masses was 103.5 ± 32.6 mm

TABLE 3 | Computed tomography (CT) features of oral or sinonasal squamous cell carcinomas in an equine and feline population.

| | CT scanner (slices) | Involved compartments (Number) | Involved tissue layers (Number) | Involved bones (Number) | Periosteal patterns (Number) | Centre of the mass (right, left) | Size |
|---|---|---|---|---|---|---|---|
| Horse 1 | multi | 4 | 1 | 3 | 1 | Paranasal sinuses (right) | large |
| Horse 2 | multi | 1 | 0 | 0 | 0 | Nasal cavity (left) | small |
| Horse 3 | multi | 3 | 1 | 2 | 1 | Paranasal sinuses (left) | large |
| Horse 4 | multi | 2 | 2 | 1 | 3 | Mandible (right) | 146 mm |
| Horse 5 | multi | 3 | 3 | 2 | 1 | Paranasal sinuses (left) | large |
| Horse 6 | multi | 3 | 4 | 2 | 2 | Paranasal sinuses (right) | medium |
| Horse 7 | single | 8 | 4 | 7 | 1 | Paranasal sinuses (left) | medium |
| Horse 8 | single | 6 | 4 | 8 | 1 | Paranasal sinuses (left) | large |
| Horse 9 | multi | 3 | 2 | 1 | 3 | Mandible (right) | 81 mm |
| Horse 10 | multi | 2 | 2 | 1 | 2 | Soft tissue–tongue (left) | 75 mm |
| Horse 11 | multi | 3 | 3 | 2 | 1 | Paranasal sinuses (right) | large |
| Horse 12 | multi | 2 | 2 | 1 | 2 | Mandible (right) | 112 mm |
| Horse 13 | multi | 4 | 4 | 3 | 1 | Paranasal sinuses (left) | large |
| Cat 1 | multi | 5 | 4 | 4 | 1 | Maxilla at the level of the orbit (left) | 32 mm |
| Cat 2 | single | 4 | 4 | 2 | 1 | Mandible (left) | 58 mm |
| Cat 3 | single | 5 | 4 | 10 | 1 | Diffuse (facial and cranial bones) (left) | 45 mm |
| Cat 4 | multi | 3 | 3 | 4 | 2 | Mandible (right) | ne |
| Cat 5 | multi | 2 | 3 | 0 | 0 | Soft tissue–buccal (left) | 26 mm |
| Cat 6 | multi | 3 | 2 | 0 | 0 | Soft tissue–tongue (right) | 34 mm |
| Cat 7 | multi | 6 | 4 | 8 | 1 | Maxilla at the level of the orbit (right) | 40 mm |
| Cat 8 | multi | 2 | 4 | 2 | 1 | Mandible (right, left) | ne |
| Cat 9 | multi | 5 | 4 | 5 | 1 | Maxilla at the level of the orbit (right) | 35 mm |
| Cat 10 | multi | 6 | 4 | 10 | 1 | Maxilla at the level of the orbit (left) | 50 mm |

*Compartments (oral cavity, pharynx, nasal cavity, nasopharynx, paranasal sinus, orbital region, cranial cavity, soft tissues); tissue layers (bone, soft tissues, fat, skin); periosteal patterns (solid/lamellar, irregular, spiculated, Codman's triangle, amorphous/pumice stone-like). Ne, not evaluable.*

(range, 75–146 mm). The mean pre-contrast attenuation values of the masses were 41.5 ± 7.7 HU (range, 30–55.1 HU). The maximum attenuation values of the two horses after contrast medium application were 64.2 and 54.2 HU.

In cats, the centre of the masses occurred at the maxilla, mandible, tongue, and buccal levels, and in one case, the tumour displayed diffuse involvement of the facial and cranial bones. In all cases, the masses were poorly marginated. Five out of eight cases showed a rim enhancement and three out of eight cases showed a heterogeneous enhancement pattern of the masses. Four of the 10 cats had a mass centred at the maxilla. Degrees of exophthalmus varied depending on mass size. Three of the 10 cats showed the centre of the mass at the mandible, two had only a soft tissue mass, one in the buccal region, and one affecting the tongue. One cat with diffuse disease showed a poorly marginated soft tissue mass along the ventral aspect of the nasal cavity, unilateral maxilla, ipsilateral buccal region, with intracranial extension and affecting the ipsilateral mandibula as well. The mean maximum length of the masses was 40 ± 10.5 mm (range, 26–58 mm) post-contrast. The masses showed a mean attenuation value of 60.6 ± 15.6 HU (range, 46.6–90.8 HU) on pre-contrast images. After contrast medium application the mean attenuation values were 106.8 ± 32.6 HU (range, 69.5–163.8 HU).

## Bone Changes

In eight equine patients tumour masses were at the paranasal sinus level. Seven of those eight horses had associated mild, solid-to-laminar periosteal reactions. One horse had a severe solid- to-laminar periosteal reaction and an additional mild irregular periosteal reaction. All cases showed some degree of cortical destruction. Cases with gross destruction were severe; cases with permeative destruction were mild. Mandibular masses in two horses showed severe periosteal reaction and cortical destruction; these periosteal reactions were solid/lamellar and spiculated, with a Codman's triangle and amorphous periosteal reactions. One horse presented only a mild, solid/lamellar, periosteal reaction

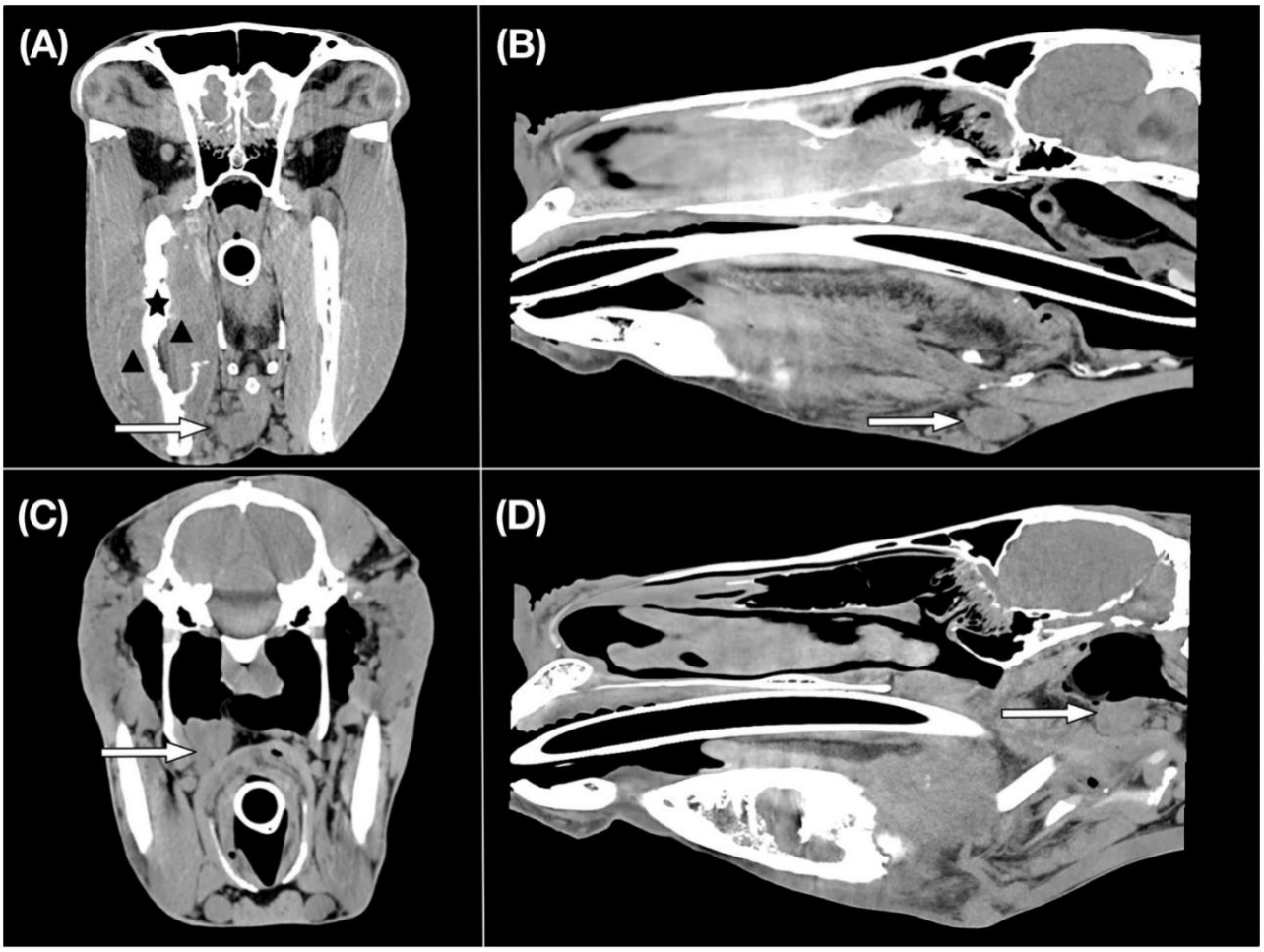


FIGURE 1 | CT images of an equine patient diagnosed with an oral squamous cell carcinoma centred at the right mandible. Transverse (A) and sagittal (B) CT images in a soft tissue window show an enlarged right mandibular lymph node which is indicated by a white arrow. Histopathological examination revealed evidence of metastasis. A black asterisk illustrates the site of osseous changes of the right mandible. The black arrowheads indicate the region of the soft tissue mass. Transverse (C) and sagittal (D) CT images in a soft tissue window display an enlarged right medial retropharyngeal lymph node shown by a white arrow.

with a Codman's triangle and severe, gross mandibular cortical destruction. One equine patient with a lingual mass showed osseous changes of the ipsilateral stylohyoid bone, including severe, gross cortical destruction, with mild, irregular, periosteal reactions and a Codman's triangle.

The feline maxillary tumours showed severe, gross, permeative destruction. Periosteal reactions were severe, irregular, and amorphous/pumice stone-like for the maxillary lesions. Mandible-associated masses in the cats showed different periosteal reactions (solid/lamellar, irregular and spiculated, or amorphous/pumice stone-like). Two cats showed mild, permeative cortical and severe, gross cortical destruction, while in one case both permeative and gross cortical destruction were severe. One cat had a diffuse soft tissue mass involving the facial and cranial bones, which showed mainly gross cortical destruction and mild, irregular periosteal reaction.

### Involved Compartments

Ten of the 13 horses had two to four compartments involved. The most common involved compartments were nasal cavity, paranasal sinuses, and soft tissues. Two-thirds of the cases (8/13) showed two and four affected tissue layers.

Cats displayed between two and six involved compartments, which were almost equally distributed, and most cats (9/10) revealed three and four affected tissue layers.

### Lymph Nodes

For regional lymph nodes in the horses, 20 of 26 mandibular and 14 of 26 medial retropharyngeal lymph nodes were available for interpretation. Eight ipsilateral and one contralateral mandibular lymph nodes and five ipsilateral and two contralateral medial retropharyngeal lymph nodes were subjectively enlarged in nine horses. The mean maximum length × short axis $_{trans}$ × long axis $_{trans}$ of the largest right and left mandibular lymph node was 28.5 × 12.8 × 18.8 mm and 35.0 × 16.5 × 20.7 mm, respectively. The mean maximum length × short axis $_{trans}$ × long axis $_{trans}$ of the largest right and left medial retropharyngeal lymph was 36.1 × 21.4 × 26.2 mm and 32.9 × 17.3 × 25.9 mm, respectively. An example of the CT appearance of regional lymph node enlargement is shown in **Figure 1**.

Twenty of 20 groups of mandibular lymph nodes and 20 of 20 medial retropharyngeal regional lymph nodes were available for interpretation. Four ipsilateral mandibular and three ipsilateral medial retropharyngeal lymph nodes were subjectively enlarged in four cats. In cats, the mean maximum length × short axis $_{trans}$ × long axis $_{trans}$ of the largest right and left mandibular lymph node was 9.5 × 3.3 × 6.5 mm and 8.9 × 3.5 × 5.8 mm, respectively. The mean maximum length × short axis $_{trans}$ × long axis $_{trans}$ of the right and left medial retropharyngeal lymph nodes was 16.7 × 3.6 × 10.5 mm and 15.6 × 3.9 × 10.3 mm, respectively.

**Table 4** lists all individual lymph node parameters for each patient.

## Histopathology

### Tumour

The majority of horses (8/13) was categorized as grade III, four cases as grade IV and one case was grade II. The degree of keratinization was distributed relatively unequal within the study population, with increasing numbers from highly keratinized cells to none keratinization. The latter group comprised almost 40 % of the study population (5/13). Four horses showed a minimal (4/13) and three a moderate degree of keratinization (4/13), whereas only one case displayed highly keratinization. Also, nuclear polymorphism and mitotic cells were quite inconsistent ranging from moderately abundant (4/13), abundant (3/13) to extreme polymorphism (6/13) and zero to more than five mitotic cells per HPF. In most horses (12/13) the tumour turned out to be highly invasive with marked and widespread cellular dissociation in small groups of cells and extensive and deep invasion. Lymphoplasmocytic infiltration was ranging between moderate to none. Eight of 10 cats were categorized as grade III. Out of them two were categorized at least grade III because the small size of the tissue sample did not allow to evaluate a total of
10 HPF for counting of mitotic cells. Each one case was designated as grade IV and II. Regarding the morphologic evaluation of the tumour cell population the degree of keratinization was quite variable ranging between moderate to none. Nuclear polymorphism was quite consistent with moderately abundant to abundant and the number of mitotic cells was quite variable lying between zero and five per HPF. Analysis of tumour-host relationship yielded a marked and widespread pattern of invasion in small groups of cells (10/10), an extensive and deep infiltration into the bone replacing most of the stromal tissue (6/10) in the majority of cats and quite variable none to marked lymphoplasmocytic infiltration. The individual scores for horses and cats are noted in **Table 5**.

### Lymph Nodes

Eight horses with enlarged lymph nodes were necropsied within 1 week after CT, except for one. Two metastatic mandibular and two metastatic medial retropharyngeal lymph nodes were detected among four horses. One horse with subjectively normal lymph nodes on CT images, showed metastasis to the left mandibular lymph node with cytology, however in this horse no histopathology of the lymph node or necropsy was performed.

Histopathological examination was performed in one cat with enlarged lymph nodes revealing metastasis of the ipsilateral mandibular lymph node.

## DISCUSSION

In the current study, we applied Anneroth's classification for cats and adopted this scheme to the best of our knowledge for its first-time use in grading equine oral and sinonasal SCC. Using Anneroth's grading system, eight horses (61%) and eight cats (80%) were categorized as grade III. For both horses and cats,

invasion pattern and stage parameters predominantly received the most points, reflecting the intensive, histological infiltrative nature of this tumour. Whereas, morphologic parameter of the tumour cell population including degree of keratinization and number of mitotic cells were quite variable in horses and cats, the evaluation of the tumour-host relationship yielded a marked and widespread as well as extensive and deep invasion into the bone in the majority of horses and cats. Regarding the proliferation of tumour cells it seems that in the majority of horses (61%) the number of mitotic cells was generally higher with up to >5 mitoses/HPF (5/13) and between four and five mitosis (3/13) when compared with cats. In the latter one, mitotic cells in general were lower and relatively evenly distributed within the study population, ranging between zero and five mitoses/HPF. However, it has to be mentioned that in three cases the sample size was too small to evaluate a total of 10 HPFs, which could alter an exact categorization at least in two cases.

Most tumours were grade III, and an interesting trend of phenotypic variation within and between the two species was seen on CT images (**Figures 2**, **3**). Consistent with a previous study on felines, similarities in the masses included poor definition, rim and heterogeneous contrast enhancement, and maxillary, mandibular, buccal, and lingual locations (12).

Potential patterns of osseous changes also occurred relative to the location and species. In cats, similar features in the maxillary region comprised severe osteolysis and similar periosteal reactions, including irregular and amorphous/pumice stone-like features. In equines, most masses (8/13) were in the paranasal sinuses, which is reported to be more common than in the nasal cavity and particularly frequent in the maxillary sinus. However, whether the mass originates from the sinus or the oral cavity cannot be determined in all cases (3). On CT images, the mass lesions of the paranasal sinuses predominantly showed mild periosteal reactions in the form of a solid-to-lamellar pattern and thus differed from the masses of the maxillary region in cats. Mandible-associated masses showed the most varied periosteal reactions and osteolysis both within species and between species. Cats with masses in the lingual and buccal region presented no osseous changes; however, one horse presented osseous changes affecting the adjacent stylohyoid bone, which indicated local infiltration. Unfortunately, the study population was too small to evaluate a statistically significant correlation between the histological grading system and CT findings.

In addition to primary lesions, regional lymph nodes are assessed in full diagnostic work-ups. The mandibular and medial retropharyngeal lymph nodes are the major lymph nodes

TABLE 4 | Features of mandibular and medial retropharyngeal lymph nodes in an equine and feline population diagnosed with oral or sinonasal squamous cell carcinoma.

| | Mandibular lymph nodes (mm) right; left | | | | | Medial retropharyngeal lymph nodes (mm) right; left | | | | |
|---|---|---|---|---|---|---|---|---|---|---|
| | Long axis | Short axis | Length | Shape | Number | Long axis | Short axis | Length | Shape | Number |
| Horse 1* | na | na | na | na | na | na | na | na | na | na |
| Horse 2 | 15.2; 16.2 | 8.9; 11.2 | 30.4; 25.8 | i; i | ≥20; ≥20 | 14.2; 17.3 | 9.1; 10.2 | 34.0; 29.8 | o; o | ≥10; ≥10 |
| Horse 3* | 15.8; 26.0 | 12.0; 21.8 | 17.6; 60.7 | o; i | ≥20; ≥20 | na | na | na | na | na |
| Horse 4* | 42.9; 17.9 | 24.8; 15.3 | 53.6; 40.5 | i; o | ≥20; ≥20 | 31.8; 9.9 | 27.6; 5.9 | 39.4; 11.1 | i; o | ≥10; ≥10 |
| Horse 5* | 7.4; 39.8 | 6.3; 29.8 | 15.5; 55.7 | o; i | ≥20; ≥20 | na | na | na | na | na |
| Horse 6* | 16.7; 12.8 | 12.1; 5.0 | 27.8; 29.1 | i; o | ≥20; ≥20 | na | na | na | na | na |
| Horse 7* | na | na | na | na | na | na | na | na | na | na |
| Horse 8* | 8.7; 21.2 | 7.3; 19.7 | 16.1; 34.0 | o; i | ≥10; ≥10 | ne | ne | ne | ne | ne |
| Horse 9* | 22.5; 6.7 | 13.4; 6.6 | 29.9; 7.6 | i; o | ≤10; ≤10 | 41.9; ne | 40.9; ne | 56.3; ne | i; ne | 1; ne |
| Horse 10 | 12.4; 15.3 | 8.9; 14.6 | 27.0; 27.7 | i; i | ≥20; ≥20 | 28.8; 29.7 | 17.0;18.7 | 31.2; 29.2 | i; i | ≥10; ≥10 |
| Horse 11* | na | na | na | na | na | na | na | na | na | na |
| Horse 12* | 27.6; 23.6 | 22.1; 15.9 | 35.8; 31.5 | i;i | ≤10; ≤10 | ne; 38.3 | ne; 28.2 | ne; 58.1 | ne; i | ne; ≤10 |
| Horse 13* | 18.9; 27.6 | 12.9; 24.6 | 31.3; 37.8 | i; i | ≥20; ≥20 | 14.4; 34.6 | 12.5; 23.7 | 19.7; 36.6 | o; i | ≤10; ≤10 |
| Cat 1 | 8.2; 8.0 | 3.0; 6.4 | 12.9; 15.2 | o; r | 1; 2 | 9.0; 11.8 | 3.3; 3.5 | 16.5; 16.4 | f; f | 1; 1 |
| Cat 2 | 8.6; ne | 5.5; ne | 10.8; ne | r; ne | 2; ne | 12.3; 15.2 | 4.0; 7.3 | 17.6; 18.0 | f; o | 1; 1 |
| Cat 3 | 2.9; 4.7 | 1.6; 2.8 | 6.0; 6.7 | o; o | 2; 2 | 7.1; 7.7 | 2.0; 2.1 | 9.9; 9.8 | f; f | 1; 1 |
| Cat 4* | ne; 5.0 | ne; 3.1 | ne; 9.3 | ne o | ne; 2 | 9.9; 10.0 | 3.8; 4.2 | 13.3; 13.8 | o; o | 1; 1 |
| Cat 5 | 9.1; 10.3 | 3.7; 4.9 | 12.2; 11.5 | r; r | 2; 2 | 11.4; 12.5 | 4.0; 4.4 | 25.7; 24.8 | f; f | 1; 1 |
| Cat 6 | 4.0; 3.4 | 3.4; 1.9 | 5.1; 6.3 | r; o | 2; 2 | 15.9; 10.4 | 4.6; 3.3 | 19.0; 17.3 | o; f | 1; 1 |
| Cat 7 | 7.5; 6.8 | 3.3; 4.7 | 10.0; 7.6 | r; o | 2; 2 | 11.0; 9.1 | 4.0; 4.2 | 19.4; 18.0 | f; f | 1; 1 |
| Cat 8* | 4.5; 4.9 | 2.2; 2.6 | 7.3; 8.6 | o; o | 2; 2 | 7.7; 6.6 | 3.5; 3.7 | 11.3; 9.1 | f; f | 1; 1 |
| Cat 9 | 6.9; 3.4 | 3.4; 1.6 | 11.9; 5.6 | r; o | 2; 2 | 10.5; 9.0 | 3.1; 2.1 | 17.8; 12.8 | f; f | 1; 1 |
| Cat 10 | 4.3; 4.8 | 2.9; 2.1 | 8.5; 7.6 | o; o | 2; 3 | 10.6; 10.0 | 4.6; 3.6 | 18.6; 14.4 | o; o | 1; 1 |

*Long and short axis are measures on transverse CT images. The maximum length is measured on sagittal CT images along the long axis of the lymph nodes. r, round; o, oval; f, fusiform; b, bilobed; *no contrast medium application; na, not available; ne, not evaluable.*

draining the oral and nasal cavity (19). In the present study we noted up to 20 mandibular and 10 medial retropharyngeal lymph nodes on soft tissue CT images on each side in horses. Interestingly, a big proportion of the lymph nodes were even smaller than 5 mm, however in addition to the largest lymph nodes measured there were multiple lymph nodes in between in the smallest and largest lymph nodes. To the authors' knowledge no detailed CT descriptions of equine head and neck lymph nodes have been published. According to an anatomical reference, 35–75 densely packed mandibular lymph nodes which can be located along a 16 cm region are reported. For the medial retropharyngeal lymph nodes it has been noted that 20–30 loosely arranged lymph nodes can be present (19).

In cats, the mean maximum length × short axis $_{trans}$ × long axis $_{trans}$ of the largest right and left mandibular lymph node and medial retropharyngeal lymph nodes within ranges of previously described dimensions. There are few studies investigating CT features of feline medial retropharyngeal lymph nodes. One study is focusing on CT measurements of medial retropharyngeal lymph nodes in clinically healthy cats reporting the mean length × rostral height × rostral width dimensions of medial retropharyngeal lymph nodes to be 20.7 × 13.1 × 4.7 mm with the maximum dimensions of ∼32 × 20 × 7 mm (20). The same authors published a study comparing medial retropharyngeal lymph node features of cats with nasal neoplasia and rhinitides and found significant association with neoplasia and medial retropharyngeal asymmetry (21). There is limited information about CT characteristics of the feline mandibular lymph nodes. Previously the mean length × height × width dimensions of the right medial and lateral (11.04 × 2.87 × 5.71 mm; 10.86 × 3.22 × 6.53 mm) and left medial and lateral mandibular lymph nodes (11.35 × 2.84 × 5.40 mm; 11.32 × 3.43 × 6.88 mm) of healthy cats have been reported, respectively (22). Gendler et al. (12) described a mean ± SD maximum width of mandibular and medial retropharyngeal lymph nodes of 4.1 ± 1.9 mm (range, 1.5–8.6 mm) and 5.3 ± 1.5 mm (range, 2–8.4 mm), respectively in cats with oral SCC.

In the current study the terms long and short axis were used for the measurements on transverse CT images. While the long and short axis corresponded to the width and height in mandibular lymph nodes and to the height and width in medial

TABLE 5 | Malignancy grading scores according to Anneroth et al. (18) in an equine and feline population diagnosed with oral or sinonasal squamous cell carcinoma.

| | Degree of keratinization | Nuclear polymorphism | Number of mitotic cells/high-power field | Pattern of invasion | Stage of invasion (depth) | Lympho-plasmocytic infiltration | Total score | Grade |
|---|---|---|---|---|---|---|---|---|
| Horse 1 | 4 | 4 | 4 | 4 | 4 | 3 | 23 | IV |
| Horse 2 | 2 | 2 | 3 | 3 | 4 | 2 | 16 | III |
| Horse 3 | 4 | 4 | 4 | 4 | 4 | 3 | 23 | IV |
| Horse 4 | 4 | 3 | 4 | 4 | 4 | 2 | 21 | IV |
| Horse 5 | 4 | 4 | 2 | 4 | 4 | 3 | 21 | IV |
| Horse 6 | 2 | 2 | 1 | 4 | 4 | 2 | 15 | II |
| Horse 7 | 3 | 4 | 2 | 4 | 4 | 2 | 19 | III |
| Horse 8 | 4 | 4 | 2 | 4 | 4 | 2 | 20 | III |
| Horse 9 | 3 | 3 | 3 | 4 | 4 | 2 | 19 | III |
| Horse 10 | 1 | 2 | 2 | 4 | 4 | 4 | 17 | III |
| Horse 11 | 3 | 4 | 4 | 4 | 3 | 2 | 20 | III |
| Horse 12 | 3 | 3 | 3 | 4 | 4 | 2 | 19 | III |
| Horse 13 | 2 | 2 | 4 | 4 | 4 | 3 | 19 | III |
| Cat 1 | 3 | 2 | 2 | 4 | 4 | 2 | 17 | III |
| Cat 2 | 4 | 2 | 3 | 4 | 3 | 3 | 19 | III |
| Cat 3 | 3 | 2 | 1* | 4 | 3 | 4 | ≥17 | III |
| Cat 4 | 3 | 3 | 1* | 4 | 4 | 3 | ≥18 | ≥III |
| Cat 5 | 2 | 2 | 3 | 4 | 3 | 2 | 16 | III |
| Cat 6 | 2 | 2 | 1 | 4 | 3 | 2 | 14 | II |
| Cat 7 | 3 | 2 | 2 | 4 | 4 | 3 | 18 | III |
| Cat 8 | 4 | 3 | 3 | 4 | 4 | 4 | 22 | IV |
| Cat 9 | 3 | 3 | 2 | 4 | 4 | 1 | 17 | III |
| Cat 10 | 3 | 2 | 1* | 4 | 4 | 4 | ≥18 | ≥III |

* *Tumour did not extend towards the margins of 10 high-power fields. Grade I = 5–10 points, Grade II = 11–15 points, Grade III = 16–20 points, Grade IV = >20 points.*

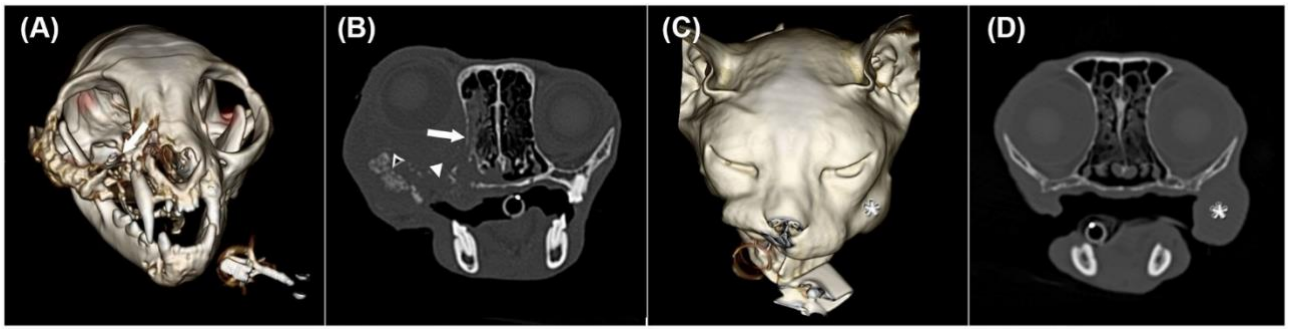


FIGURE 2 | Three-dimensional surface models (A,C) and transverse CT images in a bone window (B,D) of two cats with oral squamous cell carcinoma showing different CT phenotypes despite having the same histological grade. (A) and (B) illustrate cat 7 with the centre of the mass at the right maxillar level (white arrow) shown in image A. In image B, severe permeative (white arrow) and gross cortical (white arrowhead) destruction and amorphous/pumice stone-like (black arrowhead with a white frame) periosteal reactions are depicted. The soft tissue mass extends into the ipsilateral oral and nasal cavity, causing ipsilateral exophthalmus. (C) and (D) represent cat 5 with a mass lesion (white asterisk) at the left buccal level without osseous changes.

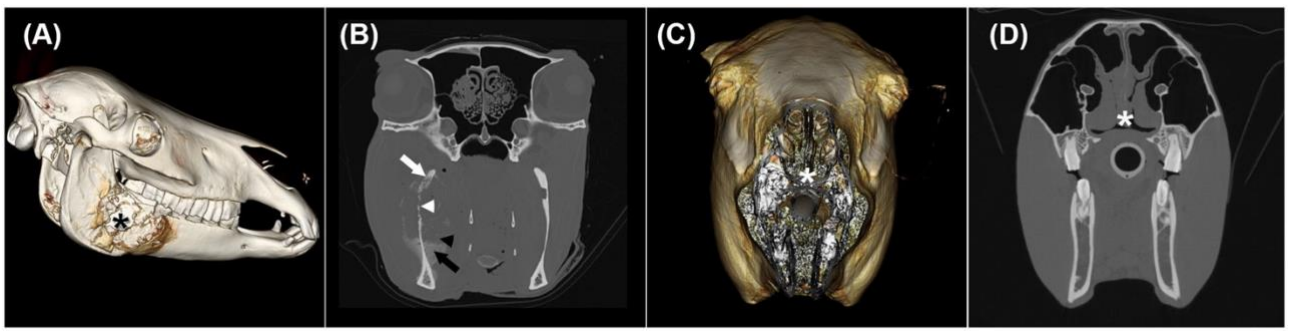


FIGURE 3 | Three-dimensional surface models (A,C) and transverse CT images in a bone window (B,D) of two horses with oral and nasal squamous cell carcinoma showing different CT phenotypes despite having the same histological grade. (A) and (B) illustrate horse 9 with a mass lesion affecting the right mandible (black asterisk) with severe permeative (white arrow) and gross cortical (white arrowhead) destruction as well as solid/lamellar (black arrow) and amorphous/pumice stone-like (black arrowhead) periosteal reactions. (C) and (D) display horse 2 with an irregularly thickened nasal septum (white asterisk).

retropharyngeal lymph nodes, respectively as described in cats, especially in equine mandibular lymph nodes width and height were not straight forward identified.

The presence of lymph node enlargement was first decided on comparison to the contralateral side. The subjectively enlarged lymph nodes corresponded to the side of the SCC in most of the cases. If no asymmetry is detected, unfortunately bilateral enlargement could not be excluded completely. Measurements of the maximum three dimensions of the largest lymph nodes of each side were made, only in one cat the width of a medial retropharyngeal lymph node was reaching the upper limit for what has been described in healthy cats (20). Unfortunately, histopathological examination of enlarged medial retropharyngeal lymph nodes in cats was not performed. Concerning oral SCC in cats, Gendler et al. (12) reported that the mean ± SD maximum width of mandibular lymph nodes measured on CT images in patients with cytologic evidence of metastasis (5.3 ± 2.1 mm) was not significantly different from the mean maximum width of mandibular lymph nodes in patients without metastatic disease (3.9 ± 1.7 mm).

In the current study few metastatic lymph nodes were detected, accounting for two of nine mandibular and two of seven medial retropharyngeal metastases of enlarged lymph nodes in horses. Equine SCC metastasis is rare, and without a histological examination, enlarged lymph nodes could also result from primary inflammation unrelated to the tumour or could be concurrent inflammation due to secondary tumour infection (3). In the present study, five cats showed subjectively enlarged lymph nodes, but only one lymph node sample was available, which showed mandibular metastasis. Previously, the prevalence of mandibular lymph node metastasis was reported to be 31% in cats. Treating metastasis may be of value in cases where long-term control of the primary tumour is feasible (23). Our results need to be cautiously interpreted since this study was a retrospective study and histopathology of the lymph nodes were only available in a proportion of the cases.

The survival times in horses ranged from 0 to 306 days in the present study. The two horses of this study, who received surgical debulking of masses in the paranasal masses had survival times of 70 days and 306 days. There is little information about the survival time of head and neck SCC in horses. A case report described an 18 year-old American Saddlebred stallion with a SCC at the base of the tongue who received palliative radiation therapy and after initial clinical improvement was euthanized 7 weeks after (24). In another case report, partial excision of the incisive bone was performed in a 27-year-old Arabian stallion with a large oral SCC and showed no gross evidence of recurrence or metastasis 5 months later (6). In the present study the survival times in cats ranged from 0 to 67 days with six of 10 cats being euthanized or lost to follow up on the day of diagnosis. Two previous studies assessed the survival time in cats with oral squamous cell carcinoma of 14–251 days (median 91 days) (23) and 14–1,020 days (median 60 days) (12), with most of the cats being part of a chemotherapeutic trial (12, 23). In another study including cats without radiation therapy or chemotherapy the overall median survival time was 44 days (95% confidence interval (CI): 31–79) (25). The survival times are variable and unfortunately the diagnosis is often achieved at an already progressed disease stage in which local disease control is the main goal. Therefore, with growing knowledge about the characteristics of this tumour, and more precise prognosis for each treatment option, the owners could be provided with more information for decision making.

Histopathological evaluation is part of the diagnostic work- up for equine and feline SCC. Histological grading of equine SCC is generally based on the descriptions of Schuh (26). Schuh's system grades the oral, pharyngeal and nasal mucosa according to morphological cellular characteristics, specifically the number of keratin "pearls," the number of cells showing keratinization and the presence of intercellular bridges (maximum, moderate, poorly differentiated, and anaplastic variants). For three grades, the amounts of differentiation and keratinization decrease as the grade increases. Grade III additionally describes some atypical mitotic figures (27). To date, more feline than equine studies have addressed the biological background of oral SCC. This is partly because cats are compatible models for research on human head and neck SCC owing to their similar tumour behaviours and response to therapy (28). In human medicine, multiple histological classifications have been used to predict disease behaviour (29). Generally reported histological subtypes in human medicine include conventional SCC (further graded as well-, moderately or poorly differentiated), verrucous carcinoma, basaloid SCC, and other variants (30). Among these classifications, Anneroth's scheme is a multifactorial and detailed human malignancy grading system for oral SCC considering tumour cell populations and tumour-host relationships (18). Akhter et al. (16) investigated Anneroth's classification for human oral SCC compared with other classification systems and concluded that Anneroth's classification can be used as a valuable diagnostic factor. In veterinary medicine, papers on feline oral SCC also used Anneroth's classification (8, 31, 32). Sparger et al. (33) graded feline oral SCC according to human and canine schemes (34, 35). Because of a detailed morphological assessment that included the tumour-host relationship used in human medicine we decided therefore to apply this classification to our study populations.

In humans, HNSCC is known for its heterogenous biological behaviour, thus, HNSCC research focuses on elucidating the genetic background to better understand tumour-specific characteristics (36). Tumours of the same histological type can show various phenotypes, making this tumour challenging to treat (37); however, similarities exist between human and feline oral SCC, thus offering potential options for using cats as animal models (38). Many studies in human medicine are addressing the association between human papillomavirus infection and HNSCC (39). In cats, accumulating studies are also focusing on molecular biology and the relationship with papillomavirus infection (8, 33, 40). Studies have also evaluated using cats as animal models for studying emerging targets in human cancer therapy (41).

In humans, diagnostic imaging shows high variation in the primary tumour locations and degree of involvement of the surrounding structures (42). In addition, the grade of the histological differentiation does not appear to strongly affect predicting the presence or extension of bone involvement (43). Likewise, in cats, oral SCCs can reportedly present as severely aggressive tumours despite being well-differentiated histologically (1). A feline study showed that the lingual location was associated with younger cats, suggesting a possible different pathogenesis, influenced by the epithelial susceptibility to develop SCC (44). In humans, the location seems crucial for the prognosis since the tongue, soft palate, and floor of the mouth present the worst prognoses (45). The squamous epithelium of the oropharynx develops from the endoderm and shows a higher ability to form poorly differentiated carcinomas. Apart from the tumour origin, the pathways by which the tumours spread, i.e., by direct extension over mucosal surfaces, muscle and bone or by lymphatic drainage and extension along neurovascular bundles, must also be considered (42). Because cats and humans have similar bone-invasive phenotypes, cat are recognized as models for characterizing bone resorption in human SCC. Feline oral SCC cells can stimulate osteoclastic bone resorption corresponding to parathyroid hormone related-protein expression (46). A large feline study revealed that bone invasion was most commonly seen in gingival-associated SCC, most likely due to the close anatomical relationship of the gingiva to the bone. New bone formation in the form of periosteal reactions and metaplastic bone as well as the ability of neoplastic cells to directly adhere to the bone matrix have also been described (44). Periosteal reactions invade the bone in human SCC at a frequency of 11% (47). In the current study, eight out of 10 cats and 12/13 horses showed periosteal new bone formation. This high periosteal reaction percentage likely occurred because cats and horses present later in the disease process showing large tumour masses and being more locally aggressive at that stage compared with humans (28). Periosteal reactions occur because of tumour displacement and infiltration.

In human medicine, a CT study on periosteal new bone formation in the jaw found a spicule pattern in 61% of malignant tumours, in addition to parallel, irregular and Codman's triangle patterns (47). Those periosteal reactions were also found in the present study. Why severe, irregular and amorphous/pumice stone-like periosteal reactions were common in the maxillary region of cats, and solid- to-lamellar periosteal reactions were seen at the paranasal sinus level in horses is unknown. Different subtypes may be associated with varying numbers of osteoproliferative mediators. Larger study populations are needed to investigate whether specific osseous changes are statistically significant to an anatomical location.

This study had some limitations relative to its retrospective nature. The small sample size prevented statistical analysis. Furthermore, histological evaluations depend on the sample size and location; therefore, biased interpretations can result. As larger tissue samples obtained by necropsy provide better survey of histological findings we generally preferred to use necropsy samples instead of biopsy material as far as possible, however necropsy was only performed in two of 10 cats (the other cats were lost to follow up or were taken home by owners), and was mainly performed in horses. Histopathological samples were acquired by clinicians according to possibilities of biopsy collection, respectively. As this was a retrospective study, an exact correlation between the histological sample location and the respective location on the CT images, which would have helped better elucidate the findings, could not be determined. Some limitations were related to the CT protocols. Because no horse with a mass lesion in the paranasal sinuses received intravenous contrast medium, the proper extent of the mass could not be delineated, and concurrent loculated fluid of varying compositions may have been a contributing factor. Besides, the regional lymph nodes were inconsistently imaged in the horses, and lymph node samples were unavailable in a proportion of animals. Since except for two cases, for all other horses only pre-contrast CT images were available and lymph nodes often presented with an overall irregular shape, it cannot be ensured that this irregular shape resulted from multiple lymph nodes in close proximity to each other and not a single lymph node. Thus, lymph node-related findings must be cautiously interpreted and further studies with healthy controls are warranted. Two horses and two cats were examined with a single-slice CT scanner, which has a lower temporal and contrast resolution in comparison to a multi-slice CT scanner. Thus, the shape of the periosteal reaction or the existence of permeative cortical destruction could have been misinterpreted. The time between CT and histological examination was $<7$ days in most animals. However, delays of 58 and 15 days occurred between these two diagnostic modalities in two cats, and a 12-day delay occurred in one horse. Whether this time difference affected the morphological changes is unknown. Unfortunately, no studies have documented morphological follow-up. Therefore, the degrees of osseous changes may be partly related to a more progressed disease.

In conclusion, the current study showed that equine and feline oral and sinonasal SCCs presented different phenotypic tendencies on CT scans while also presenting similar histological grades. These findings add diagnostic imaging and histopathological features to the present research on oral and sinonasal SCC and demonstrate the need for further studies with larger populations to investigate the heterogeneous biological behaviour of equine and feline HNSCC. Thus, gaining more specific knowledge regarding the molecular genetics and biology of SCC may help clarify the role of veterinary models in human research and help target specific therapies and redefine prognoses in animals and potentially in humans. Finally, as veterinary and human medicine get more complementary, they might benefit from one another by serving the same goal of one common health.

## DATA AVAILABILITY STATEMENT

The raw data supporting the conclusions of this article will be made available by the authors, without undue reservation.

## ETHICS STATEMENT

Ethical review and approval was not required for the animal study because the study is retrospective in nature and the study patients were clinical patients of the Vetmeduni Vienna. Written informed consent for participation was not obtained from the owners because the majority of patient owners signed a consent procedure for research when hospitalizing their patients. Due to the retrospective nature of the study, a minority of patient owners (3/23) agreed to a clinical investigation and were not aware of a subsequent systematic analysis.

## AUTHOR CONTRIBUTIONS

All authors listed have made a substantial, direct and intellectual contribution to the work, and approved it for publication.

## FUNDING

Part of the article processing charges was funded by the University Library of the University of Veterinary Medicine, Vienna, Austria.

## REFERENCES

1. Murphy BG, Bell CM, Soukup J. Oral squamous cell carcinoma. In: Murphy BG, Bell CM, Soukup JW, editors. *Veterinary Oral and Maxillofacial Pathology*. 1st ed. Hoboken, NJ: Wiley & Sons (2020). p. 139–48. doi: 10.1002/9781119221296
2. Dixon PM, Head K. Equine nasal and paranasal sinus tumours: part 2: a contribution of 28 case reports. *Vet J*. (1999) 157:279– 94. doi: 10.1053/tvjl.1999.0371
3. Head KW, Dixon PM. Equine nasal and paranasal sinus tumours. Part 1: review of the literature and tumour classification. *Vet J*. (1999) 157:261– 78. doi: 10.1053/tvjl.1998.0370

4. Stebbins KE, Morse CC, Goldschmid MH. Feline oral neoplasia: a ten-year survey. *Vet Pathol*. (1989) 26:121–8. doi: 10.1177/030098588902600204
5. Bilgic O, Duda L, Sánchez MD, Lewis JR. Feline oral squamous cell carcinoma: clinical manifestations and literature review. *J Vet Dent*. (2015) 32:30– 40. doi: 10.1177/089875641503200104
6. Orsini JA, Nunamaker DM, Jones CJ, Acland HM. Excision of oral squamous cell carcinoma in a horse. *Vet Surg*. (1991) 20:264–6. doi: 10.1111/j.1532-950X.1991.tb01259.x
7. Tannehill-Gregg S, Kergosien E, Rosol T. Feline head and neck squamous cell carcinoma cell line: characterization, production of parathyroid hormone-related protein, and regulation by transforming growth factor-beta. *In Vitro Cell Dev Biol Anim*. (2001) 37:676–83. doi: 10.1290/1071-2690(2001)037<0676:FHANSC>2.0.CO;2
8. Yoshikawa H, Ehrhart EJ, Charles JB, Custis JT, LaRue SM. Assessment of predictive molecular variables in feline oral squamous cell carcinoma treated with stereotactic radiation therapy. *Vet Comp Oncol*. (2016) 14:39– 57. doi: 10.1111/vco.12050
9. Samolyk-Kogaczewska N, Sierko E, Dziemianczyk-Pakiela D, Nowaszewska KB, Lukasik M, Reszec J. Usefulness of hybrid PET/MRI in clinical evaluation of head and neck cancer patients. *Cancers*. (2020) 12:511. doi: 10.3390/cancers12020511
10. Kowalczyk L, Boehler A, Brunthaler R, Rathmanner M, Rijkenhuizen ABM. Squamous cell carcinoma of the paranasal sinuses in two horses. *Equine Vet Educ*. (2011) 23:435–40. doi: 10.1111/j.2042-3292.2010.00141.x
11. Etienne A-L, Evrard L, Bolen G, Esman M, Grulke S, Busoni V. *Imaging Findings in Horses With Pharyngeal Squamous Cell Carcinoma*. Belgium: Diagnostic Imaging Section, Large Animal Surgical Section, Faculty of Veterinary Medicine, University of Liège (2012). Available online at: http://hdl.handle.net/2268/135597 (accessed 2020).
12. Gendler A, Lewis JR, Reetz JA, Schwarz T. Computed tomographic features of oral squamous cell carcinoma in cats: 18 cases (2002–2008). *JAVMA*. (2010) 236:319–25. doi: 10.2460/javma.236.3.319
13. Yoshikawa H, Randall EK, Kraft SL, LaRue SM. Comparison between 2-$^{18}$F-fluoro-2-deoxy-d-glucose positron emission tomography and contrast-enhanced computed tomography for measuring gross tumor volume in cats with oral squamous cell carcinoma. *Vet Radiol Ultrasound*. (2013) 54:307–13. doi: 10.1111/vru.12016
14. Randall EK, Kraft SL, Yoshikawa H, LaRue SM. Evaluation of 18F-FDG PET/CT as a diagnostic imaging and staging tool for feline oral squamous cell carcinoma. *Vet Comp Oncol*. (2016) 14:28–38. doi: 10.1111/vco.12047
15. Munday JS, Löhr CV, Kiupel M. Tumors of the alimentary tract. In: Meuten DJ, editor. *Tumors in Domestic Animals*. 5th ed. Hoboken, NJ: Wiley & Sons (2017). p. 503–6. doi: 10.1002/9781119181200.ch13
16. Akhter M, Hossain S, Rahman QB, Molla MR. A study on histological grading of oral squamous cell carcinoma and its co- relationship with regional metastasis. *J Oral Maxillofac Pathol*. (2011) 15:168–76. doi: 10.4103/0973-029X.84485
17. Modiano JF. Comparative pathogenesis of cancers in animals and humans. *Vet Sci*. (2016) 3:1–4. doi: 10.3390/vetsci3030024
18. Anneroth G, Batsakis J, Luna M. Review of the literature and a recommended system of malignancy grading in oral squamous cell carcinomas. *Scand J Dent Res*. (1987) 95:229–49. doi: 10.1111/j.1600-0722.1987.tb01836.x
19. Nickel R, Schummer A, Seiferle E. Lymphknoten und Lymphsammelgänge der Katze. Lymphknoten und Lymphsammelgänge des Pferdes. In: Nickel R, Schummer A, Seiferle E, editor. *Lehrbuch der Anatomie der Haustiere Band III: Kreislaufsystem, Haut und Hautorgane*. 4th ed. Berlin: Parey (2005). p. 366, 422. doi: 10.1024/0036-7281.147.6.275a
20. Nemanic S, Nelson NC. Ultrasonography and noncontrast computed tomography of medial retropharyngeal lymph nodes in healthy cats. *Am J Vet Res*. (2012) 73:1377–85. doi: 10.2460/ajvr.73.9.1377
21. Nemanic S, Hollars K, Nelson NC, Bobe G. Combination of computed tomographic imaging characteristics of medial retopharyngeal lymph nodes and nasal passages aids discrimination between rhinitis and neoplasia in cats. *Vet Radiol Ultrasound*. (2015) 56:617–27. doi: 10.1111/vru.12279
22. Restrepo MT. Anatomic and pathologic assessment of feline lymph nodes using computed tomography and ultrasonography. Doctoral thesis. Barcelona: Universitat Autonoma de Barcelona (2016).
23. Soltero-Rivera MM, Krick EL, Reiter AM, Brown DC, Lewis JR. Prevalence of regional and distant metastasis in cats with advanced oral squamous cell carcinoma: 49 cases (2005–2011). *J Feline Med Surg*. (2014) 16:164–9. doi: 10.1177/1098612X1350 2975
24. Morrison ML, Groover E, Schumacher J, Newton J, Pereira MM. Lingual squamous cell carcinoma in two horses. *J Equine Vet Sci*. (2019) 79:35– 8. doi: 10.1016/j.jevs.2019.05.022
25. Hayes AM, Adams VJ, Scase TJ, Murphy S. Survival of 54 cats with oral squamous cell carcinoma in United Kingdom general practice. *JSAP*. (2007) 48:394–9. doi: 10.1111/j.1748-5827.2007.00393.x
26. Schuh JCL. Squamous cell carcinoma of the oral, pharyngeal and nasal mucosa in the horse. *Vet Pathol*. (1986) 23:205–7. doi: 10.1177/030098588602300217
27. Knottenbelt DC, Patterson-Kane JC, Snalune KL. Squamous cell carcinoma. In: Knottenbelt DC, Patterson-Kane JC, Snalune KL, editors. *Clinical Equine Oncology*. St. Louis, MO: Elsevier Saunders (2015). p. 223– 5. doi: 10.1016/B978-0-7020-4266-9.00012-X
28. Tannehill-Gregg SH, Levine AL, Rosol TJ. Feline head and neck squamous cell carcinoma: a natural model for the human disease and development of a mouse model. *Vet Comp Oncol*. (2006) 4:84–97. doi: 10.1111/j.1476-5810.2006.00096.x
29. Lindenblatt RdeC, Martinez GL, Silva LE, Faria PS, Camisasca DR, Lourenço SdeQ. Oral squamous cell carcinoma grading systems – analysis of the best survival predictor. *J Oral Pathol Med*. (2012) 41:34– 9. doi: 10.1111/j.1600-0714.2011.01068.x
30. Pereira MC, Oliveira DT, Landman G, Kowalski LP. Histologic subtypes of oral squamous cell carcinoma: prognostic relevance. *J Can Dent Assoc*. (2007) 73:339–44.
31. Klobukowska HJ, Munday JS. High numbers of stromal cancer- associated fibroblasts are associated with a shorter survival time in cats with oral squamous cell carcinoma. *Vet Pathol*. (2016) 53:1124–30. doi: 10.1177/0300985816629713
32. Millanta F, Andreani G, Rocchigiani G, Lorenzi D, Poli A. Correlation between cyclo-oxygenase-2 and vascular endothelial growth factor expression in canine and feline squamous cell carcinoma. *J Comp Pathol*. (2016) 154:297–303. doi: 10.1016/j.jcpa.2016.02.005
33. Sparger EE, Murphy BG, Kamal FM, Arzi B, Naydan D, Skouritakis CT, et al. Investigation of immune cell markers in feline oral squamous cell carcinoma. *Vet Immunol Immunopathol*. (2018) 202:52–62. doi: 10.1016/j.vetimm.2018.06.011
34. Barnes L, Eveson JW, Reichart P, Sidransky D. *World Health Organization Classification of Tumours. Pathology and Genetics of Head and Neck Tumours*. Lyon: IARC Press (2005). p. 107–208.
35. Nemec A, Murphy B, Kass PH, Verstraete FJ. Histological subtypes of oral non-tonsillar squamous cell carcinoma in dogs. *J Comp Pathol*. (2012) 147:111–20. doi: 10.1016/j.jcpa.2011.11.198
36. Alsahafi E, Begg K, Amelio I, Raulf N, Lucarelli P, Sauter T, et al. Clinical update on head and neck cancer: molecular biology and ongoing challenges. *Cell Death Dis*. (2019) 10:540–57. doi: 10.1038/s41419-019-1769-9
37. Hasina R, Whipple M, Martin L, Kuo WP, Ohno-Machado L, Lingen MW. Angiogenic heterogeneity in head and neck squamous cell carcinoma: biologic and therapeutic implications. *Lab Invest*. (2008) 88:342–53. doi: 10.1038/labinvest.2008.6
38. Junior CR, D'Silva NJ. Non-murine models to investigate tumor- immune interactions in head and neck cancer. *Oncogene*. (2019) 38:4902–14. doi: 10.1038/s41388-019-0776-8
39. Panarese I, Aquino G, Ronchi A, Longo F, Montella M, Cozzolino I, et al. Oral and Oropharyngeal squamous cell carcinoma: prognostic and predictive parameters in the etiopathogenetic route. *Expert Rev Anticancer Ther*. (2019) 19:105–19. doi: 10.1080/14737140.2019. 1561288
40. Altamura G, Cardeti G, Cersini A, Eleni C, Cocumelli C, Bartolomé del Pino LE, et al. Detection of felis catus papillomavirus type-2 DNA and viral gene expression suggest active infection in feline oral squamous cell carcinoma. *Vet Comp Oncol*. (2020). doi: 10.1111/vco.12569
41. Cannon CM, Trembley JH, Kren BT, Unger GM, O'Sullivan MG, Cornax I, et al. Therapeutic targeting of protein kinase CK2 gene expression in feline oral squamous cell carcinoma: a naturally occurring large-animal model of head and neck cancer. Hum Gene Ther Clin Dev. (2017) 28:80– 6. doi: 10.1089/humc.2017.008

42. Trotta BM, Pease CS, Rasamny JJ, Raghavan P, Mukherjee S. Oral cavity and oropharyngeal squamous cell cancer: key imaging findings for staging and treatment planning. Radiographics. (2011) 31:339–54. doi: 10.1148/rg.312105107
43. Lukinmaa PL, Hietanen J, Söderholm AL, Lindqvist C. The histologic pattern of bone invasion by squamous cell carcinoma of the mandibular region. Br J Oral Maxillofac Surg. (1992) 30:2–7. doi: 10.1016/0266-4356(92)90 128-6
44. Martin CK, Tannehill-Gregg SH, Wolfe TD, Rosol T. Bone- invasive oral squamous cell carcinoma in cats: pathology and expression of parathyroid hormone-related protein. Vet Pathol. (2011) 48:302–12. doi: 10.1177/030098581038 4414
45. de Araújo RF Jr., Barboza CAG, Clebis NK, de Moura SAB, Lopes Costa AdeL. Prognostic significance of the anatomical location and TNM clinical classification in oral squamous cell carcinoma. Med Oral Patol Oral Cir Bucal. (2008) 13:E344–7.
46. Martin CK, Dirksen WP, Shu ST, Werbeck JL, Thudi NK, Yamaguchi M, et al. Characterization of bone resorption in novel in vitro and in vivo models of oral squamous cell carcinoma. Oral Oncol. (2012) 48:491– 9. doi: 10.1016/j.oraloncology.2011.12.012
47. Ida M, Tetsumura A, Kurabayashi T, Sasaki T. Periosteal new bone formation in the jaws. A computed tomographic study. Dentomaxillofac Radiol. (1997) 26:169–76. doi: 10.1038/sj.dmfr.4600234

**Conflict of Interest:** The authors declare that the research was conducted in the absence of any commercial or financial relationships that could be construed as a potential conflict of interest.

pathogens

MDPI

*Article*

# Tumor Cell Plasticity in Equine Papillomavirus-Positive Versus-Negative Squamous Cell Carcinoma of the Head and Neck

Carina Strohmayer [1,†], Andrea Klang [2,†], Stefan Kummer [3], Ingrid Walter [3,4], Christoph Jindra [5], Christiane Weissenbacher-Lang [2], Torben Redmer [6], Sibylle Kneissl [1] and Sabine Brandt [5,*]

1 Clinical Unit of Diagnostic Imaging, Department for Companion Animals and Horses, University of Veterinary Medicine, 1210 Vienna, Austria; carina.strohmayer@vetmeduni.ac.at (C.S.); sibylle.kneissl@vetmeduni.ac.at (S.K.)
2 Institute of Pathology, Department of Pathobiology, University of Veterinary Medicine, 1210 Vienna, Austria; andrea.klang@vetmeduni.ac.at (A.K.); christiane.weissenbacher-lang@vetmeduni.ac.at (C.W.-L.)
3 VetCore Facility for Research, University of Veterinary Medicine, 1210 Vienna, Austria; stefan.kummer@vetmeduni.ac.at (S.K.); ingrid.walter@vetmeduni.ac.at (I.W.)
4 Institute of Morphology, Department of Pathobiology, University of Veterinary Medicine, 1210 Vienna, Austria
5 Research Group Oncology (RGO), Clinical Unit of Equine Surgery, Department for Companion Animals and Horses, University of Veterinary Medicine, 1210 Vienna, Austria; christoph.jindra@vetmeduni.ac.at
6 Institute of Medical Biochemistry, Department of Biomedical Sciences, University of Veterinary Medicine, 1210 Vienna, Austria; torben.redmer@vetmeduni.ac.at
* Correspondence: sabine.brandt@vetmeduni.ac.at; Tel.: +43-12-5077-5308
† These authors contributed equally to this work.



**Citation:** Strohmayer, C.; Klang, A.; Kummer, S.; Walter, I.; Jindra, C.; Weissenbacher-Lang, C.; Redmer, T.; Kneissl, S.; Brandt, S. Tumor Cell Plasticity in Equine Papillomavirus-Positive Versus-Negative Squamous Cell Carcinoma of the Head and Neck. *Pathogens* **2022**, *11*, 266. https://doi.org/10.3390/pathogens11020266

Academic Editor: Laura Gallina

Received: 22 December 2021
Accepted: 14 February 2022
Published: 18 February 2022

**Publisher's Note:** MDPI stays neutral with regard to jurisdictional claims in published maps and institutional affiliations.



**Abstract:** Squamous cell carcinoma of the head and neck (HNSCC) is a common malignant tumor in humans and animals. In humans, papillomavirus (PV)-induced HNSCCs have a better prognosis than papillomavirus-unrelated HNSCCs. The ability of tumor cells to switch from epithelial to mesenchymal, endothelial, or therapy-resistant stem-cell-like phenotypes promotes disease progression and metastasis. In equine HNSCC, PV-association and tumor cell phenotype switching are poorly under- stood. We screened 49 equine HNSCCs for equine PV (EcPV) type 2, 3 and 5 infection. Subsequently, PV-positive versus -negative lesions were analyzed for expression of selected epithelial (keratins, β-catenin), mesenchymal (vimentin), endothelial (COX-2), and stem-cell markers (CD271, CD44) by immunohistochemistry (IHC) and immunofluorescence (IF; keratins/vimentin, CD44/CD271 double-staining) to address tumor cell plasticity in relation to PV infection. Only EcPV2 PCR scored positive for 11/49 equine HNSCCs. IHC and IF from 11 EcPV2-positive and 11 EcPV2-negative tumors revealed epithelial-to-mesenchymal transition events, with vimentin-positive cells ranging between <10 and >50%. CD44- and CD271-staining disclosed the intralesional presence of infiltrative tumor cell fronts and double-positive tumor cell subsets independently of the PV infection status. Our findings are indicative of (partial) epithelial–mesenchymal transition events giving rise to hybrid epithelial/mesenchymal and stem-cell-like tumor cell phenotypes in equine HNSCCs and suggest CD44 and CD271 as potential malignancy markers that merit to be further explored in the horse.

**Keywords:** horse; HNSCC; papillomavirus; immunohistochemistry; immunofluorescence; tumor cell plasticity

## 1. Introduction

Squamous cell carcinoma (SCC) is a common epithelial tumor type in humans and animals that arises from cutaneous or mucosal keratinocytes. In humans, virtually 100% of cervical carcinomas, about 50% of anogenital SCCs, and approximately 25% of head and neck SCCs (HNSCC) are causally associated with infection by carcinogenic papillomaviruses (PVs) [1]. These PVs termed high-risk human PVs (hrHPVs) belong to the genus α-PVs.

Despite their high genetic heterogeneity, hrHPVs share common features. These include their ability to transform normal keratinocytes into highly proliferative neoplastic cells by a concerted action of the oncoproteins E6 and E7 [2], and to escape from immune surveillance via E5 oncoprotein-mediated downregulation of the MHC class I [3].

HNSCCs refer to SCCs of the nasal and oral cavity, the larynx, and the pharynx, i.e., the naso-, oro-, and hypopharynx. It is widely accepted today that hrHPV-induced and -unrelated HNSCCs constitute two different disease entities. Whilst hrHPV-associated HNSCCs predominantly affect the oropharynx, including the tonsils and base of the tongue, hrHPV-unrelated tumors have no defined predilection sites in the HN region and develop upon exposure to various carcinogens, e.g., alcohol and tobacco [4,5]. In addition, there is evidence of Epstein-Barr virus—a γ-Herpesvirus—contributing to the onset and progression of certain HNSCC subtypes, such as oral SCC [6].

SCCs are malignant tumors, i.e., they have the potential to invade surrounding tissues and establish metastases in other parts of the body. Yet, hrHPV-positive and -negative HNSCCs have different clinical behavior in terms of infiltrative growth and metastasis, with hrHPV-induced lesions showing higher sensitivity to multiple-type therapy and thus having a better prognosis than their hrHPV-unrelated counterparts [7].

In horses and other equids, SCCs preferentially develop at muco-cutaneous junctions, notably the anogenital, ocular, and HN region [8]. Meanwhile, there is ample evidence that equine papillomavirus type 2 (EcPV2) infection causes virtually 100% of anogenital SCCs [9,10]. In contrast, ocular SCCs seem to be unrelated to PV infection. There is general agreement that overexposure to UV-radiation constitutes a major risk factor for ocular SCC development [8,11]. The etiology of equine HNSCC is still poorly understood. Occasional detection of EcPV2 DNA from HNSCCs reported by different groups suggests that a subset of these tumors may be associated with EcPV2 infection [12,13]. However, in-depth research is needed to ascertain that EcPV2 has an active role in the development and progression of some HNSCCs.

Cancer progression and metastasis is a multistep event initiated by genetic and non- genetic cell transforming processes. The latter mechanism, termed cellular plasticity enables the rapid switching of tumor cell phenotypes in response to extracellular cues such as changes in the composition of growth factor or oxygen supply [14]. Consequently, cellular transformation modulates cell–cell interactions, enabling tumor cells to detach from the primary mass, invade and migrate through the extracellular matrix (ECM), enter the microvasculature, and spread via the blood stream and the lymphatics [15,16]. This cascade of events closely resembles an embryologic cellular program termed epithelial–mesenchymal transition (EMT). This program is activated in embryonic development and wound heal- ing and orchestrates the conversion of various types of epithelial cells into mesenchymal cells [15–18]. EMT can be grossly characterized by the loss of typical epithelial properties (e.g., apical–basolateral polarization, basement membrane integrity, cell– cell adhesion) and the gain of mesenchymal characteristics. This transition is mediated by E-cadherin suppression, allowing EMT transcription factors to promote enhanced expression of mesenchymal proteins. The latter, including, e.g., N-cadherin, vimentin, and matrix metalloproteinases (MMPs), promote ECM degradation, cell motility, invasion, and metastasis [16,19]. EMT- mediated changes confer poor immunogenicity, prevent senescence and apoptosis, and enhance the migratory capacity and invasiveness of tumor cells, thus promoting infiltrative growth and metastasis of solid tumors, including HNSCCs [20–23]. Under in vitro conditions, human tumor cells commonly undergo complete EMT as represented by the E- to N-cadherin switch. Under natural in vivo conditions however, human epithelial cancer cells preferentially switch to a hybrid E/M phenotype in a process termed partial EMT (pEMT), which is regulated by ECM components, soluble factors, and exosomes [24]. In human HNSCC, pEMT is well-documented [25]. It is characterized by the concurrent expression of both epithelial and mesenchymal proteins that allows epithelial/mesenchymal (E/M) hybrid tumor cells to migrate collectively as cell clusters. E/M-phenotype tumor cells are thus regarded as best-suited for metastasis [24,25].

In the past years, it has been shown that EMT not only allows tumor cells to acquire a hybrid E/M or mesenchymal phenotype, but is also associated with a second program promoting transition of epithelial tumor cells to a "cancer stem(-like) cell" (CSC) phenotype [21,26]. CSCs are long-lived tumor cells with typical stem-cell properties that notably include the abilities for self-renewal and multidirectional differentiation [27]. CSCs show pronounced resistance to stress factors such as DNA damage [28], reactive oxygen species [29], or hypoxia [30], and by this, to various therapeutic approaches including chemo- and radiation therapy. Thus, CSCs are recognized as crucial promoters of tumor progression and reoccurrence, immune evasion, and metastasis [31,32]. This in turn explains why CSCs are also termed tumor-initiating cells (TICs) [33].

Meanwhile, an increasing number of reports help pave the way towards a better understanding of human CSC biology in cancer diseases, including HNSCC [31,34–37].

In horses, the etiology of HNSCC is largely unclear, and there is only scarce information on cancer cell plasticity in this tumor type. Only three studies have addressed EMT in equine SCC so far. Suárez-Bonnet and colleagues provided consistent evidence of EMT events occurring at the infiltration front of equine penile SCCs [38]. This finding was further corroborated by Armando et al. [39], who also reported on EMT in the case of an EcPV2-positive laryngeal SCC [40]. No information is available on CSCs in equine HNSCCs or any other equine tumor disease so far.

The higher multidrug-sensitivity of hrHPV-induced HNSCCs in comparison to their hrHPV-unrelated counterparts, and the crucial role of EMT and related CSCs as promotors of malignant progression and multidrug resistance (MDR) are suggestive of PV oncoproteins mitigating EMT processes. Given the still-prevailing paucity of knowledge on the pathobiological events underlying equine HNSCC development and metastatic dissemination, the role of EMT and related CSC in this context, and the impact of PV infection on EMT, the objective of this study was (i) to screen a series of equine HNSCCs for the presence of EcPV DNA, and (ii) comparatively analyze EcPV-positive versus -negative lesions for expression of selected epithelial (keratins, β-catenin), mesenchymal (vimentin), endothelial (COX-2), and stem-cell markers (CD271, CD44) by immunohistochemical (IHC) and immunofluorescent staining (IF). The major findings of this study indicate that equine HNSCCs can be categorized into EcPV2-related and -unrelated HNSCC subtypes, at a similar ratio as determined for hrHPV-induced versus -unrelated HNSCCs in humans. We provide evidence of (p)EMT occurring in virtually all lesions to a various extent, and, importantly, of the presence $CD44^+$ $CD271^+$ tumor cell subsets that likely represent CSCs. No significant correlation between (p)EMT/CSC- and EcPV2 infection status was observed.

## 2. Results

### *2.1. Twenty-Two Percent of HNSCC Samples Harbor EcPV2 DNA*

DNA isolated from 49 equine HNSCCs (49 equine patients) was assessed for the presence of EcPV type 2, 3, and 5 DNA on the grounds that these three EcPV2 types are reported to occur in equine SCC [9,10,41,42]. As expected, EcPV2 PCR from 4/15 native lesions previously shown to contain EcPV2 DNA [13] yielded amplicons of anticipated size (173 bp; Table 1; Figure 1). DNA extracted from another native tumor (VLU) also scored positive for this virus type. From the DNA aliquots derived from 27 FFPE tumor samples, six tested positive by EcPV2 PCR (Table 1; Figure 1). None of the tumor DNA samples harbored EcPV3 or EcPV5 DNA (not shown). PCR from positive, negative, and no-template controls included in every reaction yielded anticipated results, thus confirming the experimental accuracy and the validity of results (Figure 1).

### *2.2. Histopathological Findings*

Sections from six noncornifying and 16 cornifying HNSCCs were subjected to histopathological examination. The well-differentiated cornifying tumors consisted of broad and anastomosing trabeculae, cords, and islands of tumor cells displaying varying degrees of keratinization including concentrically laminated keratin formation—so-called keratin pearls. Tumor cells were characterized by minimal

cellular atypia, mild anisocytosis and anisokaryosis, and a moderate mitotic index. The six poorly differentiated, noncornifying HNSCCs exhibited irregular trabeculae, nests, and clusters of tumor cells without keratinization that showed moderate to marked cellular atypia and pronounced anisocytosis. Interspersed dyskeratotic cells were also noted. The tumor cells displayed prominent nuclear pleomorphism with anisokaryosis, high mitotic index including pathologic mitotic figures, and one or multiple prominent nucleoli. Multinucleated tumor cells and macronuclei were occasionally observed. Tumorous infiltrates were commonly accompanied by multifocal areas of necrosis, proliferation of fibrous tissue, desmoplasia and infiltration of the adjacent tumor stroma by lymphocytes, plasma cells and, in some cases, numerous neutrophils.

Individual tumor locations, evidence and location of metastasis, and additional findings such as osteolysis of adjacent structures are provided in Table 1.

**Table 1.** Patient and sample specifications including EcPV2 PCR results.

| Code | Breed | Age | Color | Sex | Sample Origin/Histopathological Diagnosis | Cornification | Native, FFPE | EcPV2 DNA |
|---|---|---|---|---|---|---|---|---|
| **EQUINE HNSCC PATIENTS AND TUMOR SAMPLES THEREFROM SELECTED FOR IHC ANALYSIS (n = 22)** | | | | | | | | |
| DAN | WB | 22 | Chestnut | G | Nasal and oral SCC, retropharyngeal LN metastases | + | N, F | YES |
| MAL | Arabian TB | 19 | Grey | M | Nasal SCC with orbital infiltration | + | F | YES |
| VAL | Icelandic horse | 18 | Black | M | SCC of dorsal nasal concha, osteolysis | ++ | N, F | No |
| DIA | Trotter | 17 | Black | M | SCC of the left nasal cavity and paranasal sinus, osteolysis | + | N, F | No |
| MMO | Haflinger mix | 13 | Bay | G | Sinus SCC | No | F | No |
| PRI | Shetland pony | 26 | Black | G | Nasal SCC | ++ | N, F | YES |
| HJA | Icelandic horse | 16 | Bay | G | Maxillary sinus SCC, oral and retropharyngeal LN metastases | + | F | YES |
| KLU | Noriker horse | 17 | Piebald | G | Maxillary sinus SCC invading lymphatics and blood vessels | + | F | YES |
| FIL | WB | 26 | Chestnut | G | Maxillary sinus SCC | No | N, F | No |
| PER | Trotter | 20 | Bay | G | Maxillary sinus SCC, mandibular and retropharyngeal LN metastases | + | F | No |
| SHM | Cob | 23 | Piebald | G | Sinonasal SCC | ++ | F | No |
| MEC | Shetland pony | 25 | Black | M | Oral SCC right mandibula, maxilla | ++ | F | No |
| BLE | WB | 11 | Piebald | M | Intermandibular SCC (recurrent lesion) | + | F | No |
| SHA | Pinto | 17 | Skewbald | M | Lingual and intermandibular SCC | + | N, F | YES |
| BOM | WB | 24 | Bay | M | Lingual SCC, retropharyngeal and tracheal LNs metastases | No | F | No |
| JON | Pony | 25 | Chestnut | G | Gingival/palatal SCC | No | N, F | YES |
| LUK | WB | 17 | Grey | G | Palatal SCC invading maxillary sinus | ++ | F | No |
| SIR | WB | 11 | Fuchs | M | Mandibular SCC | ++ | F | YES |
| KRA | Icelandic horse | 21 | Fuchs | G | Oral SCC, regional LNs metastases | No | F | No |
| VLU | Icelandic horse | 30 | Chestnut | G | Oral SCC | ++ | N, F | YES |
| SAM | Haflinger-WB | 13 | Sorrel | G | Pharyngeal SCC, retropharyngeal LN metastases | + | N, F | YES |
| MCH | Connemara | 15 | Grey | M | Periocular SCC with metastases (parotis, larynx, jugular notch) | + | N, F | YES |
| **EQUINE HNSCC PATIENTS AND TUMOR SAMPLES THEREFROM (NO IHC ANALYSIS) (n = 27)** | | | | | | | | |
| MIL | WB | 22 | Chestnut | M | Maxillary sinus SCC | + | N, F | No |
| GER | Trakehner | 18 | Black | G | Sinonasal SCC with mandibular LN metastases | No | N, F | No |
| STA | Haflinger | 7 | Sorrel | G | Nasal SCC, mandibular LN metastases | No | N, F | No |
| ATH | Haflinger | 22 | Sorrel | G | Oral vestibule SCC | + | N, F | No |
| BEL | Haflinger | 22 | Sorrel | M | Paranasal sinus SCC with pronounced osteolysis | No | N, F | No |
| JAN | Hungarian WB | 17 | Bay | M | Maxillary sinus SCC, retropharyngeal LN metastases | ++ | F | No |
| CAT | Trotter | 7 | Bay | M | Sinonasal SCC, osteolysis right maxilla | + | F | No |
| CHI | Trotter | 23 | Bay | M | Maxillary SCC invading oral cavity and brain | No | F | No |
| ANG | Haflinger | 16 | Chestnut | M | Maxillary SCC, suspected metastatic activity | No | F | No |
| SNI | Connemara | 16 | Grey | M | Mandibular SCC invading lymphatics, LN metastases | No | N, F | No |
| PEN | Shetland pony | 26 | Piebald | M | Mandibular SCC, osteolysis | ++ | F | No |
| ARR | TB | 21 | Bay | M | Mandibular SCC left, osteolysis | + | N, F | No |
| FEX | Pony | 27 | Sorrel | G | Mandibular SCC invading tongue, trachea, esophagus | No | F | No |
| GAJ | Trotter | 13 | Bay | G | Palatal/gingival SCC, bone arrosion | + | N, F | No |
| WHI | WB | 20 | Skewbald | M | Ulcerative, lingual SCC, invading left stylohyoid | ++ | F | No |
| IAS | Arabian TB | 22 | Grey | M | Lingual SCC, retropharyngeal LN metastases | ++ | F | No |
| NEP | Lusitano | 21 | Grey | G | Lingual base SCC | + | F | No |
| MOZ | WB | 27 | Grey | G | Lingual base SCC, retropharyngeal LNs metastases | + | F | No |
| KAR | Haflinger | 23 | Sorrel | M | Lingual SCC, retropharyngeal, mandibular, cranial LN metastases | + | F | No |
| GOL | Haflinger | 23 | Sorrel | G | Labial SCC (+conjunctival and cutaneous CIS) | ++ | F | No |
| NAV | Haflinger | 17 | Sorrel | G | Labial SCC (+right eye: CIS; left eye: SCC) | ++ | N, F | No |
| JOY | Haflinger | 20 | Sorrel | M | Labial SCC (recurrent lesion), mandibular LN metastases | + | F | No |
| LEN | WB | 23 | Chestnut | M | Maxillary SCC, mandibular LN metastases | + | F | No |
| RIG | Haflinger | 9 | Sorrel | G | Mandibular and labial SCC, mandibular LN metastases | + | F | No |
| GRA | Arabohaflinger | 20 | Sorrel | G | Nasal CIS | ++ | F | No |
| ARM | Haflinger | 12 | Sorrel | M | Cutaneous perinasal CIS (+conjunctival SCC) | No | F | No |
| DAL | Trotter | 12 | Bay | G | Paranasal sinus and oral SCC | + | F | No |

SCC: squamous cell carcinoma; CIS: carcinoma in situ; G: gelding; M: mare; N: native; FFPE: Formalin-fixed paraffin-embedded; LN(s): lymph node(s). ++: cornified; +: partly cornified, No: no cornification.

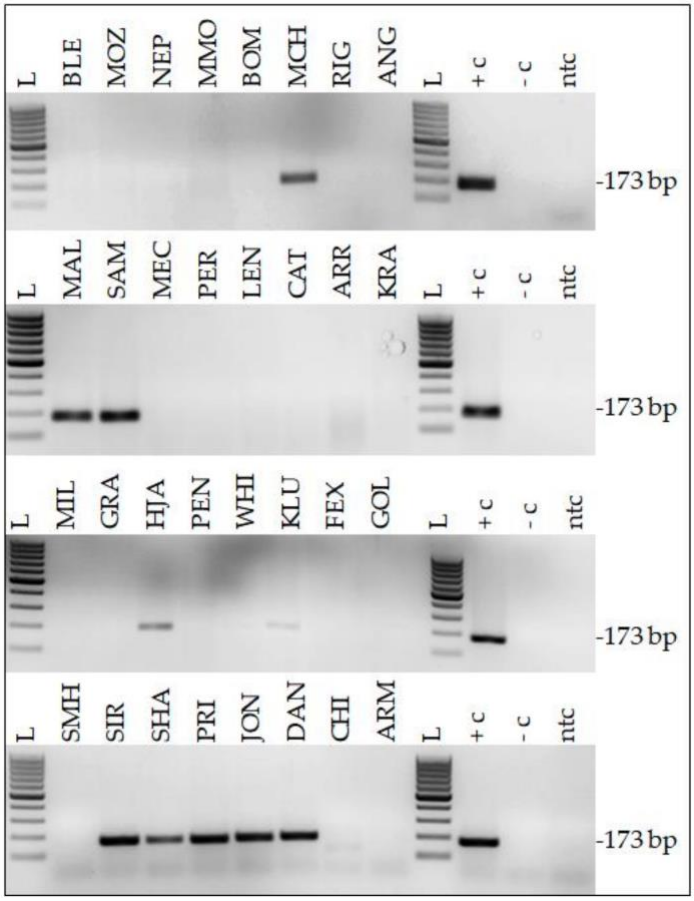


**Figure 1.** A subset of equine HNSCCs harbored EcPV2 DNA. Amplification products (16 µL) were run on 2% TAE gels and visualized by ethidium staining. PCR results are exemplarily shown for 32/49 samples, with PCR yielding amplicons of anticipated size (173 bp) in 10 of the 32 presented cases. L: Gene Ruler 100 bp DNA ladder (Thermo Scientific); +c: positive control (EcPV2- positive equine penile SCC); -c: negative control (PV-free equine skin DNA); ntc: no template control (sterile water).

### 2.3. *Immunohistochemical Staining Reveals Tumor Cell Plasticity in Equine HNSCC*

#### 2.3.1. Keratin (KRT)

Keratins (KRT) are a group of intermediate filament cytoskeletal proteins. Stratified epithelial KRTs can be classified as Type 1 (or low molecular weight; LMW) acidic, and type 2 (or high MW; HMW) basic KRTs [43,44]. EMT-driven changes in cellular morphology are based on cytoskeletal intermediate filament rearrangements mediated by modulated KRT expression [45]. Consequently, we first assessed EcPV2-positive and -negative equine HNSCCs for KRT expression using a pan-KRT antibody cocktail (AE1, AE3) confirmedly reacting with basic KRTs 1, 3, 4, 5, 6, and 8, and acidic KRTs 10, 14, 15, 16, and 19 according to the manufacturer (Cell Marque). All lesions scored positively to various extents, with KRT expression being confined to the cytoplasm, the physiological location of KRT intermediate filaments [44]. Various KRT staining intensities and patterns were noted, as exemplarily depicted in Figure 2. A pronouncedly central signal was observed in case of sections from four EcPV2-positive, and five EcPV2-negative HNSCCs (Table 2). Equine skin sections used as positive control exhibited intense KRT-labeling of mucosal epithelial cells. No signal was exhibited by the no-primary Ab control section (Figure 2).

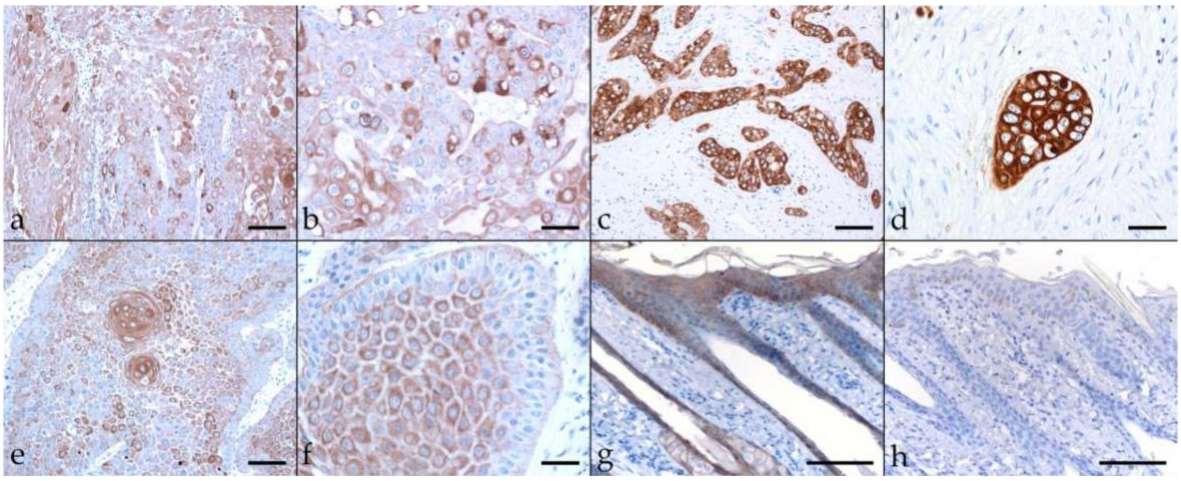


**Figure 2.** Cytokeratin labeling of EcPV2-positive and EcPV2-negative HNSCC sections. The figure depicts a representative selection of immunohistochemical staining results. a/b: Detection of KRTs in an EcPV2-positive, gingivopalatinal HNSCC (JON). Note the patchy distribution and varying intensity of KRT labeling, and the pronounced disorganization within the lesion. (**a**) Bar = 80 µm, (**b**) bar = 40 µm. c/d: diffuse, intensive KRT labeling of cell islets in an EcPV2-negative, palatinal squamous cell carcinoma (LUK). (**c**) Bar = 80 µm, (**d**) bar = 40 µm. (**e**,**f**): Mild to moderate KRT labeling in an EcPV2-positive, mandibular HNSCC (SIR) revealing the presence of keratin pearls (**e**), a typical feature of well differentiated SCCs, and signal intensity increasing from the basal to the squamous layers (**f**); (**e**) bar = 80 µm, (**f**) bar = 40 µm. (**g**): KRT labeling (positive control), and (**h**): mock labeling of equine skin (no-primary Ab control). Bars = 100 µm.

**Table 2.** Compiled β-catenin, vimentin, and keratin single-labeling results.

| HNSCC (n = 22) | | Keratin | | | | β-Catenin | | | Vimentin | | | |
|---|---|---|---|---|---|---|---|---|---|---|---|---|
| **Code** | **Tumor Analyzed** | **I** | **D** | **% +Cells** | **P** | **I** | **D** | **% +Cells** | **I** | **D** | **% +Cells** | **P** |
| *DAN* | *nasal* | 1–3 | *diffuse* | ≤100 | central+ | 3 | *diffuse* | ≤100 | 3 | *patchy* | <50 | |
| *MAL* | *nasal* | 2–3 | *diffuse* | ≤*100* | | 3 | *diffuse* | ≤*100* | 3 | *patchy* | <10 | |
| VAL | sinonasal | 3 | diffuse | ≤100 | | 1–2 | diffuse | ≤100 | 3 | patchy | <10 | |
| DIA | sinonasal | 1–2 | diffuse | ≤100 | central+ | 1 | patchy | >50 | 3 | patchy | <10 | |
| MMO | sinonasal | 2–3 | diffuse | ≤100 | | 2 | diffuse | ≤100 | 1–3 | patchy | <50 | |
| *PRI* | *sinonasal* | *3* | *diffuse* | ≤*100* | | *3* | *diffuse* | ≤*100* | *2–3* | *patchy* | *<50* | *marginal* |
| *HJA* | *sinonasal* | *1–3* | *diffuse* | ≤*100* | | *1–3* | *diffuse* | ≤*100* | *3* | *patchy* | *<10* | |
| *KLU* | *maxillary sinus* | *1–2* | *diffuse* | ≤*100* | | *1–3* | *patchy* | ≤*100* | *1–3* | *patchy* | *>50* | |
| FIL | maxillary sinus | 3 | diffuse | ≤100 | | 1 | diffuse | ≤100 | 3 | patchy | >50 | |
| PER | maxillary sinus | 2–3 | diffuse | ≤100 | central+ | 2–3 | diffuse | ≤100 | 2–3 | patchy | <50 | |
| SHM | sinus | 2–3 | diffuse | ≤100 | central+ | 3 | patchy | ≤100 | 3 | patchy | <50 | |
| MEC | mandibular | 2–3 | diffuse | ≤100 | central+ | 1–2 | patchy | >50 | 2–3 | patchy | <50 | |
| BLE | intermandibular | 2–3 | diffuse | ≤100 | central+ | 3 | diffuse | ≤100 | 3 | patchy | <10 | |
| *SHA* | *linguomandibular* | *3* | *diffuse* | ≤*100* | | *3* | *diffuse* | ≤*100* | *3* | *patchy* | *<10* | |
| BOM | lingual | 3 | diffuse | ≤100 | | 1 | diffuse | ≤100 | 3 | patchy | <10 | |
| *JON* | *gingivopalatal* | *1–3* | *diffuse* | ≤*100* | *central+* | *1* | *diffuse* | ≤*100* | *3* | *patchy* | *<10* | |
| LUK | palatal | 3 | diffuse | ≤100 | | 2 | diffuse | ≤100 | 3 | patchy | <50 | |
| *SIR* | *labiopalatal* | *1–2* | *diffuse* | ≤*100* | *central+* | *2* | *diffuse* | ≤*100* | *3* | *patchy* | *<10* | |
| KRA | oral | 2–3 | diffuse | ≤100 | | 1–2 | patchy | >50 | 3 | patchy | <10 | |
| *VLU* | *oral* | *1–2* | *diffuse* | ≤*100* | *central+* | *1* | *patchy* | *>50* | *1* | *patchy* | *<10* | |
| *SAM* | *laryngeal* | *3* | *diffuse* | ≤*100* | | *3* | *diffuse* | ≤*100* | *3* | *patchy* | *<10* | |
| *MCH* | *periocular* | *3* | *diffuse* | ≤*100* | | *1* | *diffuse* | ≤*100* | *3* | *patchy* | *<10* | |

I: intensity, D: distribution, and P: pattern of labeling; *Italics*: EcPV2-positive tumors.

### 2.3.2. β-Catenin

Epithelial cell adhesion is mediated by E-cadherin. It builds on the intracellular attachment to the actin cytoskeleton by interaction with catenins, including β-catenin. There is growing evidence that reduced assembly of membranous β-catenin in favor of nuclear expression of this protein is associated with human head-and-neck and equine SCC invasiveness and metastasis [39,40,46–48]. Hence, we also stained equine HNSCCs for β-catenin, revealing low-to-pronounced membranous expression in most tumor sections, with diffuse (16 tumors) predominating over patchy signal distribution (two EcPV2-positive and EcPV2- negative HNSCCs) (Table 2).

In some cases, β-catenin labeling was particularly intense within infiltration fronts of lesions. Cytoplasmic/nuclear β-catenin expression was only observed occasionally. Equine skin sections used as positive control exhibited β-catenin labeling whilst no-primary Ab control sections of equine skin scored negatively (Figure 3).

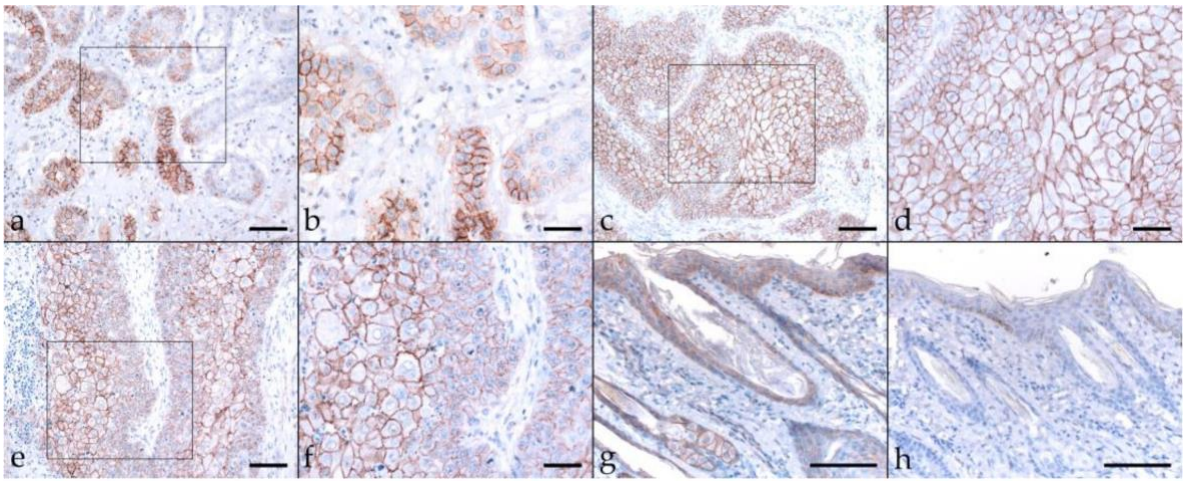


**Figure 3.** β-catenin labeling of EcPV2-positive and EcPV2-negative HNSCC sections. The figure depicts a representative selection of β-catenin labeling results. (**a**,**b**): patchy, strong membranous β-catenin labeling of >50% of tumor cells in an EcPV2-negative oral SCC (KRA). (**a**) Bar = 150 µm, (**b**) bar = 80 µm. (**c**,**d**): Strong, diffuse β-catenin labeling in an EcPV2-positive, pharyngeal SCC (SAM). (**c**) Bar = 150 µm, (**d**) bar = 80 µm. (**e**,**f**): Centrally focused β-catenin labeling pattern in an EcPV-positive, maxillary sinusoidal SCC (HJA). (**e**) Bar = 150 µm, (**f**) bar = 80 µm. (**g**,**h**): Positive and negative control, i.e., β-catenin labeled (**g**) and mock labeled ((**h**); no primary Ab) equine skin sections. Bars = 100 µm. Framed areas are presented at higher magnification.

### 2.3.3. Vimentin

EMT is inter alia characterized by loss of cell adhesion properties and acquisition of mesenchymal features via downregulation of E-cadherin. This allows EMT transcription factors to promote expression of mesenchymal proteins including vimentin that confer the ability on tumor cells to cross tissue barriers. Therefore, vimentin is considered as a reliable EMT marker [16,19,49]. Vimentin labeling yielded an intensive cytoplasmic signal in most cases. The signal exhibited a patchy distribution. Percentages of vimentin-positive cells greatly varied, ranging from <10% (eight $EcPV2^{+}$ and five $EcPV2^{-}$ tumors), and <50% (two $EcPV2^{+}$ and five $EcPV2^{-}$ tumors), to >50% ($EcPV2^{+}$ tumor KLU, and $EcPV2^{-}$ tumor FIL) (Table 2). The equine skin positive control exhibited vimentin labeling of mesenchymal cells. No-primary Ab equine skin sections scored consistently negative (Figure 4).

### 2.3.4. Cyclooxygenase-2 (COX-2)

The enzyme COX-2 is known to promote the development and progression of various cancers including HNSCCs via pleiotropic functions that also include the induction of EMT [50]. COX-2-staining of equine HNSCC sections revealed a cytoplasmic and/or membranous localization of the enzyme, with variable staining intensities observed in <10% to >50% of tumor cells. In two EcPV2-positive (VLU, KLU) and two EcPV2-negative HNSCCs (PER, VAL), COX-2-staining was most pronounced within tumorous infiltration fronts (Table 3). Equine skin sections that served as positive controls exhibited labeling of COX-2 antigen, whereas no signal was exhibited when omitting the primary Ab (Figure 5).

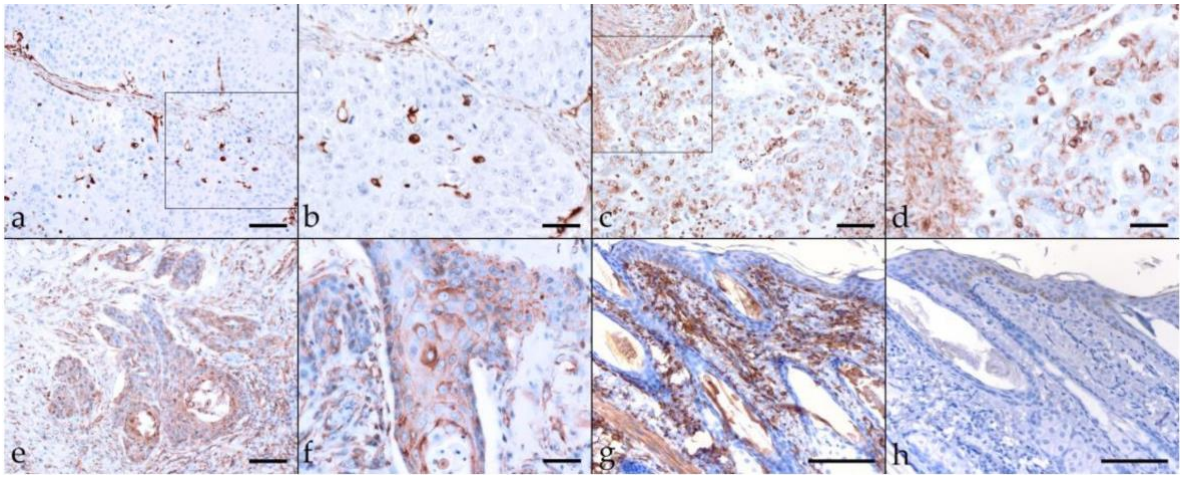


**Figure 4.** Vimentin staining of EcPV2-positive and EcPV2-negative HNSCC sections. The figure depicts a representative selection of vimentin labeling results. (**a**,**b**): Detection of vimentin in an EcPV2-positive maxillary sinusoidal SCC (HJA) in <10% of tumor cells, (**a**) bar = 80 µm, (**b**) bar = 40 µm. (**c**,**d**): Vimentin staining of <50% of tumor cells in an EcPV2-negative sinusoidal SCC (MMO), (**c**) bar = 80 µm, (**d**) bar = 40 µm. (**e**,**f**): Detection of vimentin in >50% of tumor cells in an EcPV2-negative maxillary sinusoidal SCC (FIL), (**e**) bar = 80 µm, (**f**) bar = 40 µm. (**g**,**h**): Vimentin (**g**) and mock labeling (**h**) of mesenchymal equine skin cells, bar = 100 µm. Framed areas are presented at higher magnification.

**Table 3.** Compiled COX-2, CD44, and CD271 single-labeling results.

| HNSCC (n = 22) | | COX-2 | | | CD44 | | | CD271 | | | |
|---|---|---|---|---|---|---|---|---|---|---|---|
| **Code** | **Tumor Analyzed** | **I** | **% +Cells** | **P** | **I** | **D** | **% +Cells** | **I** | **D** | **% +Cells** | **P** |
| *DAN* | *nasal* | *0–3* | *>50* | | *0–2* | *patchy* | *>50* | *1–2* | *diffuse* | *≤100* | |
| *MAL* | *nasal* | *0–3* | *<50* | | *0–1* | *patchy* | *<50* | *1–3* | *diffuse* | *≤100* | |
| VAL | sinonasal | 0–3 | <10 | marginal | 0–2 | patchy | <50 | 1 | diffuse | ≤100 | |
| DIA | sinonasal | 0–1 | <10 | | 0–2 | patchy | <50 | 0–1 | diffuse | >50 | |
| MMO | sinonasal | 0–3 | >50 | | 0–3 | patchy | >50 | 1 | diffuse | ≤100 | |
| *PRI* | *sinonasal* | *2–3* | *>50* | | *1–2* | *diffuse* | *na* | *0–2* | *diffuse* | *>50* | *central+* |
| *HJA* | *sinonasal* | *0–3* | *>50* | | *0–1* | *patchy* | *<50* | *1–2* | *diffuse* | *≤100* | |
| *KLU* | *maxillary sinus* | *0–3* | *<50* | *marginal* | *0–3* | *patchy* | *>50* | *1–2* | *patchy* | *≤100* | |
| FIL | maxillary sinus | 0–3 | <50 | | 0–2 | patchy | <50 | 1–2 | diffuse | ≤100 | |
| PER | maxillary sinus | 0–3 | <50 | marginal | 0–2 | patchy | >50 | 1–2 | diffuse | ≤100 | |
| SHM | sinus | 0–3 | >50 | | 1–3 | patchy | >50 | 1–3 | diffuse | ≤100 | |
| MEC | mandibular | 0–3 | <50 | | 0–3 | patchy | >50 | 0–1 | patchy | >50 | |
| BLE | intermandibular | 0–3 | <50 | | 1–2 | patchy | <50 | 1–2 | diffuse | ≤100 | |
| *SHA* | *linguomandibular* | *0–2* | *<50* | | *0–2* | *patchy* | *<50* | *1–2* | *diffuse* | *≤100* | |
| BOM | lingual | 0–1 | <10 | | 0–2 | patchy | >50 | 0–1 | patchy | >50 | |
| *JON* | *gingivopalatal* | *0–3* | *<50* | | *0–3* | *patchy* | *>50* | *1–2* | *diffuse* | *≤100* | |
| LUK | palatal | 0–3 | >50 | | 0–2 | patchy | >50 | 1–2 | diffuse | ≤100 | |
| *SIR* | *labiopalatal* | *0–3* | *<50* | | *0–2* | *patchy* | *>50* | *2–3* | *diffuse* | *≤100* | |
| KRA | oral | 0–3 | <50 | | 0–1 | patchy | <50 | 1 | diffuse | ≤100 | |
| *VLU* | *oral* | *0–3* | *<10* | *marginal* | *0–2* | *patchy* | *>50* | *1–2* | *diffuse* | *≤100* | *central+* |
| *SAM* | *laryngeal* | *0–3* | *>50* | | *1–3* | *patchy* | *<50* | *1–2* | *patchy* | *>50* | |
| *MCH* | *periocular* | *0–3* | *<50* | | *0–2* | *patchy* | *<10* | *1* | *diffuse* | *100* | |

I: intensity, D: distribution, and P: pattern of labeling; *Italics*: EcPV2-positive tumors.

2.3.5. CD44

CD44 is a transmembrane glycoprotein, which acts as a major hyaluronan (HA) receptor, and by this, mediates cell–cell and cell–ECM interactions. In many tumors, CD44 has been recognized as a CSC marker [51]. CD44-staining of EcPV2-positive and -negative equine HNSCCs yielded membranous signals of varying intensity, and a predominantly patchy distribution, with <50% to >50% of tumor cells scoring positive. Of note, 12 sections displayed an aberrant, cytoplasmic signal irrespective of the EcPV2 infection status. In some cases, staining was evident in the margins of tumor islets (Table 3). Basal equine salivary gland cells (positive control) scored CD44-positive, no-primary Ab sections tested negative (Figure 6).

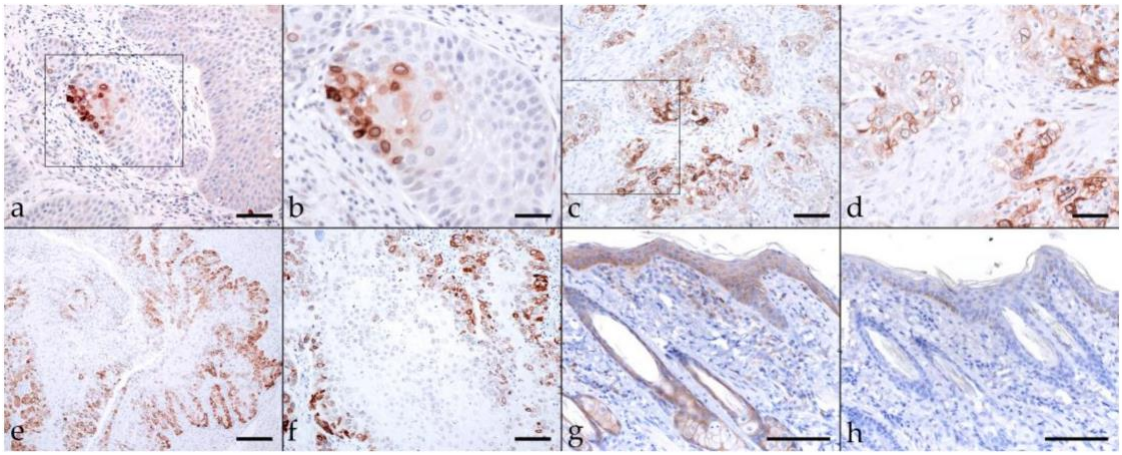


**Figure 5.** COX-2-staining of EcPV2-positive and EcPV2-negative HNSCC sections. The figure depicts a representative selection of COX-2 staining results. (**a**,**b**): Strong membranous and cytoplasmic COX-2 staining of <10% of tumor cells in an EcPV2-positive, mandibular SCC (SIR), (**a**) bar = 80 µm, (b) bar = 40 µm. (**c**,**d**): COX-2 staining of most tumor cells in an EcPV2-negative, sinusoidal SCC (MMO), (**c**) bar = 80 µm, (**d**) bar = 40 µm. (**e**,**f**): Pronounced COX-2-staining of cells within the infiltration front in an EcPV2-negative, maxillary sinusoidal SCC (PER), (**e**) bar = 150 µm, (**f**) bar = 80 µm. (**g**,**h**): Positive (**g**) and negative control (**h**) (equine skin ± primary Ab), bar = 100 µm. Framed areas are presented at higher magnification.

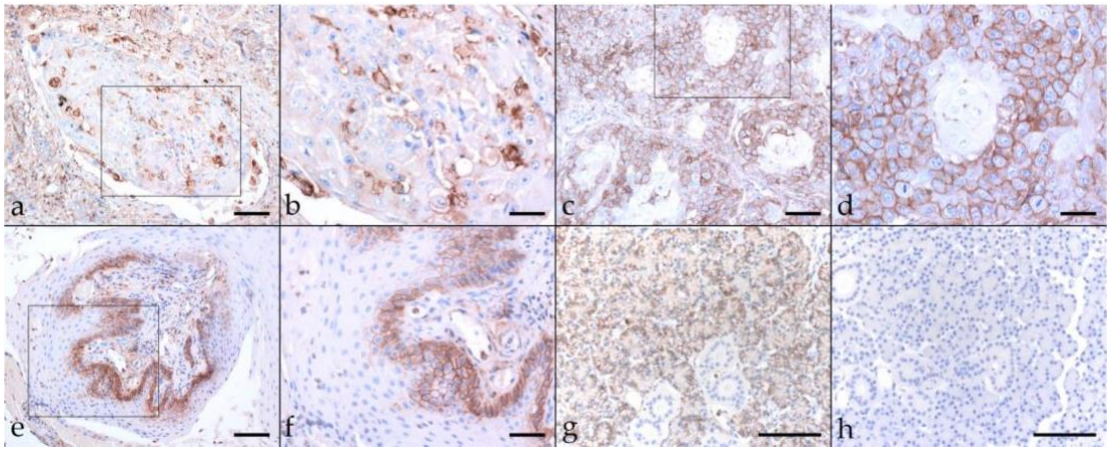


**Figure 6.** CD44-staining of EcPV2-positive and EcPV2-negative HNSCC sections. The figure depicts a representative selection of CD44-staining results. (**a**,**b**): patchy, cytoplasmic, and membranous CD44-staining in an EcPV2-negative, lingual SCC (BOM), (**a**) bar = 150 µm, (**b**) bar = 80 µm. (**c**,**d**): Patchy, membranous CD44-staining of >50% of tumor cells in an EcPV2-negative oral SCC (MEC), (**c**) bar = 150 µm, (**d**) bar = 80 µm. (**e**,**f**): Strong marginal CD44-staining pattern in an EcPV2- postive, pharyngeal SCC (SAM), (**e**) bar = 150 µm, (**f**) bar = 80 µm. (**g**,**h**): CD44- (**g**, positive control) and mock-staining (**h**, negative control) of an equine salivary gland section, bar = 100 µm. Framed areas are presented at higher magnification.

#### 2.3.6. CD271 ($p75^{NTR}$)

The nerve growth factor receptor known as CD271 (or $p75^{NTR}$) is a member of the tumor necrosis factor receptor (TNFR) superfamily. In recent years, CD271 has emerged as a promising marker for specific identification of CSC subpopulations in several types of human solid cancers including HN cancers [32,51]. In most tumor sections (17/22), CD271 labeling was mild to moderate, with a diffuse or patchy distribution.

Focally intense CD271 labeling was noted in tumor sections derived from two EcPV2-positive (MAL, SIR) horses and one EcPV2-negative (SHM) horse. Centrally accentuated CD271 labeling patterns were noted in two EcPV2-positive cases (PRI, VLU) (Table 3; Figure 7a–f). An equine SCC previously established as a positive control exhibited Ab-binding to the CD271 antigen (Figure 7g), whilst mock labeled sections scored negatively (Figure 7h).

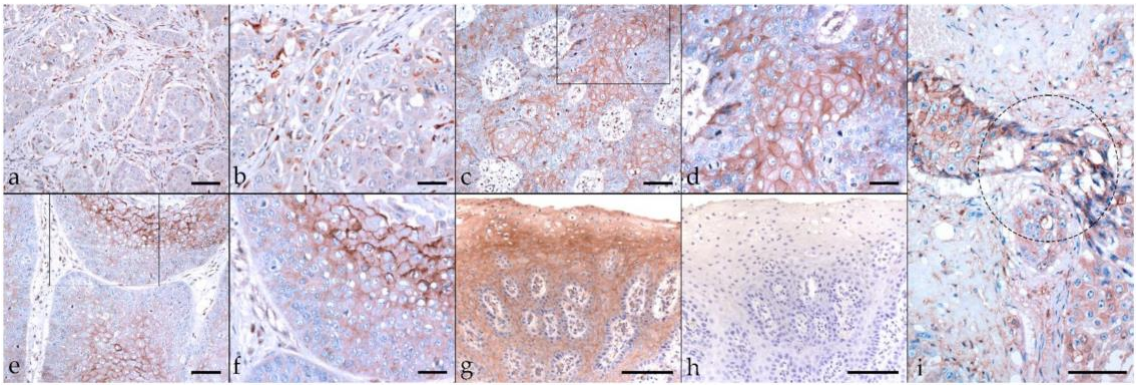


**Figure 7.** CD271 labeling of EcPV2-positive and EcPV2-negative HNSCC sections. The figure depicts a representative selection of CD271 labeling results. (**a,b**): Cytoplasmic CD271 labeling of only <10% of tumor cells in an EcPV2-negative, lingual SCC (BOM), (**a**) bar = 80 µm, (**b**) bar = 40 µm. (**c,d**): Mild to moderate, diffuse, membranous CD271 labeling in an EcPV2-positive, oral SCC (VLU). This horse has a history of penile SCC harboring the same genetic EcPV2 variant as the oral tumor, (**c**) bar = 80 µm, (**d**) bar = 40 µm. (**e,f**): Central CD271 labeling is likewise observed in sections of this oral SCC (VLU), (**e**) bar = 80 µm, (**f**) bar = 40 µm. (**g,h**): CD271 positive (**g**) and negative control (**h**) (equine SCC ± primary Ab), bar = 100 µm. Framed areas are presented at higher magnification. (**i**): EMT in a lingual SCC, as revealed by CD271-staining. Transition of tumor cells of typically polygonal epithelial phenotype into spindle-type cells (encircled area) within the infiltration front of an EcPV2-negative, metastasizing lingual SCC (BOM). Bar = 100 µm.

### *2.4. Immunofluorescent Double-Staining of HNSCCs for Keratins and Vimentin Reveals pEMT*

Single immunohistochemical analysis of EcPV2-positive and negative HNSCCs yielded KRT labeling in all lesions to different extents, with varying labeling intensities and pat- terns (Figure 2; Table 2). Vimentin labeling revealed variable amounts of positive cells that were patchily distribution in most cases (Table 2; Figure 4). To further analyze EMT by studying the localization of KRT and vimentin expression in more detail, we subjected EcPV2-positive and EcPV2-negative tumor sections to double IF staining for these molecules. KRT and vimentin co-expression was noted in all HNSCC sections examined. Signals localized at the infiltrative fronts of the tumors or were irregularly distributed. Representative KRT/vimentin double-staining results from EcPV2-positive (Figure 8a–d) and EcPV2-negative (Figure 8e–h) tumors are depicted in Figure 8.

### *2.5. Immunofluorescent Double-Staining of HNSCC Sections Reveals CD44$^+$ CD271$^+$ Tumor Cells*

In human HNSCCs, CSCs have been previously described as a CD44$^+$CD271$^+$ tumor cell subpopulation within the CD44$^+$ compartment [52]. Given that single CD44- and CD271 staining revealed the presence of variable amounts of positive cells in all tumor sections analyzed (Table 3), we finally screened HNSCC sections for CD44$^+$CD271$^+$ tumor cells in an IF double-staining approach. Signal co-localization was observed with variable intensity in virtually all EcPV2-positive and -negative tumors. In some cases, CD44$^+$CD271$^+$ cells were predominantly detected within tumor margins representing infiltrative tumor fronts. In other cases, the CD44$^+$CD271$^+$ staining patterns were less organized, irrespective of tumor differentiation. Representative results are depicted in Figure 9.

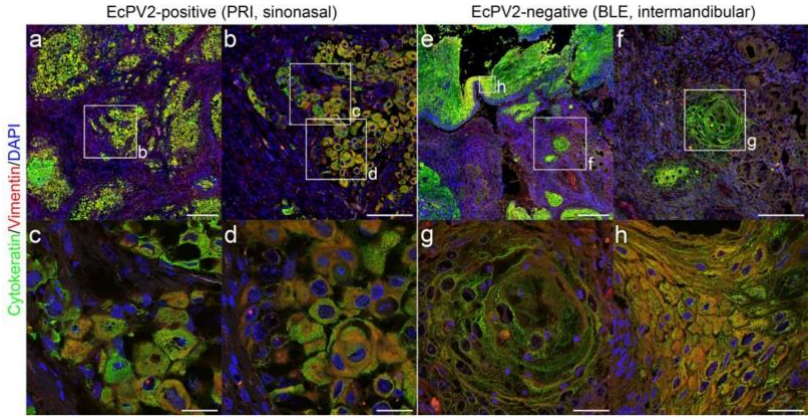


**Figure 8.** IF double-staining reveals KRT$^+$ vimentin$^+$ tumor cells consistent with pEMT. Overview: (**a**,**e**), 20× magnification: (**b**,**f**), and 63× magnification: (**c**,**d**,**g**,**h**) images of representative HNSCC sections (PRI, EcPV2-positive, sinonasal SCC: top panels, respectively; BLE, EcPV2-negative inter- mandibular SCC: bottom panels, respectively). Framed areas (**c**,**d**,**g**,**h**) depict representative sites of EMT and pEMT shown enlarged in the lower row. Immunofluorescent staining revealed cytoplasmic labeling of KRT (green) and vimentin (red). Note the yellow–orange double-positive cells represent- ing mesenchymal transdifferentiated epithelial cells (pEMT). Nuclei were visualized by DAPI (blue). Scale bar = 250 µm (**a**,**e**), 100 µm (**b**,**f**), 25 µm (**c**,**d**,**g**,**h**).

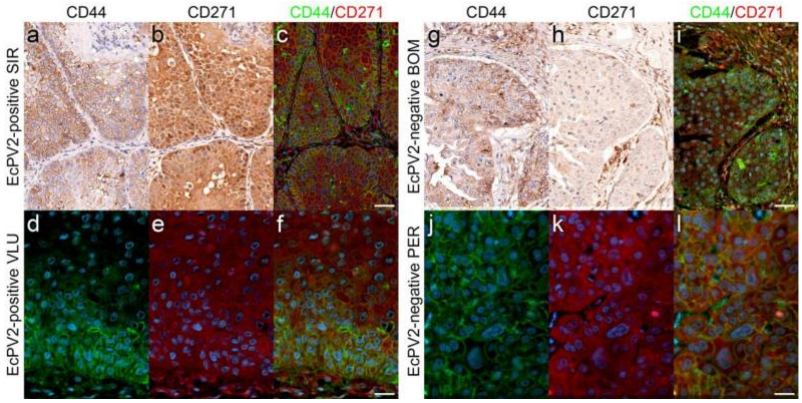


**Figure 9.** IF double-staining revealed CD44$^+$CD271$^+$ tumor cell subsets. Top: Sections of EcPV2- positive (SIR, VLU; left panels) and EcPV2-negative (BOM, PER; right panels) HNSCCs were comparatively assessed for single expression of CD44 (**a**,**g**) and CD271 (**b**,**h**) by IHC, and double expression of these stem-cell markers (**c**,**i**) by IF. IHC-staining revealed confinement of CD44 expression to the cell surface (**a**,**g**), whilst CD271 expression was cytoplasmic (**b**,**h**), with varying signal intensities and distributions. High CD44 and CD271 expression within tumor margins was observed for sections of the EcPV2-positive HNSCC (SIR) (**a**–**c**) in contrast to diffuse, mild to moderate expression in the EcPV2-negative tumor (**g**–**i**). Bottom: IF single staining for CD44 (**d**,**j**) and CD271 (**e**,**k**) and double-staining for both stem-cell markers (**f**,**l**) revealed a subset of CD44$^+$CD271$^+$ tumor cell sub- populations. Whereas double staining was most pronounced within the infiltration front in an EcPV2-positive HNSCC (VLU; (**d**–**f**)), the double-signal distribution seemed to be more disorganized in the EcPV2-negative lesion (PER; (**j**–**l**)). Diaminobenzidine chromogen was used for IHC staining, and hematoxylin counterstaining was performed to visualize cell nuclei. In the IF-based experiment, CD44-Alexa 488 produced a green, and CD271-Alexa 568 a red signal. Nuclei were visualized by DAPI (blue). Scale bar = 50 µm (top panels); scale bar = 20 µm (bottom panels).

## 3. Discussion

In humans, HNSCC constitutes a potentially lethal disease. However, early diagnosis and treatment of HNSCC precursor lesions such as plaques or papillomas can help prevent the development of late-stage lesions and metastasis [53]. In horses and other equids, benign SCC precursor lesions usually remain unnoticed when affecting the HN region.

Owners commonly consult a veterinarian when noticing ingestion problems, head deformity, nasal discharge, weight loss, or ataxia. This leads to disease being diagnosed when precursor lesions have already progressed to large tumor masses invading adjacent tissue and bone, and impairing physiological functions [54]. At this stage, euthanasia usually represents the only ethically justifiable escape strategy [54–56]. In cases where disease is accidently detected at an earlier stage, e.g., during routine dental examination, the therapeutic repertoire is still very limited, with surgical tumor excision constituting the most common approach [55]. The considerable lack of therapeutic alternatives is due to the location of the tumor within the complex, highly innervated, and interrelated compartments of the HN region [57], and the poor understanding of the mechanisms underlying HNSCC development and progression in the horse.

To help pave the way towards a better understanding of the pathobiology of equine HNSCC, we first screened 49 tumors with confirmed diagnosis of HNSCC for the presence of equine papillomavirus infection. We opted to target EcPV2, EcPV3, and EcPV5, as these EcPV types have already been reported in association with muco-cutaneous lesions [9]. Notably EcPV2 DNA and transcripts were previously detected in HNSCCs by several groups [12,13,40,58,59]. In agreement with these findings, EcPV2 PCR yielded amplicons of expected size in 22% (11/49) of cases, whilst EcPV3 and EcPV5 PCRs scored consistently negative. Despite the still limited number of equine HNSCCs tested for EcPV2 infection so far, the herein-reported EcPV2 detection rate of 22% suggests that similar proportions of equine and human HNSCCs are PV-related [1]. Together with the previously reported finding of EcPV2 infection in <10% of apparently healthy equids [9,13,60,61], detection of EcPV2 DNA in a subset of HNSCCs points to a causal association of viral infection with these tumors. In-depth in vitro and ex vivo studies are beginning to help to clarify this issue.

Recently, Armando et al. reported on the detection of EcPV2 DNA from a laryngeal SCC affecting an elderly Maremmano mare. The group provided evidence of viral E6 oncogene transcription, indicating that EcPV2 was actively involved in neoplastic cell transformation, and by this, in disease progression [40]. In addition, this group was the first to address intralesional EMT in an equine case of HNSCC. The reported cadherin switch, and expression of EMT-associated transcription factors TWIST-1, ZEB-1, and HIF- 1α were highly indicative for EMT events in the tumor, possibly explaining the metastatic behavior [40]. In the herein-presented study, we assessed 11 EcPV2-positive and 11 EcPV2- negative tumors with confirmed diagnosis of (metastasizing) HNSCCs for expression of selected EMT and CSC markers using IHC and IF.

Intratumoral presence of the epithelial tumor cell phenotype was assessed by immunohistological staining for keratins (KRTs) and β-catenin. All tumor sections scored consistently positive for KRT expression, with up to 100% of tumor cells displaying a cytoplasmic signal. In many lesions, KRT-staining patterns reflected the high degree of tissue disorganization, as recently described for EcPV2-positive equine penile SCCs and three- dimensional rafts established therefrom [62]. Over 50 to 100% of tumors cells also scored positive for β-catenin expression that was predominantly confined to the cell membrane irrespective of the EcPV2 infection status. This finding contrasts with other reports describing translocation of β-catenin expression to the nucleus in human and equine HNSCC cells [40,46,47,63]. Nuclear translocation results in β-catenin acquiring tumor-promoting properties by activating the expression of various oncogenes such as fibronectin, cyclin D1, or c-myc, leading to deregulation of cell-cycle progression [47,64]. Interestingly, nuclear β-catenin translocation is particularly observed in hrHPV-induced carcinomas. There are indications that membranous β-catenin expression in favor of nuclear expression of the protein is mediated by overexpressed E6 and E7 [47]. On these grounds, it may be speculated that E6 and E7 expression levels in EcPV2-positive equine HNSCCs were too low to allow for interference with β-catenin expression.

EMT is characterized by the so-called cadherin switch, i.e., downregulation of E- cadherin and upregulation of N-cadherin. Loss of E-cadherin entails the loss of epithelial KRTs, and expression of the

mesenchymal protein vimentin, providing the tumor cells with migratory properties [16,19]. In the equine HNSCCs analyzed, vimentin was expressed by tumor cells to a various extent in 100% of lesions, irrespective of the precise tumor location and the EcPV2 infection status. This finding agrees with the histopathological classification of all tumors as late-stage lesions, with metastasis confirmed in 10/22 lesions subjected to expression analyses. Overall, vimentin-staining revealed a patchy distribution within tumor islets. Pronounced confinement of vimentin expression to neoplastic cells of the infiltration front was observed in a single EcPV2-positive case. This contrasts with reported occasional expression of vimentin only in the infiltratively growing portion of EcPV2 associated penile SCCs [39]. To further characterize EcPV2-positive and –negative HNSCCs with respect to the localization of KRT and vimentin expression, we analyzed tumor sections by IF KRT/vimentin double-staining and generated high-resolution images. The latter provided robust evidence of $KRT^+vimentin^+$ tumor cells in all lesions that very likely represent E/M hybrid cells that had undergone pEMT. This finding agrees with the concept that epithelial tumor cells do not complete EMT in vivo, but rather remain in a pEMT state in human patients [24]. This state is characterized by simultaneous expression of epithelial- and mesenchymal-type proteins providing E/M hybrid cells with the abilities to attach and migrate, and hence, to migrate collectively [24,25]. The observation that equine HNSCC cells had undergone pEMT rather than complete EMT also provides a sound explanation for the predominantly membranous expression of β-catenin by tumor cells.

COX-2 is a cyclooxygenase isoform that acts as inflammatory enzyme in chronic inflammation. Importantly, there is substantial evidence that COX-2 overexpression orchestrates EMT via creation of an inflammatory tumor microenvironment [65]. In equine HNSCC, COX-2 expression was consistently detected, with <10 up to >50% of tumor cells staining positive. Although statistically not significant at $p < 0.1$, there was a tendency of EcPV2-positive HNSCCs harboring more COX-2 positive tumor cells than their EcPV2- negative counterparts. This observation is in accordance with the finding of HPV type 16 E6 and E7 oncoproteins promoting COX-2 overexpression [66].

EMT is also associated with a second program promoting the transition of epithelial- type tumor cells to CSCs. The latter are characterized by MDR, and also known as tumor-initiating cells (TICs) due to their intrinsic ability to form tumors in vivo, and promote tumor growth, recurrence, and metastasis [67]. In human HNSCCs, the presence of CSCs is well-documented, and their frequency positively correlates with severity of disease [51,52,68,69]. In horses and other equids, no information is available on CSCs in any tumor disease. This substantial lack of knowledge prompted us to put a special focus on the detection of CSCs in equine HNSCC.

Since the discovery of CSCs, CD44 has evolved as useful marker for detection and isolation of this particular tumor cell subset [51]. CD44 labeling of equine HNSCC sections revealed the presence of $CD44^+$ tumor cells in 100% of tumors analyzed, with positive tumor cells ranging between >10 and >50%. A lower percentage was only determined for a periocular tumor. Of note, CD44 is also expressed by a wide range of immune cells that reside in HNSCCs as infiltrates and are also part of the tumor stroma [51]. This fact was kept in mind when assessing the numbers of $CD44^+$ tumor cells.

In the past two decades, another surface molecule, i.e., CD271, has been identified as potent CSC marker in human melanoma [70] and HNSCC [71–73]. Labeling of equine HNSCCs revealed CD271 expression in up to 100% of tumor cells. This finding is not completely surprising, since CD271 is also expressed by undifferentiated cells in normal epithelium [51]. It can be speculated, that both undifferentiated tumor cells and CSCs may express CD271 in equine HNSCC. Since the specificity of all antibodies was evaluated prior to this study, high CD271 labeling due to unspecific binding appears rather unlikely.

Combined use of CD44 and CD271 markers in HNSCC research recently led to the identification of CSCs as a $CD271^+$ subpopulation within the $CD44^+$ tumor cell compartment [51,52,68,69]. Based on this intriguing discovery, we subjected equine HNSCC section to immunofluorescent CD44/CD271 double staining, revealing the intralesional presence of $CD44^+CD271^+$ tumor cells in all tumors analyzed.

This finding provides the first evidence of CSCs in high-grade equine SCCs affecting different parts of the HN region.

When comparing EMT and CSC marker expression intensities and rates in EcPV2- positive versus -negative equine HNSCCs, no significant differences attributable to presence or absence of EcPV2 infection were noted. This was somewhat disappointing as we expected to disclose some distinctive features, e.g., in relation to nuclear translocation of β-catenin in EcPV2-positive tumors, as described for hrHPV-induced versus -unrelated HNSCCs [47] or CSC percentages. Sole inclusion of late-stage equine HNSCCs in the study may represent a limiting factor, since differences regarding (p)EMT/CSC-induced malignant progression of EcPV2-related versus -unrelated lesions may be particularly encountered in premalignant HNSCC precursor lesions. Such differences, if existent, would determine the fate of these lesions. In addition, comparison of tumors affecting the same location within the HN region would certainly help obtain a more concise picture. More in-depth research is needed to elucidate the pathobiological role of EcPV2 in equine HNSCCs and related precursor lesions, with particular focus on the impact of E6 and E7 oncoprotein expression on (p)EMT-mediated tumor cell plasticity.

To conclude, this study provides evidence of (p)EMT constituting a common event in partly metastasizing equine EcPV2-positive and -unrelated HNSCCs, with epithelial tumor cells adopting an E/M hybrid or CSC phenotype. The observed phenotype switching em- phasizes the high tumor cell plasticity in equine HNSCC and provides a sound explanation for the malignancy and potential metastatic behavior of the disease.

## 4. Method

### *4.1. Sample Material*

A total of 49 histopathologically confirmed equine HNSCC were included in the study. Archival, formalin-fixed paraffin-embedded (FFPE) tumor material was available in 49/49, native tumor material and whole DNA extracted therefrom in 16/49 cases. All tumor samples were collected at the Veterinary University of Vienna, Austria, during therapeutic surgical excisions or during requested necropsies with the owners' written consent. Patient, disease, and sample specifications are provided in Table 1.

### *4.2. DNA Extraction*

DNA aliquots from 15/16 native tumor samples were already available [13]. The one additional native sample (VLU) was subjected to DNA extraction using a DNeasy Blood & Tissue Kit (Qiagen, Hilden, Germany) according to instructions of manufacturer. Obtained DNA was stored at - 20°C until use.

To prepare FFPE samples for DNA isolation, 10-µm tissue sections were deparaffinized according to an established protocol [74]. In brief, sections were vortexed with 1 mL xylene (Merck, Darmstadt, Germany) and incubated at room temperature for 5 min. Following a centrifugation step at 13,000 x g for 5 min, supernatants were discarded, and the procedure was repeated. Then, resulting pellets were vortexed in 1 mL 96% ethanol each (Merck, Darmstadt, Germany) and centrifuged at 13,000 x g for 5 min. Supernatants were discarded and the washing procedure was repeated. In a final step, ethanol was removed, and pellets were dried under vacuum using a desiccator for up to 1.5 h. Subsequently, pellets were subjected to DNA extraction as described above.

### *4.3. EcPV PCR*

Following assessment of DNA concentrations per photometry, equine β-actin PCR was performed to test all DNA isolates for PCR compatible quality. Reactions were carried out as described previously [75], with the only difference that the published forward primer was combined with reverse primer 3 β-actin-683 (5 - gccatctcttgctcgaagtccagg-3 ) for generation of a shorter amplification product (208 bp) to assure successful amplification also from FFPE-derived template DNA. Given that β-actin PCR scored positive for all DNA isolates, the latter were subsequently assessed for the presence of EcPV types 2,

3, and 5 using type-specific PCR. The primer pairs used for amplification of a 173 to 270 bp region within the respective E6 or E7 open reading frames were the following: 5 and 3 EcPV2 E7 (5 -ggatcctgcagcaactgc-3 ; 5 -atcactatcacagtcgctacacagc-3 ; product size: 173 bp), 5 and 3 EcPV3 E6 (5 -ctgttgaagctcgctactgagtcac-3 ; 5 -gtctccactgcttctccctaaactc; product size: 270 bp), and 5 and 3 EcPV5 E6 (5 -cgctacagcggggacgac-3 ; 5 -ggaggtgagcagtgacgaagag-3 ; product size: 257 bp). Reactions were conducted with Thermo Scientific™ Phusion Hot Start II DNA-Polymerase (Fisher Scientific GmbH, Schwerte, Germany), or PCRBIO HS VeriFi™ Polymerase (PCR Biosystems Ltd., London, UK) according to instructions of the manufacturer. The amplification program consisted of an initial denaturation step at 95 ˚C for 5 min, followed by 40 cycles (95 ˚C for 15 sec, 67 ˚C for 30 sec, 72 ˚C for 45 sec), and a final elongation step at 72 ˚C for 5 min. Amplification products (16 µL) were subjected to gel-electrophoresis using 2%TAE agarose gels, and visualized by ethidium staining.

Every PCR reaction included a positive (EcPV type 2-, 3- or 5-positive equine DNA), a negative (PV-free equine DNA), and a no-template control (ntc; sterile water).

### *4.4. Histopathological Examination*

We matched 11 EcPV2-positive HNSCC with 11 EcPV2-negative HNSCC according to the grade of differentiation, the anatomical tumor location, and, as far as possible, the patient's age. Hematoxylin- and eosin-stained (HE) sections of FFPE tissue material of selected cases were histopathologically re-examined for verification of sample matching. To characterize the degree of histological differentiation, archived FFPE tissue from necropsies and biopsies were evaluated with respect to tumor cell morphology and grade of cornification.

### *4.5. Immunohistochemical Staining (IHC)*

In a first step, fresh 2.5 µm-sections of 11 EcPV2-positive and 11 EcPV2-negative tumor FFPE samples were assessed by a single labeling approach for expression of keratins (KRT), β-catenin, vimentin, COX-2, CD271 ($p75^{NTR}$), and CD44. To this end, sections were deparaffinized with xylene, and successively dehydrated in 100%, 96%, and 70% ethanol. Then, sections were treated with 0.3% $H_2O_2$/methanol to block peroxidase activity. Heat-induced epitope retrieval (HIER) was performed in 0.1 M citrate buffer (pH 6) or TRIS-EDTA (pH 9; Table 2) for 30 min in a steamer at 94–100 ˚C. To minimize unspecific binding, slides were blocked with 1.5% normal goat serum. Incubation with primary antibody (Ab; for Ab specifications see Table 4) was conducted at 4 ˚C overnight. After washing with phosphate-buffered saline (PBS), sections were incubated with secondary horseradish per- oxidase (HRP)-conjugated Ab (Table 4) for 30 min at room temperature. Ab-bound protein was visualized with diaminobenzidine (DAB) chromogen. Hematoxylin (HE) was used for nuclear counterstaining. Evaluation of signals was semiquantitatively performed by blinded investigator AK using an Olympus BX45 light microscope. The following staining characteristics were assessed: (i) intracytoplasmic versus membranous immunostaining; (ii) DAB signaling intensity that was classified as absent (negative), mild, moderate, or strong.; (iii) the labeling pattern, i.e., diffuse labeling of all tumor cell layers, patchy labeling with irregular distribution, and special labeling patterns in the center of tumor islets or the infiltrative front; and (iv) estimated percentage of positive tumor cells (<10%, <50%, and >50%). For evaluation of larger tissue samples, five highly representative fields were selected in 100x magnification. Images were captured using an Olympus BX51 microscope equipped with an Olympus camera UC90 (Olympus, Vienna, Austria). High-resolution images were captured using a Zeiss LSM880 Airyscan confocal microscope (Carl Zeiss AG, Jena, Germany).

**Table 4.** Antibody and pretreatment specifications.

| Host | Type | Clone | Target Protein | Provider | Dilution | HIER |
|---|---|---|---|---|---|---|
| **IHC (single staining)** | | | | | | |
| **Primary Abs** | | | | | | |
| Mouse | Monoclonal | AE1 | LMW keratins | Cell Marque, Sigma-Aldrich, Vienna, Austria | 1:650 | pH 9 |
| Mouse | Monoclonal | AE3 | HMW keratins | Cell Marque, Sigma-Aldrich, Vienna, Austria | 1:650 | pH 9 |
| Mouse | Monoclonal | 9G2 | Beta-catenin | Acris Antibodies, Herford, Germany | 1:500 | pH 9 |
| Mouse | Monoclonal | V9 | Vimentin | Dako, Hamburg, Germany | 1:500 | pH 6 |
| Rabbit | Recombinant | EPR3208 | CD146 | Abcam, Cambridge, UK | 1:500 | pH 6 |
| Rabbit | Monoclonal | SP21 | COX2 | Thermo Fisher Scientific, Vienna, Austria | 1:400 | pH 6 |
| Rat | Monoclonal | IM7 | CD44 | Santa Cruz Biotechnology, Dallas, Texas, USA | 1:200 | pH 6 |
| Rabbit | Monoclonal | D4B3 | CD271 (p75NTR) | Cell Signaling Technology, Frankfurt, Germany | 1:1000 | pH 9 |
| **Secondary Abs** | | | | | | |
| BrightVision Poly-HRP anti-mouse Ab | | | | ImmunoLogic, Duiven, The Netherlands | | |
| BrightVision Poly-HRP anti-rabbit Ab | | | | ImmunoLogic, Duiven, The Netherlands | | |
| Goat anti-rat HRP conjugated | | | | Abcam, Cambridge, UK | | |
| **IF (double staining)** | | | | | | |
| **Primary Abs** | | | | | | |
| Mouse | Monoclonal | AE1 | LMW keratins | Cell Marque, Sigma-Aldrich, Vienna, Austria | 1:400 | pH 9 |
| Mouse | Monoclonal | AE3 | HMW keratins | Cell Marque, Sigma-Aldrich, Vienna, Austria | 1:400 | pH 9 |
| Rabbit | Polyclonal | | Vimentin | Sigma Prestige, Merck, Vienna, Austria | 1:500 | pH 9 |
| Rat | Monoclonal | IM7 | CD44 | Santa Cruz Biotechnology, Dallas, Texas, USA | 1:500 | pH 9 |
| Rabbit | Monoclonal | D4B3 | CD271 ($p75^{NTR}$) | Cell Signaling Technology, Frankfurt, Germany | 1:250 | pH 9 |
| **Secondary Abs** | | | | | | |
| Donkey anti-mouse Ab A488 1:800 | | | | Jackson ImmunoResearch Europe, LTD, Ely, UK | | |
| Donkey anti-rabbit Ab A568 1:400 | | | | Invitrogen, Thermo Fisher Scientific, Vienna, Austria | | |
| Goat anti-rat Ab A488 1:800 | | | | Invitrogen, Thermo Fisher Scientific, Vienna, Austria | | |
| Goat anti-rabbit Ab A568 1:1500 | | | | Invitrogen, Thermo Fisher Scientific, Vienna, Austria | | |

### *4.6. Immunofluorescent Staining (IF)*

In a second step, sections were subjected to KRT/vimentin and CD44/CD271 double immunofluorescent (IF) staining. Sections were rehydrated and pretreated with TRIS-EDTA- buffer at pH9 for 30 min in the steamer for epitope retrieval as described above. Following blocking with goat serum, sections were incubated with mixtures of primary anti-KRT and anti-vimentin, or anti-CD44 and anti-CD271 Abs (Table 4). Alexa Fluor®(Thermo Fisher Scientific, Vienna, Austria) 488 (green signal) and 568 (red signal) conjugated Abs were used as secondary Abs (Table 4). Following incubation with 4 , 6-diamidino-2-phenylindole (DAPI) for nuclear counterstaining and rinsing with water, slides were mounted with Aqua-PolyMount (Polysciences, Szabo-Scandic, Vienna, Austria) and digitized using a Panoramic Scan II Slide scanner (3DHistech, Budapest, Hungary).

### *4.7. Statistical Analyses*

The significance of differences between respective labeling intensities and % positive cells in EcPV2-positive versus -negative HNSCC sections were assessed by the Mann–Whitney U test (https://www.socscistatistics.com/tests/mannwhitney/; accessed on 10 February 2022). Statistical significance was set at $p < 0.1$.

**Author Contributions:** Conceptualization, S.K. (Sibylle Kneissl), C.S. and S.B.; methodology, C.W.-L., I.W., S.K. (Stefan Kummer) and S.B.; formal analysis, C.S., A.K., C.J., T.R. and S.K. (Stefan Kummer); investigation, C.S., A.K., C.W.-L., S.K. (Stefan Kummer) and C.J.; resources, I.W., S.B.; data cura- tion, A.K., C.S., I.W., S.K. (Stefan Kummer), T.R. and S.B.; writing—original draft preparation, S.B., A.K. and C.S.; writing—review and editing, all authors; visualization, A.K., S.K. (Stefan Kummer), T.R.; supervision, S.B., S.K. (Sibylle Kneissl) and I.W.; project administration, C.J., S.B. and S.K. (Sibylle Kneissl); funding acquisition, S.K. (Sibylle Kneissl). All authors have read and agreed to the published version of the manuscript.

**Funding:** This research was funded by the Clinical Unit of Diagnostic Imaging, University of Veterinary Medicine, Vienna, Austria.

**Institutional Review Board Statement:** Not applicable.

**Informed Consent Statement:** Not applicable.

**Data Availability Statement:** All data are presented in this article.

**Acknowledgments:** We wish to thank Nora Nedorost for her valuable technical assistance, Klaus Bittermann for excellent photographic work and Eberhard Ludewig for financing this project. This research was also supported using resources of the VetCore Facility (VetImaging|VetBioBank) of the University of Veterinary Medicine, Vienna, Austria. Open Access Funding by the University of Veterinary Medicine Vienna.

**Conflicts of Interest:** The authors declare no conflict of interest.

## References

1. Dayyani, F.; Etzel, C.J.; Liu, M.; Ho, C.H.; Lippman, S.M.; Tsao, A.S. Meta-analysis of the impact of human papillomavirus (HPV) on cancer risk and overall survival in head and neck squamous cell carcinomas (HNSCC). Head Neck Oncol. 2010, 2, 15. [CrossRef]
2. Gissmann, L. Linking human papillomaviruses to cervical cancer: A long and winding road. In Papillomavirus Research: From Natural History to Vaccines and Beyond; Campo, M.S., Ed.; Caister Academic Press: Wymondham, UK, 2006; pp. 3–9.
3. Ashrafi, G.H.; Brown, D.R.; Fife, K.H.; Campo, M.S. Down-regulation of MHC class I is a property common to papillomavirus E5 proteins. Virus Res. 2006, 120, 208–211. [CrossRef]
4. Pullos, A.N.; Castilho, R.M.; Squarize, C.H. HPV Infection of the Head and Neck Region and Its Stem Cells. J. Dent. Res. 2015, 94, 1532–1543. [CrossRef]
5. Secretan, B.; Straif, K.; Baan, R.; Grosse, Y.; El Ghissassi, F.; Bouvard, V.; Benbrahim-Tallaa, L.; Guha, N.; Freeman, C.; Galichet, L.; et al. A review of human carcinogens—Part E: Tobacco, areca nut, alcohol, coal smoke, and salted fish. *Lancet Oncol.* **2009**, *10*, 1033–1034. [CrossRef]
6. Kikuchi, K.; Inoue, H.; Miyazaki, Y.; Ide, F.; Kojima, M.; Kusama, K. Epstein-Barr virus (EBV)-associated epithelial and non- epithelial lesions of the oral cavity. *Jpn. Dent. Sci. Rev.* **2017**, *53*, 95–109. [CrossRef]
7. Fleming, J.C.; Woo, J.; Moutasim, K.; Mellone, M.; Frampton, S.J.; Mead, A.; Ahmed, W.; Wood, O.; Robinson, H.; Ward, M.; et al. HPV, tumour metabolism and novel target identification in head and neck squamous cell carcinoma. *Br. J. Cancer* **2019**, *120*, 356–367. [CrossRef]
8. Scott, D.W.; Miller, W.H., Jr. Squamous cell carcinoma. In *Equine Dermatology*, 2nd ed.; Scott, D.W., Miller, W.H., Jr., Eds.; Saunders Elsevier: St. Louis, MO, USA, 2011; pp. 473–476.
9. Sykora, S.; Brandt, S. Papillomavirus infection and squamous cell carcinoma in horses. *Vet. J.* **2017**, *223*, 48–54. [CrossRef]
10. Scase, T.; Brandt, S.; Kainzbauer, C.; Sykora, S.; Bijmholt, S.; Hughes, K.; Sharpe, S.; Foote, A. *Equus caballus* papillomavirus-2 (EcPV-2): An infectious cause for equine genital cancer? *Equine Vet. J.* **2010**, *42*, 738–745. [CrossRef]
11. Lassaline, M.; Cranford, T.L.; Latimer, C.A.; Bellone, R.R. Limbal squamous cell carcinoma in Haflinger horses. *Vet. Ophthalmol.* **2015**, *18*, 404–408. [CrossRef]
12. Knight, C.G.; Dunowska, M.; Munday, J.S.; Peters-Kennedy, J.; Rosa, B.V. Comparison of the levels of *Equus caballus* papillomavirus type 2 (EcPV-2) DNA in equine squamous cell carcinomas and non-cancerous tissues using quantitative PCR. *Vet. Microbiol.* **2013**, *166*, 257–262. [CrossRef]
13. Sykora, S.; Jindra, C.; Hofer, M.; Steinborn, R.; Brandt, S. Equine papillomavirus type 2: An equine equivalent to human papillomavirus 16? *Vet. J.* **2017**, *225*, 3–8. [CrossRef] [PubMed]
14. Yuan, S.; Norgard, R.J.; Stanger, B.Z. Cellular Plasticity in Cancer. *Cancer Discov.* **2019**, *9*, 837–851. [CrossRef]
15. Baum, B.; Settleman, J.; Quinlan, M.P. Transitions between epithelial and mesenchymal states in development and disease. *Semin. Cell Dev. Biol.* **2008**, *19*, 294–308. [CrossRef]
16. Yang, J.; Weinberg, R.A. Epithelial-mesenchymal transition: At the crossroads of development and tumor metastasis. *Dev. Cell* **2008**, *14*, 818–829. [CrossRef]
17. Greenburg, G.; Hay, E.D. Epithelia suspended in collagen gels can lose polarity and express characteristics of migrating mesenchymal cells. *J. Cell Biol.* **1982**, *95*, 333–339. [CrossRef]

18. Greenburg, G.; Hay, E.D. Cytodifferentiation and tissue phenotype change during transformation of embryonic lens epithelium to mesenchyme-like cells in vitro. *Dev. Biol.* **1986**, *115*, 363–379. [CrossRef]
19. Thiery, J.P.; Acloque, H.; Huang, R.Y.; Nieto, M.A. Epithelial-mesenchymal transitions in development and disease. *Cell* **2009**, *139*, 871–890. [CrossRef]
20. Chen, C.; Wei, Y.; Hummel, M.; Hoffmann, T.K.; Gross, M.; Kaufmann, A.M.; Albers, A.E. Evidence for epithelial-mesenchymal transition in cancer stem cells of head and neck squamous cell carcinoma. *PLoS ONE* **2011**, *6*, e16466. [CrossRef]
21. Chen, C.; Zimmermann, M.; Tinhofer, I.; Kaufmann, A.M.; Albers, A.E. Epithelial-to-mesenchymal transition and cancer stem(-like) cells in head and neck squamous cell carcinoma. *Cancer Lett.* **2013**, *338*, 47–56. [CrossRef]
22. Mandal, M.; Myers, J.N.; Lippman, S.M.; Johnson, F.M.; Williams, M.D.; Rayala, S.; Ohshiro, K.; Rosenthal, D.I.; Weber, R.S.; Gallick, G.E.; et al. Epithelial to mesenchymal transition in head and neck squamous carcinoma: Association of Src activation with E-cadherin down-regulation, vimentin expression, and aggressive tumor features. *Cancer* **2008**, *112*, 2088–2100. [CrossRef]
23. Nijkamp, M.M.; Span, P.N.; Hoogsteen, I.J.; van der Kogel, A.J.; Kaanders, J.H.; Bussink, J. Expression of E-cadherin and vimentin correlates with metastasis formation in head and neck squamous cell carcinoma patients. Radiother. Oncol. 2011, 99, 344–348. [CrossRef]
24. Saitoh, M. Involvement of partial EMT in cancer progression. J. Biochem. 2018, 164, 257–264. [CrossRef]
25. Liao, C.; Wang, Q.; An, J.; Long, Q.; Wang, H.; Xiang, M.; Xiang, M.; Zhao, Y.; Liu, Y.; Liu, J.; et al. Partial EMT in Squamous Cell Carcinoma: A Snapshot. Int. J. Biol. Sci. 2021, 17, 3036–3047. [CrossRef] [PubMed]
26. Mani, S.A.; Guo, W.; Liao, M.J.; Eaton, E.N.; Ayyanan, A.; Zhou, A.Y.; Brooks, M.; Reinhard, F.; Zhang, C.C.; Shipitsin, M.; et al. The epithelial-mesenchymal transition generates cells with properties of stem cells. Cell 2008, 133, 704–715. [CrossRef] [PubMed]
27. Ben-Porath, I.; Thomson, M.W.; Carey, V.J.; Ge, R.; Bell, G.W.; Regev, A.; Weinberg, R.A. An embryonic stem cell-like gene expression signature in poorly differentiated aggressive human tumors. Nat. Genet. 2008, 40, 499–507. [CrossRef]
28. Vitale, I.; Manic, G.; De Maria, R.; Kroemer, G.; Galluzzi, L. DNA Damage in Stem Cells. Mol. Cell 2017, 66, 306–319. [CrossRef] [PubMed]
29. Diehn, M.; Cho, R.W.; Lobo, N.A.; Kalisky, T.; Dorie, M.J.; Kulp, A.N.; Qian, D.; Lam, J.S.; Ailles, L.E.; Wong, M.; et al. Association of reactive oxygen species levels and radioresistance in cancer stem cells. Nature 2009, 458, 780–783. [CrossRef] [PubMed]
30. Keith, B.; Simon, M.C. Hypoxia-inducible factors, stem cells, and cancer. Cell 2007, 129, 465–472. [CrossRef]
31. Oshimori, N. Cancer stem cells and their niche in the progression of squamous cell carcinoma. Cancer Sci. 2020, 111, 3985–3992. [CrossRef]
32. Vidal, A.; Redmer, T. Decoding the Role of CD271 in Melanoma. Cancers 2020, 12, 2460. [CrossRef]
33. Nassar, D.; Blanpain, C. Cancer Stem Cells: Basic Concepts and Therapeutic Implications. Annu. Rev. Pathol. Mech. Dis. 2016, 11, 47–76. [CrossRef] [PubMed]
34. Bourguignon, L.Y.; Earle, C.; Wong, G.; Spevak, C.C.; Krueger, K. Stem cell marker (Nanog) and Stat-3 signaling promote MicroRNA-21 expression and chemoresistance in hyaluronan/CD44-activated head and neck squamous cell carcinoma cells. *Oncogene* **2012**, *31*, 149–160. [CrossRef] [PubMed]
35. Bourguignon, L.Y.; Wong, G.; Earle, C.; Chen, L. Hyaluronan-CD44v3 interaction with Oct4-Sox2-Nanog promotes miR-302 expression leading to self-renewal, clonal formation, and cisplatin resistance in cancer stem cells from head and neck squamous cell carcinoma. *J. Biol. Chem.* **2012**, *287*, 32800–32824. [CrossRef] [PubMed]
36. Gomez, K.E.; Wu, F.; Keysar, S.B.; Morton, J.J.; Miller, B.; Chimed, T.S.; Le, P.N.; Nieto, C.; Chowdhury, F.N.; Tyagi, A.; et al. Cancer Cell CD44 Mediates Macrophage/Monocyte-Driven Regulation of Head and Neck Cancer Stem Cells. *Cancer Res.* **2020**, *80*, 4185–4198. [CrossRef]
37. Keysar, S.B.; Le, P.N.; Miller, B.; Jackson, B.C.; Eagles, J.R.; Nieto, C.; Kim, J.; Tang, B.; Glogowska, M.J.; Morton, J.J.; et al. Regulation of Head and Neck Squamous Cancer Stem Cells by PI3K and SOX2. *J. Natl. Cancer Inst.* **2017**, *109*, djw189. [CrossRef]
38. Suarez-Bonnet, A.; Willis, C.; Pittaway, R.; Smith, K.; Mair, T.; Priestnall, S.L. Molecular carcinogenesis in equine penile cancer: A potential animal model for human penile cancer. *Urol Oncol. Semin. Orig. Investig.* **2018**, *36*, 532.e9–532.e18. [CrossRef] [PubMed]
39. Armando, F.; Mecocci, S.; Orlandi, V.; Porcellato, I.; Cappelli, K.; Mechelli, L.; Brachelente, C.; Pepe, M.; Gialletti, R.; Ghelardi, A.; et al. Investigation of the Epithelial to Mesenchymal Transition (EMT) Process in Equine Papillomavirus-2 (EcPV-2)-Positive Penile Squamous Cell Carcinomas. *Int. J. Mol. Sci.* **2021**, *22*, 10588. [CrossRef]
40. Armando, F.; Godizzi, F.; Razzuoli, E.; Leonardi, F.; Angelone, M.; Corradi, A.; Meloni, D.; Ferrari, L.; Passeri, B. Epithelial to Mesenchymal Transition (EMT) in a Laryngeal Squamous Cell Carcinoma of a Horse: Future Perspectives. *Animals* **2020**, *10*, 2318. [CrossRef]
41. Lange, C.E.; Tobler, K.; Ackermann, M.; Favrot, C. Identification of two novel equine papillomavirus sequences suggests three genera in one cluster. *Vet. Microbiol.* **2011**, *149*, 85–90. [CrossRef]
42. Lange, C.E.; Vetsch, E.; Ackermann, M.; Favrot, C.; Tobler, K. Four novel papillomavirus sequences support a broad diversity among equine papillomaviruses. *J. Gen. Virol.* **2013**, *94*, 1365–1372. [CrossRef]
43. Moll, R.; Divo, M.; Langbein, L. The human keratins: Biology and pathology. *Histochem. Cell Biol.* **2008**, *129*, 705–733. [CrossRef] [PubMed]
44. Moll, R.; Franke, W.W.; Schiller, D.L.; Geiger, B.; Krepler, R. The catalog of human cytokeratins: Patterns of expression in normal epithelia, tumors and cultured cells. *Cell* **1982**, *31*, 11–24. [CrossRef]

45. Makarova, G.; Bette, M.; Schmidt, A.; Jacob, R.; Cai, C.; Rodepeter, F.; Betz, T.; Sitterberg, J.; Bakowsky, U.; Moll, R.; et al. Epidermal growth factor-induced modulation of cytokeratin expression levels influences the morphological phenotype of head and neck squamous cell carcinoma cells. *Cell Tissue Res.* **2013**, *351*, 59–72. [CrossRef] [PubMed]
46. Kudo, Y.; Kitajima, S.; Ogawa, I.; Hiraoka, M.; Sargolzaei, S.; Keikhaee, M.R.; Sato, S.; Miyauchi, M.; Takata, T. Invasion and metastasis of oral cancer cells require methylation of E-cadherin and/or degradation of membranous beta-catenin. *Clin. Cancer Res.* **2004**, *10*, 5455–5463. [CrossRef]
47. Stenner, M.; Yosef, B.; Huebbers, C.U.; Preuss, S.F.; Dienes, H.P.; Speel, E.J.; Odenthal, M.; Klussmann, J.P. Nuclear translocation of beta-catenin and decreased expression of epithelial cadherin in human papillomavirus-positive tonsillar cancer: An early event in human papillomavirus-related tumour progression? *Histopathology* **2011**, *58*, 1117–1126. [CrossRef]
48. Wang, W.; Wen, Q.; Luo, J.; Chu, S.; Chen, L.; Xu, L.; Zang, H.; Alnemah, M.M.; Li, J.; Zhou, J.; et al. Suppression of beta- catenin Nuclear Translocation By CGP57380 Decelerates Poor Progression and Potentiates Radiation-Induced Apoptosis in Nasopharyngeal Carcinoma. *Theranostics* **2017**, *7*, 2134–2149. [CrossRef]
49. Usman, S.; Waseem, N.H.; Nguyen, T.K.N.; Mohsin, S.; Jamal, A.; Teh, M.T.; Waseem, A. Vimentin Is at the Heart of Epithelial Mesenchymal Transition (EMT) Mediated Metastasis. *Cancers* **2021**, *13*, 4985. [CrossRef]
50. Watanabe, Y.; Imanishi, Y.; Ozawa, H.; Sakamoto, K.; Fujii, R.; Shigetomi, S.; Habu, N.; Otsuka, K.; Sato, Y.; Sekimizu, M.; et al. Selective EP2 and Cox-2 inhibition suppresses cell migration by reversing epithelial-to-mesenchymal transition and Cox-2 overexpression and E-cadherin downregulation are implicated in neck metastasis of hypopharyngeal cancer. *Am. J. Transl. Res.* **2020**, *12*, 1096–1113.
51. Sadasivam, S.; Subramanian, R. A perspective on challenges and opportunities in characterizing oral cancer stem cells. *Front. Biosci.* **2020**, *25*, 1011–1021. [CrossRef]
52. Murillo-Sauca, O.; Chung, M.K.; Shin, J.H.; Karamboulas, C.; Kwok, S.; Jung, Y.H.; Oakley, R.; Tysome, J.R.; Farnebo, L.O.; Kaplan, M.J.; et al. CD271 is a functional and targetable marker of tumor-initiating cells in head and neck squamous cell carcinoma. *Oncotarget* **2014**, *5*, 6854–6866. [CrossRef]
53. Gale, N.; Poljak, M.; Zidar, N. Update from the 4th Edition of the World Health Organization Classification of Head and Neck Tumours: What is New in the 2017 WHO Blue Book for Tumours of the Hypopharynx, Larynx, Trachea and Parapharyngeal Space. *Head Neck Pathol.* **2017**, *11*, 23–32. [CrossRef] [PubMed]
54. Scott, D.W.; Miller, W.H., Jr. Squamous cell carcinoma. In *Equine Dermatology*, 1st ed.; Scott, D.W., Miller, W.H., Jr., Eds.; Saunders Elsevier: St. Louis, MO, USA, 2003; pp. 707–712.
55. Knottenbelt, D.C. Squamous cell carcinoma. In *Pascoe's Principles and Practice of Equine Dermatology*, 2nd ed.; Knottenbelt, D.C., Ed.; Saunders Elsevier: London, UK, 2009; pp. 427–433.
56. Pascoe, R.R.; Knottenbelt, D.C. Squamous cell carcinoma. In *Manual of Equine Dermatology*; Saunders, W.B., Ed.; Harcourt Publishers: London, UK, 1999; pp. 261–266.
57. Budras, K.-D.; Sack, W.O.; Röck, S. Head. In *Anatomy of the Horse*, 6th ed.; Schlütersche Verlagsgesellschaft: Hannover, Germany, 2011.
58. Hibi, H.; Hatama, S.; Obata, A.; Shibahara, T.; Kadota, K. Laryngeal squamous cell carcinoma and papilloma associated with Equus caballus papillomavirus 2 in a horse. *J. Vet. Med. Sci.* **2019**, *81*, 1029–1033. [CrossRef] [PubMed]
59. Kainzbauer, C.; Rushton, J.; Tober, R.; Scase, T.; Nell, B.; Sykora, S.; Brandt, S. Bovine papillomavirus type 1 and *Equus caballus* papillomavirus 2 in equine squamous cell carcinoma of the head and neck in a Connemara mare. *Equine Vet. J.* **2012**, *44*, 112–115. [CrossRef] [PubMed]
60. Bogaert, L.; Willemsen, A.; Vanderstraeten, E.; Bracho, M.A.; De Baere, C.; Bravo, I.G.; Martens, A. EcPV2 DNA in equine genital squamous cell carcinomas and normal genital mucosa. *Vet. Microbiol.* **2012**, *158*, 33–41. [CrossRef]
61. Sykora, S.; Samek, L.; Schonthaler, K.; Palm, F.; Borzacchiello, G.; Aurich, C.; Brandt, S. EcPV-2 is transcriptionally active in equine SCC but only rarely detectable in swabs and semen from healthy horses. *Vet. Microbiol.* **2012**, *158*, 194–198. [CrossRef]
62. Ramsauer, A.S.; Wachoski-Dark, G.L.; Fraefel, C.; Ackermann, M.; Brandt, S.; Grest, P.; Knight, C.; Favrot, C.; Tobler, K. Establishment of a Three-Dimensional In Vitro Model of Equine Papillomavirus Type 2 Infection. *Viruses* **2021**, *13*, 1404. [CrossRef]
63. Van der Velden, L.A. Expression of cytokeratin subtypes and vimentin in squamous cell carcinoma of the floor of the mouth and the mobile tongue. *Otorhinolaryngol. Nova* **2001**, *11*, 186–192. [CrossRef]
64. Jung, A.; Schrauder, M.; Oswald, U.; Knoll, C.; Sellberg, P.; Palmqvist, R.; Niedobitek, G.; Brabletz, T.; Kirchner, T. The invasion front of human colorectal adenocarcinomas shows co-localization of nuclear beta-catenin, cyclin D1, and p16INK4A and is a region of low proliferation. *Am. J. Pathol.* **2001**, *159*, 1613–1617. [CrossRef]
65. Gomez-Valenzuela, F.; Escobar, E.; Perez-Tomas, R.; Montecinos, V.P. The Inflammatory Profile of the Tumor Microenvironment, Orchestrated by Cyclooxygenase-2, Promotes Epithelial-Mesenchymal Transition. *Front. Oncol.* **2021**, *11*, 686792. [CrossRef]
66. Subbaramaiah, K.; Dannenberg, A.J. Cyclooxygenase-2 transcription is regulated by human papillomavirus 16 E6 and E7 oncoproteins: Evidence of a corepressor/coactivator exchange. *Cancer Res.* **2007**, *67*, 3976–3985. [CrossRef]
67. Dawood, S.; Austin, L.; Cristofanilli, M. Cancer stem cells: Implications for cancer therapy. *Oncology* **2014**, *28*, 1101–1107. [PubMed]
68. Chung, M.K.; Jung, Y.H.; Lee, J.K.; Cho, S.Y.; Murillo-Sauca, O.; Uppaluri, R.; Shin, J.H.; Sunwoo, J.B. CD271 Confers an Invasive and Metastatic Phenotype of Head and Neck Squamous Cell Carcinoma through the Upregulation of Slug. *Clin. Cancer Res.* **2018**, *24*, 674–683. [CrossRef] [PubMed]
69. Elkashty, O.A.; Abu Elghanam, G.; Su, X.; Liu, Y.; Chauvin, P.J.; Tran, S.D.; Elkashty, O. Cancer stem cells enrichment with surface markers CD271 and CD44 in human head and neck squamous cell carcinomas. *Carcinogenesis* **2020**, *41*, 458–466. [CrossRef] [PubMed]
70. Boiko, A.D.; Razorenova, O.V.; van de Rijn, M.; Swetter, S.M.; Johnson, D.L.; Ly, D.P.; Butler, P.D.; Yang, G.P.; Joshua, B.; Kaplan, M.J.; et al. Human melanoma-initiating cells express neural crest nerve growth factor receptor CD271. *Nature* **2010**, *466*, 133–137. [CrossRef]
71. Huang, S.D.; Yuan, Y.; Liu, X.H.; Gong, D.J.; Bai, C.G.; Wang, F.; Luo, J.-H.; Xu, Z.-Y. Self-renewal and chemotherapy resistance of p75NTR positive cells in esophageal squamous cell carcinomas. *BMC Cancer* **2009**, *9*, 9. [CrossRef]
72. Imai, T.; Tamai, K.; Oizumi, S.; Oyama, K.; Yamaguchi, K.; Sato, I.; Satoh, K.; Matsuura, K.; Saijo, S.; Sugamura, K.; et al. CD271 defines a stem cell-like population in hypopharyngeal cancer. *PLoS ONE* **2013**, *8*, e62002.

73. Okumura, T.; Shimada, Y.; Imamura, M.; Yasumoto, S. Neurotrophin receptor p75 characterizes human esophageal keratinocyte stem cells in vitro. *Oncogene* **2003**, *22*, 4017–4026. [CrossRef]
74. Weissenbacher-Lang, C.; Kristen, T.; Mendel, V.; Brunthaler, R.; Schwarz, L.; Weissenbock, H. Porcine circovirus type 2 (PCV2) genotyping in Austrian pigs in the years 2002 to 2017. *BMC Vet. Res.* **2020**, *16*, 198. [CrossRef]
75. Brandt, S.; Haralambus, R.; Schoster, A.; Kirnbauer, R.; Stanek, C. Peripheral blood mononuclear cells represent a reservoir of bovine papillomavirus DNA in sarcoid-affected equines. *J. Gen. Virol.* **2008**, *89*, 1390–1395. [CrossRef]

Preliminary cell culture experiments in terms of a theranostic approach

The aim was to target cancer stem-cells (CSC) with MRI. CSC, which can develop from tumor cells during EMT are known for multidrug resistance and are involved in tumor progression (76). Cancer theranostics, namely using substances that allow diagnosis and treatment simultaneously, have gained more interest in the field of cancer research (39). A recent theranostic agent, targeting CSC and thus acting as an inhibitor of EMT, has been introduced and studied in human medicine (56). Salinomycin (SAL), a polyether antibiotic, has been proposed *in vitro* and murine data to eradicate multidrug resistant CSC through various cancer progression pathways (52, 56). In this context MRI can be used to enable diagnostic imaging of the tumor and follow up response of treatment by combining anticancer drugs with MRI contrast agents. MRI is a non-invasive imaging modality with high spatial and temporal resolution. Applying intravenous contrast agents allows to visualize regions of tissue perfusion. Most clinically used MRI contrast agents are based on Gadolinium ($Gd^{3+}$) complexes of DTPA (diethylenetriamine pentaacetic acid) or DOTA (1,4,7,10-Tetraazacyclododecane1,4,7,10-tetraacetic acid) derivatives (45). Traditional contrast agents shorten the T1 relaxation time and therefore show a high signal, which differentiates it from the adjacent tissues. Therefore, a gadolinium-based specific targeted contrast agent (SAL-Gd) may help to pave the way for a refined diagnosis and therapy for patients in terms of the ultimate principle from bench to clinic (Fig.1.).

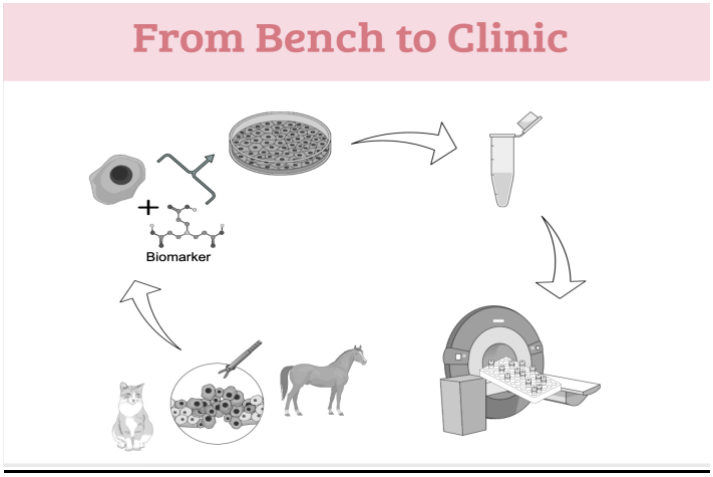


Fig.1. From Bench to Clinic-principle (created by Mind the Graph®)

Protocol establishment

The overall aim was to use SAL-Gd to test the effect of SAL on SCC cells and evaluate the results of this interaction by measuring the signal intensity via MRI. Therefore, we wanted to establish the optimal concentration range of SAL-Gd and technical parameters for MR imaging (1.5 and 9.4 T scanners) and cell culture protocol.

**MRI**

In a first step we analyzed synthesized complexes composed of SAL and two commonly used MRI contrast agents each (ProHance®, Magnevist®) in different concentrations and to choose the optimal concentration range for MR imaging. The synthesis of those complexes was carried out according to an established protocol. Two dilution series of SAL-Gd (0.012, 0.037, 0.11, 0.33, 1, 2 mM) a positive control (Dilution series 1: 1 mM ProHance, Dilution series 2: Magnevist) and a negative control (Dilution series 1: MeOH, Dilution series 2: MeOH:Acetat) were examined. The samples were placed in a rack and surrounded by a flexible coil (Fig.2). Those samples were then analyzed by a 1.5 T scanner (Siemens Magnetom, Erlangen, Germany) at the Vetmeduni. The relative T1 signal intensities were measured individually by manually placing a region of interest for each sample.

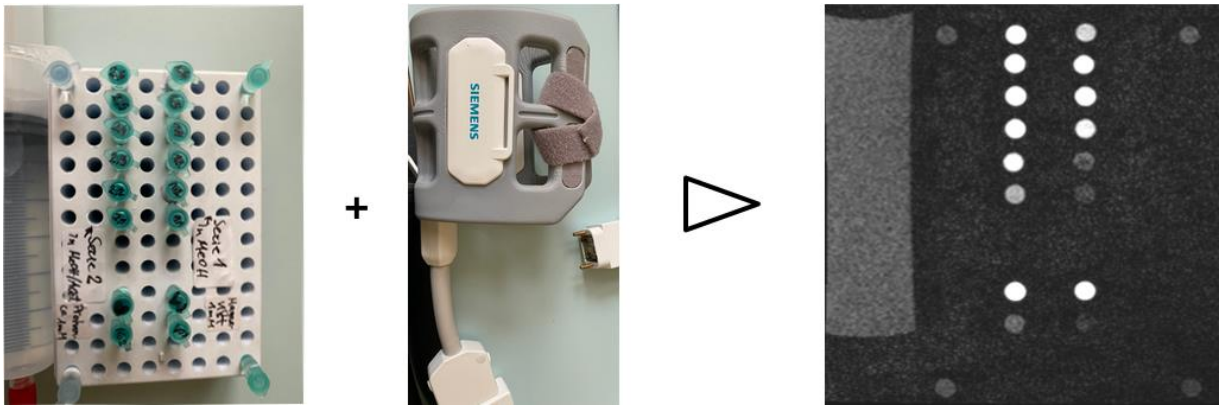


Fig. 2. Experimental setting

| Series 1 | c [mM] | Mean signal | Series 2 | c [mM] | Mean signal |
|---|---|---|---|---|---|
| SAL-Gad 1,1 | 0,012 | 140,86 | SAL-Gad 2,1 | 0,012 | 471,86 |
| SAL-Gad 1,2 | 0,037 | 265,83 | SAL-Gad 2,2 | 0,037 | 758,25 |
| SAL-Gad 1,3 | 0,11 | 728,16 | SAL-Gad 2,3 | 0,11 | 1127,52 |
| SAL-Gad 1,4 | 0,33 | 1281,98 | SAL-Gad 2,4 | 0,33 | 1449,98 |
| SAL-Gad 1,5 | 1 | 1023,31 | SAL-Gad 2,5 | 1 | 1473,18 |
| SAL-Gad 1,6 | 2 | 592,52 | SAL-Gad 2,6 | 2 | 1235,43 |
| | | | | | |
| ProHance | 1 | 1065,18 | Magnevist | 1 | 1508,07 |
| MeOH | | 98,7 | MeOH:Acetate | | 231,69 |

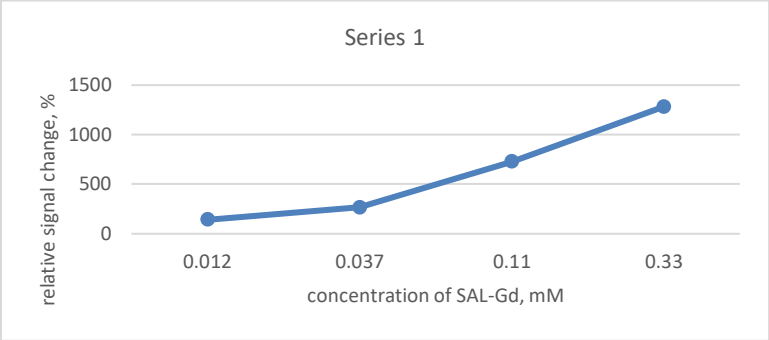


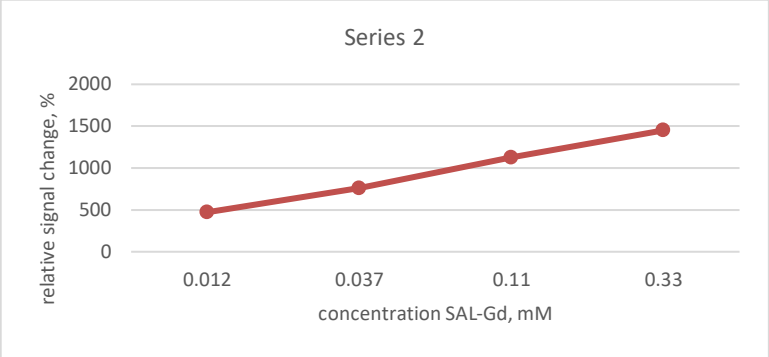


Results showed expected concentration-dependent increase in relative signal change accounting for 1 282 % and 1 450 % at 0.33 mM for SAL-Gd(III).

**Cell culture**

In the next step, feline oral SCC cells were incubated with different concentrations of SAL to evaluate the effect of SAL on these cells and to choose concentrations to further continue with.

Cells were quickly defrosted and transferred to Dulbecco's Modified Eagle Medium with high glucose (4.5 g/L) and GlutaMAX (DMEM+GlutaMAX). At a confluence of 80-90 % cells were trypsinized and the percentage of viable cells and total amount of live cells/ml were measured using ChemoMetec NucleoView NC-250. Concurrently, mycoplasma contamination was excluded by PCR. A dilution series of the SAL-Na of 0.25, 0.5, 1, 2, 4, 8, 16, 32, 64, 128 µmol/l and a positive and negative (DMSO) control were incubated with 2500 cells/well. At multiple time points (0, 24, 48, 72, 96 hours) the proliferation index was measured (Fig. 3, 4).

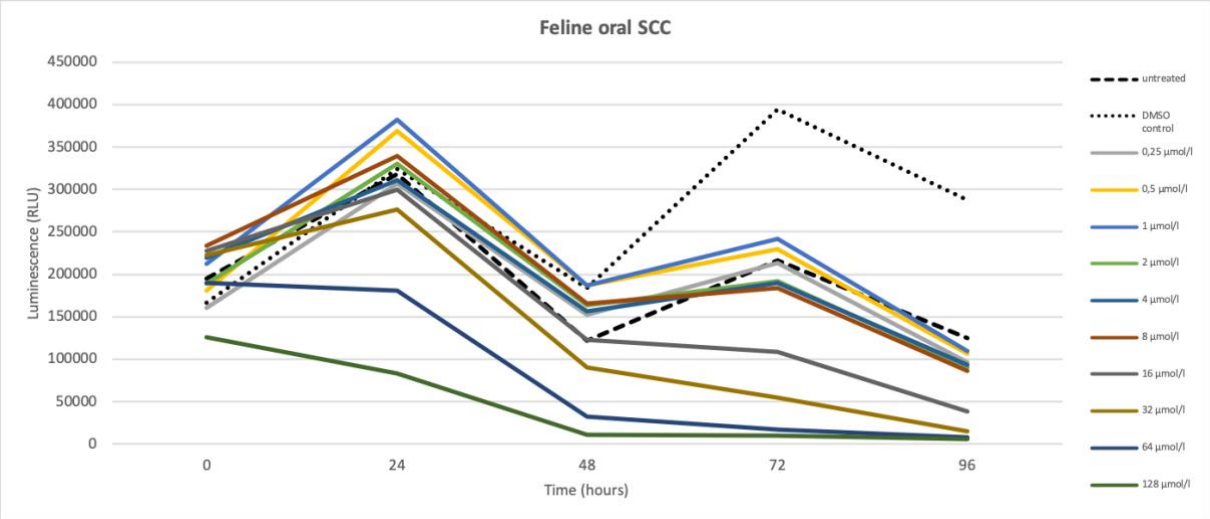


Fig. 3. Viability of feline oral squamous cell carcinoma (SCC) cells treated with Salinomycin over a time course of 96 hours.

A dose-dependent response on cell viability was seen. Within the first 24 h, cell growth is maintained in a dose-dependent manner, whereas cell viability decreases after this time point. Following these steps, feline SCC cells were considered not adequate and therefore equine SCC cells were used and the overall number of cells was reduced to 1500 cells/well.

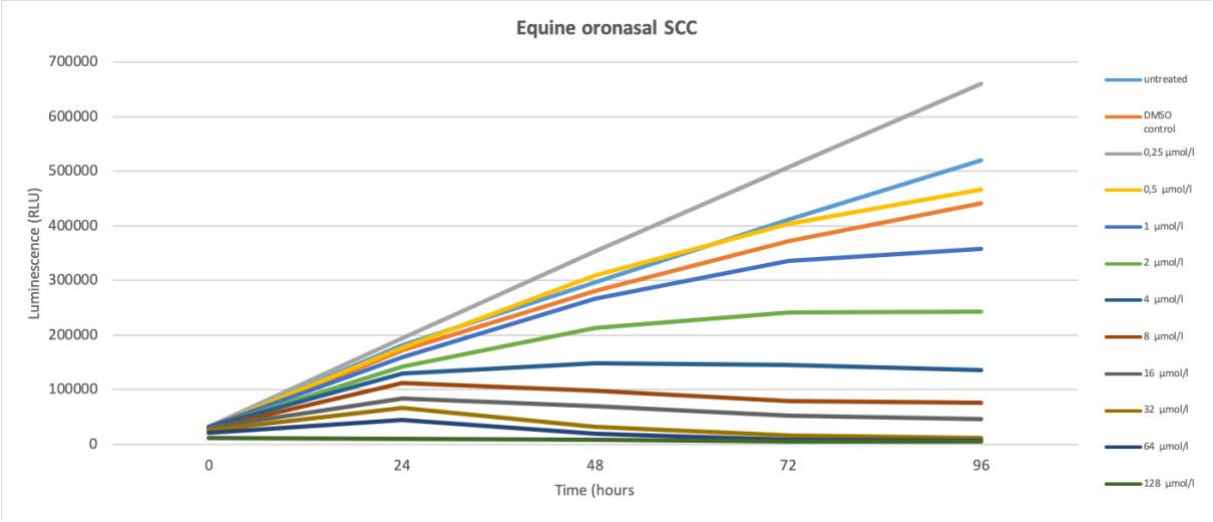


Fig. 4. Viability of equine oronasal squamous cell carcinoma (SCC) cells treated with Salinomycin over a time course of 96 hours.

A dose-dependent response on cell viability was seen. Again, in the first 24 h, cell growth is maintained in a dose-dependent manner but showed a slower growth rate. After 24 hours the cell viability decreased moreover slower and more linear.

Trial 1

Combining the previous steps, customized combined MRI-contrast agent (Gd) and SAL was synthesized and incubated with the SCC cells.

Two concentration (0.295, 0.118 mM) in duplicates with a positive (ProHance®) and negative control (DMSO) were incubated with 1500 cells/well. Following a 24 hours incubation the samples were microscopically checked. Most cells were detached, therefore suspected to be dead. Both cells in suspension and those attached to the well were harvested and centrifuged. They were resuspended with 0.6 ml of with phosphate-buffered saline (PBS) in a 0.6 ml Eppendorf tube and transferred to MR imaging.

Samples were intended to be measured with a 1.5 T scanner (Siemens Health Care, Erlangen, Germany) at the Vetmeduni and with a 9.4 T scanner (Bruker, BioSpec) at the Medical University of Vienna. While a scanning protocol for those settings is already established at the Medical University, we had to develop a protocol for measuring relaxation times at the Vetmeduni. Together with a physicist we developed the following adapted sequences adapted:

T2 Relaxivity

Multi Spin Echo Sequence: 15 echo times (8.2, 16.4, 24.6, 32.8, 41, 49.2, 57.4, 65.6, 73.8, 82, 90.2, 98.4, 106.6, 114.8 and 123 ms), TR: 1000 ms, Matrix size:256x256x1, Field of view: 20x20x1, Resolution: 0.078x0.078x1 mm, Flip angle: 90°, Bandwidth 50 000 Hz.

T1 Relaxivity

Inversion times TI: 0, 25, 50, 80, 100, 150, 200, 250, 300, 400, 500, 750, 1000, 1250, 1500, 1750, 2000, 2500, 3500 ms, TR/TE: max 15000/10 ms, Flip angle: 130°, Resolution: 0.6 $mm^2$, Slice thickness 1 mm

No signal was detected with the 9.4 T scanner, supporting the death of the cells.

# 3 Discussion

## 3.1 General discussion

This thesis focused on addressing the knowledge gap of OSCC and HNSCC in the most affected companion animals namely cats and horses respectively.

Historically, feline OSCC and equine HNSCC have a poor prognosis. This is attributed on the one hand to a late diagnosis as animals often start showing clinical symptoms when the tumor has already reached a considerable size. On the other hand, the infiltrative nature of SCC and the complexity of the anatomical region often hinders complete excision (57, 110). In addition, other treatment options such as radiation therapy has only shown limited effects. Little is known about the poor response to radiation therapy and the pathogenesis in general (27, 37, 58). Additionally, collecting data is a major challenge. First, due to the poor prognosis the owner's decision for euthanasia might occur at an early diagnostic stage without a histological sample or advanced diagnostic imaging and often owners opt for cremation preventing further scientific research. Besides, the prevalence of this tumor in comparison to the overall prevalence of neoplasms is rather small (17). Therefore, these factors might account for limited sample sizes and diagnostic imaging, histopathological and molecular information being sparse to date. However, in order to improve therapy and prognosis the pathogenesis of this tumor needs to be further examined. Consequently, the interest in investigating this tumor has grown, nonetheless because links to human medicine have been suggested and efforts to elucidate the pathogenesis in humans are promising. Overall, the pathogenesis seems to be multifactorial on a cellular and molecular level and requires further investigation in this direction (4, 12, 16, 28).

Focusing on these issues, we were able to give morphologic information by means of CT and histopathology, the prevalence of species-specific papillomavirus types, identification of tumor-type-specific proteins as biomarkers and present first data for cell culture experiments in terms of a theranostic approach in cats and horses with OSCC and HNSCC respectively (93, 94). In the following, the discussion points are therefore focused on these specific results of the three milestones.

## 3.2 Identification of morphologic differences between feline OSCC and equine HNSCC by means of computed tomography and histopathology (milestone 1).

First of all, we aimed to identify morphological characteristics by means of computed tomography (CT) and histopathology of oral and sinonasal SCC in 10 cats and 13 horses, respectively (93). CT was used to assess morphological information of the masses, as it is the main clinical diagnostic imaging modality used for non-neurologic diseases of the head in veterinary medicine. Specifically, CT is part of the routine work-up of oral cancer in terms of staging, planning for surgery or radiation therapy and can be used to monitor treatment responses. Most important imaging features of oral masses include the size of the mass and the infiltrative nature in terms of soft tissue and osseous changes (26, 44, 50, 91). We could confirm the hypothesis that all feline OSCC and equine HNSCC could be detected with CT but could not support our hypothesis that the majority of feline and equine CT cases show similar aggressive osseous features, in terms of irregular osteolysis and periosteal reactions. In our study we noticed a variety of osseous changes and phenotypes. A consistent finding with the current literature was the appearance of severe osteolysis and periosteal reaction with exophthalmos of maxillary masses in cats (26). In horses however we noticed osseous changes to a lesser degree in comparison to cats. The reason for this is unclear, however as no imaging-based articles exist on CT features of SCC in horses to date, we add morphologic CT information for further studies. The time of imaging at different disease stages and species-specific factors might be potential explanations. Interestingly, masses associated with the mandible overall showed very different appearances within species and when compared with each other. The reason for this is as well unclear and it might be attributed to different progressed disease stages or the impact of different tumor subtypes with a predilection to specific locations with a variable morphology. In human medicine on the other hand, it is well known that oral SCC can be morphologically and biologically divers (1, 12). In addition, it has been suggested that SCC from different locations of the head and neck also might differ in the carcinogenesis (89). Lingual SCC for example in humans seems quite different in behavior and carries a higher metastatic rate (114).

In addition to the oral mass itself, we evaluated the regional lymph nodes, as this is routinely performed during staging. The size of the lymph nodes was variable, nevertheless asymmetry of the lymph nodes could be detected in some cases. Unfortunately, due to the retrospective nature of the study we only have an even

smaller number of histopathological diagnoses without statistically significance. On the other hand, enlargement of a lymph nodes needs to be cautiously interpreted as an enlargement could also results from concurrent unrelated oral inflammation such as gingivitis. Additionally, little is known about CT differentiation of benign and malignant regional lymph nodes and there are quite big ranges reported regarding the size (71-74, 82). In human medicine, identifying metastatic lymph nodes based on size is one of the biggest prognostic aspect (46). In veterinary medicine however as prognosis is poor, efforts are mainly based on locoregional control of the primary tumor rather than on metastasis (57). However, as more is known about this tumor and the diagnosis and the treatment options might be refined, also the importance of lymph node metastasis is increasing in veterinary medicine. As a step towards a refined diagnosis, in recent years indirect CT lymphography has been introduced to identify the sentinel lymph node for tumors of the head, however only in dogs. During this procedure iodinated contrast medium is injected in four quadrants around the tumor (31). The lymph node to which the tumor first is supposed to drain is imaged therefore and called sentinel lymph node. Indirect CT lymphography can therefore help in guiding which lymph node to sample even in the absence of morphological alteration (55). Therefore, even micrometastasis can be detected. As little significant information about the size of metastatic lymph node is known, efforts are increasing to gain relevant information by analyzing large data. As already used in human medicine routinely, machine-based learning has been recently emerged in veterinary medicine. As a first step deep convolutional neural networks for segmenting normal medial retropharyngeal lymph node in dogs has been introduced very recently. The ability to automatically delineate the contour of lymph nodes helps in quantifying the size. This can be applied to a large data set and potentially used in clinical research in future (87). As these methods have been studied in dogs, future investigations in other species might follow. Consequently, with advanced knowledge in veterinary medicine, more advanced imaging techniques might become more and more relevant. Besides the clinical use of CT, also magnetic resonance imaging (MRI) is routinely performed and reported to be comparable in detecting tumors in human medicine (78). In veterinary medicine on the other hand, CT in comparison to MRI is generally more available, has a shorter examination time and is used because radiation planning is based on CT images (92). As MRI will be more accessible with time in veterinary medicine, the clinical role in tumor staging and monitoring might increase.

Despite our CT data we also histopathologically analyzed the samples of our CT cases and could support our hypothesis that the majority of feline OSCC and equine HNSCC show aggressive cellular features. Findings included various features of keratinization and number of mitotic cells in addition to a wide and deep invasion in adjacent bones in both horses and cats, that are representative of the infiltrative nature of this tumor. Although our study population was too small to draw statistical conclusion, we obtained more detailed histopathological data for this tumor that can be used in future studies. Findings like these could be used as first steps towards correlated imaging of SCC in veterinary medicine. No association between the histologic type and prognosis or other features are reported in veterinary medicine in comparison to human medicine (48). In human medicine, diagnostic imaging does not only macroscopically display tumors but can also obtain information about the tumor microenvironment and microstructures through advanced techniques. There are multiple emerging techniques, one of them is CT texture analysis which quantifies the heterogeneity of masses on CT images. This heterogeneity might correlate histologically with the heterogeneity of the tumors, the cellularity or other features. Therefore, the correlation with histopathology could be beneficial for evaluation of treatment response or prognosis (61). However, there are also some limitations as clinical CT and MRI do have their limitations as they overestimate the depth of invasion in comparison to histology in humans (106). Additionally, positron emission tomography (PET), a functional imaging technique, has been shown to be useful in detecting an aggressive phenotype. The principle of PET is based on radioactive substances to display and measure alterations in the metabolic processes (32). Besides efforts to subclassify SCC histopathologically and with imaging methods, combinations with other promising methods such as next generation sequencing are evolving. This tool studies the impact of genetic alterations in cancer cells and can potentially subclassify SCC based on genetics in addition (13). Therefore, future research will likely involve advanced imaging modalities building up on the knowledge of basic CT or MRI imaging with large study populations. Unfortunately, our retrospective study population was small being limited by patients that had a histopathological diagnosis. Therefore, a small sample size of 10 cats and 13 horses in our study (93) precluded us from achieving statistically significant results. The small study populations likely result from multiple factors. Often a cytologic sample is done first and together with the tentative diagnosis of SCC the owners do not want to proceed with expensive treatment since the prognosis is still considered poor. This

is reflected by the fact that in veterinary imaging articles about oral SCC usually struggle with larger study populations (26).

### 3.3 Species-specific papillomavirus types (milestone 2).

The human papillomavirus (HPV) is a major pathogenic risk factor in development of HNSCC (29, 79). With this background, we screened the available equine HNSCC and feline oral SCC samples for species-specific papillomavirus (PV) types (EcPV- 2, 3, 5 and FcaPV- 1, 2, 3). The hypothesis that the prevalence of a papillomavirus infection of the feline OSCC and equine HNSCC samples is equivalent between these two species was not supported by our findings. For our equine HNSCC-samples we observed EcPV-2 infection in 22 % of the specimen. A similar percentage is described in human medicine in association with an HPV infection, which has shown to be distinct from HNSCC without an HPV infection, that are mainly associated with tobacco and alcohol consumption (12, 108). Interestingly, HPV-positive HNSCC in contrast to its negative counterpart were found to respond better to radiation therapy and chemotherapy and thus carry a better prognosis (8). Therefore, elucidating the impact of a papillomavirus infection seems crucial. In human medicine, HPV has been demonstrated to develop various strategies to escape immune surveillance. Strategies include holding a low profile, showing low expression of MHC-class I and II, interfering with T-cell function and releasing immunosuppressive inflammatory mediators in order to escape antigen presentation and immune recognition (108). Knowledge about the pathogenesis of a papillomavirus infection and SCC can be further important when it comes to a potential vaccination against papillomaviruses in animals. Recently, Thomson *et al*. (101) developed a well-tolerated FcaPV-2 virus-like particle vaccine, which was safe but did not show an impact on the viral load of adult cats. The authors suggested that further investigations should focus on vaccinating younger cats in order to evaluate a subsequent potential reduced viral load. In comparison to humans, cats are suspected to resemble more an HPV-negative HNSCC phenotype (15). This is in conjunction with our findings of a prevalence of under 10 %. As papillomavirus infection does not appear to be a common cause of oral SCC, therefore vaccination as a main target might be not indicated (63). In contrast, the prevalence of papillomavirus infection associated with HNSCC in horses is comparable with human medicine (18, 94). As most genital tumors in horses are associated with EcPV-2 there has been emphasis in developing a targeted vaccine. Since the transmission mechanisms of PV

infection have not been elucidated, it is not known if via this vaccination in horses, as is proposed in humans, is advantageous in preventing from developing HNSCC (86).

### 3.4 Identification of tumor-type-specific proteins as biomarkers (milestone 2).

In the continuous search for an effective treatment of HNSCC in both animals and humans, domestic animals with spontaneously occurring HNSCC have potential for investigating novel therapeutic targets which could be beneficial for all. Domestic animals and humans share multiple aspect of HNSCC. They have similarities regarding clinical, pathologic, and molecular characteristics. Animals show comparable resistance to radiation and chemotherapy. Above that, they share the same environment and live in the same household (25, 28, 83, 95, 98, 111). In human medicine, HNSCC is known for its genomic, cellular, and immunological heterogeneity. This heterogeneity appears to make successful treatment challenging despite lots of efforts for new therapeutic strategies (12). Therefore, the tumor microenvironment is extensively investigated in its relationship to survival of tumor cells and tumor progression. The microenvironment overall consists of surrounding immune cells, stromal cells, angiogenesis, and cancer stem-cells. Elucidating the signal pathways and regulatory mechanisms to better understand the tumor behavior and refine therapeutic approaches are the core objectives of the current research field in human medicine (107). In this context a process called epithelial-mesenchymal transition (EMT) has been focused on widely. EMT is a process, through which epithelial cells acquire mesenchymal characteristics and thus gain the potential to metastasize and promote cancer progression (20, 49, 70).

We therefore consequently focused on cellular characteristics of this tumor in horses for the identification of tumor-specific proteins as potential biomarker by analyzing for expression of epithelial, mesenchymal, endothelial and stem-cell markers in papillomavirus-positive versus -negative HNSCC samples. In addition, we confirmed our hypotheses that biomarkers for OSCC established in human medicine can be detected in the majority of equine HNSCC samples and that the identified biomarkers help in elucidating the pathogenesis of equine HNSCC. We noted commonly partial epithelial-mesenchymal transition (EMT) by expression of the epithelial marker cytokeratin and the mesenchymal marker vimentin in our study population of partly metastasizing equine HNSCCs unrelated to a papillomavirus infection. Besides we detected stem-cell markers CD271 and CD44 in all samples. This is an interesting

finding, since there is little amount of literature about EMT published in horses and warrants further investigation (7). On the other hand, there are more studies focusing on cats as companion animal model in translational oncology. Harris et al. (34) found that N-cadherin, which is well known in human medicine to be associated with EMT, was hardly detected. Instead, biopsies and cell lines of feline OSCC frequently expressed E-cadherin, P-cadherin, hypoxia inducible factor 1a (HIF-1a), programmed death ligand 1, and Twist. Hamilton (33) has addressed EMT-events to the biggest extent in veterinary medicine. The authors studied a drug-resistant phenotype and the association of EMT. They worked with gefitinib, an epidermal growth factor (EGFR)-inhibitor to produce a resistant phenotype of human HNSCC and feline oral SCC cell lines. The results showed a biphasic response and two phenotypes, namely an early invasive mesenchymal type and then a pronounced epithelial phenotype when the drug-resistance was more established. The authors further demonstrated that through the anti-apoptotic PI3K/AKT pathway tumor cells might develop resistance due to the prevention of apoptosis. Similar to human medicine, CD147, an activator of matrix metalloproteinases was identified in feline OSCC gaining more information about potential biomarkers (70). Another potential target as treatment option of SCC is NAD(P)H:quinone oxidoreductase 1 (NQO1), a 2-electron reductase which is overexpressed in HNSCC (53). Moreover, Khammanivong *et al*. (42) targeted MD-1, an inhibitor of monocarboxylate transporters (MCTs), involved in tumor growth. The authors showed in in-vitro experiments of feline cell culture lines and in-vivo xenografts in a mouse model, that feline OSCC cell lines died, and tumor growth was reduced. Since we published the results of the equine HNSCC (94), we are focusing in near future on evaluating our feline OSCC samples for EMT events.

### 3.5 Early results for establishing a theranostic approach (milestone 3).

Theranostics, namely the combination of a therapeutic and a diagnostic agent seems a promising approach in dealing with cancer. Until now few approaches are reported for OSCC in veterinary medicine. Beltrán Hernández *et al*. (9) reported a new nanobody-targeted photodynamic therapy for feline OSCC using nanobodies to transport a photosensitizer specifically to neoplastic cells. During light application reactive oxygen species develop which ultimately lead to cell death. Another approach was used by Van Nimwegen *et al*. (105) performing an intratumoral injection of radioactive holmium-166 ($^{166}$Ho) microspheres in cats with OSCC. $^{166}$Ho emits β-

radiation, intended as a minimally invasive treatment. The study showed promising response in terms of further investigating $^{166}$Ho microspheres as treatment option for OSCC.

With our intended approach we wanted to investigate a method that can be used in a clinical setting in future. Therefore, we decided to study a compound of a diagnostic agent, namely gadolinium a contrast agent used for a readily available diagnostic modality, namely MRI with a therapeutic agent, namely Salinomycin, which has been shown to have anti-tumorigenic properties (52, 56). Building an interdisciplinary research group with a collaboration with the Medical University of Vienna, made us reinforced and motivated. With our results we laid the corner stone for advancements of tumor theranostics and were not able to support our hypothesis that the cell viability of feline OSCC cells and equine HNSCC cells will be equivalent when incubated with the theranostic agent, SAL-Gd. Despite our efforts we faced challenges inherent to the process of establishing a new approach. While equine HNSCC cells showed a more linear decrease in cell viability to the theranostic agent, SAL-Gd, we faced challenges regarding the feline OSCC cells themselves, which appeared slowly growing and morphologically divers. To the authors knowledge articles based on feline OSCC cell lines (33, 34, 70, 80) derive from cell lines by Dr. Rosol from the Ohio State University (97). An improvement of cell culture conditions for the SCC cell lines according to Tannehill-Gregg *et al*. (97) by the addition of cholera toxin (0.1 nM; Merck Sigma) and mouse EGF recombinant protein (Thermo Fisher) may provide more conclusive results in further experiments. So adapting our protocol and comparing our cell line to the well characterized cell lines of Tannehill-Gregg *et al*. (97) seems crucial.

Other challenges included the amount of SAL-Gd which must be balanced between clinically relevant concentration, toxicity and enough signal to be detected. Concentrations in the range of mmol/l are necessary to be detected by MRI, however those concentrations seem very high and toxic for the cells. Therefore, a concentration of 0,02 mmol/l was suggested for future attempts. Also using two different MRI scanners and magnet field strength of different sensitivities might help overcome this. In this context likely also the duration of the incubation time of the cells with SAL-Gd needs to be refined. Therefore, different settings of one, three and six hours of incubation are anticipated to evaluate in the next trial.

The research group submitted a proposal to the FWF 1000 ideas call, for continuation of the project, but unfortunately this was not successful. To further develop this protocol

the group submitted to the recent One Health Call of the University of Veterinary Medicine, Vienna.

## 3.6 Conclusion and Future prospects

Our research group added value to the current research on feline OSCC and equine HNSCC based on diagnostic imaging, pathomorphologic and molecular features. Information about diagnostic imaging findings, such as the wide range of morphological appearances up to severe osseous changes, can help the clinician in adding SCC on the differential list in case of an oral mass. Additionally, as more and more cross-sectional imaging data exist, future studies could also focus on advanced techniques, such as texture analysis. The identified histopathological information of a predominant invasive pattern seems in conjunction with the infiltrative nature of the tumor, however due to the small study population no statistically significant conclusions can be drawn. Therefore, further studies addressing this topic are warranted. Despite putting efforts into scientific questions, we came across challenges in the everyday clinical life. We experienced difficulties inherent to the nature of submitting biopsies. To add an overall clinical value from our observations in collaboration with the Institute of Pathology of the Vetmeduni (Dr.med.vet. Andrea Klang) we analyzed the workflow and created an educational videoclip for correctly submitting samples to improve the quality of the resulting diagnosis. From this collaboration a video (“From Clinic to Bench”) was created and will be available (e.g., VetMediathek) for students and university members in aiding them to optimize the results.

Taking a step further we identified 22 % and < 10 % papillomavirus positive samples in equine HNSCC and feline OSCC respectively. Although no difference in epithelial, mesenchymal, endothelial and stem-cell markers regarding the papillomavirus infection status in horses could be demonstrated, the overall majority of samples are suggestive of partial epithelial-mesenchymal transition events that are indicative for epithelial/mesenchymal and stem-cell-like tumor cell phenotypes.

Having studied potential biomarker, we focused on the cornerstones for a potential therapeutic approach. In cell culture experiments we tested the effect of a therapeutic agent, salinomycin combined with gadolinium, a diagnostic MRI contrast agent for both imaging and treatment. First results were promising, and we are keen on continuing this research field. As future prospects therefore, establishing a Medical Imaging Cluster at the Vetmeduni, including the Rodents Centre (according to the Development

Plan Vetmeduni 2030, https://www.vetmeduni.ac.at/fileadmin/v/z/mitteilungsblatt/organisation/Development_Plan-2030_en_screen.pdf), which connects pre-clinical and clinical research of companion animals and human medicine in terms of one health, would pave the way for scientific advances.

Besides the individual scientific results, it was motivating to witness a dedicated working group developing. In a change management project, being a member of an interdisciplinary and interinstitutional scientific working group, collaborating with different veterinary disciplines at the Vetmeduni (Research Group Oncology, Vetcore Facility for Research, Institute of Morphology, Institute of Pathology, Institute of Medical Biochemistry and Radiooncology & Nuclear Medicine Platform) and the Medical University of Vienna, respectively holds a lot of potential. Combining preclinical and clinical knowledge, breaking it down to a common language, with constant reflexion and refinement are key components for success by science for animals and humans in terms of “one health”-principles.

In conclusion, results of this thesis help in elucidating equine HNSCC and feline OSCC on a multifactorial level and hold a lot of potential for further studies of our established working group and other researchers in this scientific field.

## 4 References


1. Alsahafi E, Begg K, Amelio I, Raulf N, Lucarelli P, Sauter T, et al. Clinical update on head and neck cancer: molecular biology and ongoing challenges. Cell Death Dis. 2019;10(8):540.

2. Altamura G, Cardeti G, Cersini A, Eleni C, Cocumelli C, Bartolome Del Pino LE, et al. Detection of Felis catus papillomavirus type-2 DNA and viral gene expression suggest active infection in feline oral squamous cell carcinoma. Vet Comp Oncol. 2020;18(4):494-501.

3. Altamura G, Corteggio A, Borzacchiello G. Felis catus papillomavirus type 2 E6 oncogene enhances mitogen-activated protein kinases and Akt activation but not EGFR expression in an in vitro feline model of viral pathogenesis. Vet Microbiol. 2016;195:96-100.

4. Altamura G, Corteggio A, Pacini L, Conte A, Pierantoni GM, Tommasino M, et al. Transforming properties of Felis catus papillomavirus type 2 E6 and E7 putative oncogenes in vitro and their transcriptional activity in feline squamous cell carcinoma in vivo. Virology. 2016;496:1-8.

5. Altamura G, Cuccaro B, Eleni C, Strohmayer C, Brandt S, Borzacchiello G. Investigation of multiple Felis catus papillomavirus types (-1/-2/-3/-4/-5/-6) DNAs in feline oral squamous cell carcinoma: a multicentric study. J Vet Med Sci. 2022;84(6):881-4.

6. Altamura G, Martano M, Licenziato L, Maiolino P, Borzacchiello G. Telomerase Reverse Transcriptase (TERT) Expression, Telomerase Activity, and Expression of Matrix Metalloproteinases (MMP)-1/-2/-9 in Feline Oral Squamous Cell Carcinoma Cell Lines Associated With Felis catus Papillomavirus Type-2 Infection. Front Vet Sci. 2020;7:148.

7. Armando F, Godizzi F, Razzuoli E, Leonardi F, Angelone M, Corradi A, et al. Epithelial to Mesenchymal Transition (EMT) in a Laryngeal Squamous Cell Carcinoma of a Horse: Future Perspectives. Animals (Basel). 2020;10(12).

8. Belgioia L, Morbelli SD, Corvo R. Prediction of Response in Head and Neck Tumor: Focus on Main Hot Topics in Research. Front Oncol. 2020;10:604965.

9. Beltrán Hernández I, Grinwis GCM, Di Maggio A, van Bergen en Henegouwen PMP, Hennink WE, Teske E, et al. Nanobody-targeted photodynamic therapy for the treatment of feline oral carcinoma: a step towards translation to the veterinary clinic. Nanophotonics. 2021;10(12):3075-87.

10. Bertone ER, Snyder LA, Moore AS. Environmental and lifestyle risk factors for oral squamous cell carcinoma in domestic cats. J Vet Intern Med. 2003;17(4):557–62.

11. Boston SE, van Stee LL, Bacon NJ, Szentimrey D, Kirby BM, van Nimwegen S, et al. Outcomes of eight cats with oral neoplasia treated with radical mandibulectomy. Vet Surg. 2020;49(1):222-32.

12. Canning M, Guo G, Yu M, Myint C, Groves MW, Byrd JK, et al. Heterogeneity of the Head and Neck Squamous Cell Carcinoma Immune Landscape and Its Impact on Immunotherapy. Front Cell Dev Biol. 2019;7:52.

13. Chai AWY, Lim KP, Cheong SC. Translational genomics and recent advances in oral squamous cell carcinoma. Seminars in Cancer Biology. 2020;61:71-83.

14. Chen SH, Hsiao SY, Chang KY, Chang JY. New Insights Into Oral Squamous Cell Carcinoma: From Clinical Aspects to Molecular Tumorigenesis. Int J Mol Sci. 2021;22(5).

15. Chu S, Wylie TN, Wylie KM, Johnson GC, Skidmore ZL, Fleer M, et al. A virome sequencing approach to feline oral squamous cell carcinoma to evaluate viral causative factors. Vet Microbiol. 2020;240:108491.

16. Coletta RD, Yeudall WA, Salo T. Grand Challenges in Oral Cancers. Front Oral Health. 2020;1:3.

17. Cray M, Selmic LE, Ruple A. Demographics of dogs and cats with oral tumors presenting to teaching hospitals: 1996-2017. J Vet Sci. 2020;21(5):e70.

18. de Martel C, Plummer M, Vignat J, Franceschi S. Worldwide burden of cancer attributable to HPV by site, country and HPV type. Int J Cancer. 2017;141(4):664-70.

19. Dixon PM, Head KW. Equine Nasal and Paranasal Sinus Tumours: Part 2: A Contribution of 28 Case Reports. Vet J. 1999;157(3):279-94.

20. Dongre A, Weinberg RA. New insights into the mechanisms of epithelial-mesenchymal transition and implications for cancer. Nat Rev Mol Cell Biol. 2019;20(2):69-84.

21. Doorbar J, Quint W, Banks L, Bravo IG, Stoler M, Broker TR, et al. The biology and life-cycle of human papillomaviruses. Vaccine. 2012;30 Suppl 5:F55-70.

22. Falcão F, Faísca P, Viegas I, de Oliveira JT, Requicha JF. Feline oral cavity lesions diagnosed by histopathology: a 6-year retrospective study in Portugal. J Feline Med Surg. 2020;22(10):977-83.

23. Fidel J, Lyons J, Tripp C, Houston R, Wheeler B, Ruiz A. Treatment of Oral Squamous Cell Carcinoma with Accelerated Radiation Therapy and Concomitant Carboplatin in Cats. J Vet Intern Med. 2011;25(3):504–10.

24. Fidel JL, Sellon RK, Houston RK, Wheeler BA. A nine-day accelerated radiation protocol for feline squamous cell carcinoma. Vet Radiol Ultrasound. 2007;48(5):482-5.

25. Gardner DG. Spontaneous squamous cell carcinomas of the oral region in domestic animals: a review and consideration of their relevance to human research. Oral Dis. 1996;2(2):148-54.

26. Gendler A, Lewis JR, Reetz JA, Schwarz T. Computed tomographic features of oral squamous cell carcinoma in cats: 18 cases (2002–2008). JAVMA. 2010;236(3):319–25.

27. Gillen A, Mudge M, Caldwell F, Munsterman A, Hanson R, Brawner W, et al. Outcome of external beam radiotherapy for treatment of noncutaneous tumors of the head in horses: 32 cases (1999-2015). J Vet Intern Med. 2020;34(6):2808-16.

28. Giuliano A. Companion Animal Model in Translational Oncology; Feline Oral Squamous Cell Carcinoma and Canine Oral Melanoma. Biology (Basel). 2021;11(1).

29. Graham SV. The human papillomavirus replication cycle, and its links to cancer progression: a comprehensive review. Clin Sci (Lond). 2017;131(17):2201-21.

30. Greenwood S, Chow-Lockerbie B, Ramsauer S, Wachoski-Dark G, Knight C, Wobeser B. Prevalence of Equus caballus Papillomavirus Type-2 Infection and Seropositivity in Asymptomatic Western Canadian Horses. Vet Pathol. 2020;57(5):632-41.

31. Grimes JA, Secrest SA, Northrup NC, Saba CF, Schmiedt CW. Indirect computed tomography lymphangiography with aqueous contrast for evaluation of sentinel lymph nodes in dogs with tumors of the head. Vet Radiol Ultrasound. 2017;58(5):559-64.

32. Grönroos TJ, Lehtiö K, Söderström KO, Kronqvist P, Laine J, Eskola O, et al. Hypoxia, blood flow and metabolism in squamous-cell carcinoma of the head and neck: correlations between multiple immunohistochemical parameters and PET. BMC Cancer. 2014;14.

33. Hamilton J. Targeting epithelial-to-mesenchymal transition (EMT) in feline oral squamous cell carcinoma (FOSCC): The University of Edinburgh; 2018.

34. Harris K, Gelberg HB, Kiupel M, Helfand SC. Immunohistochemical Features of Epithelial-Mesenchymal Transition in Feline Oral Squamous Cell Carcinoma. Vet Pathol. 2019;56(6):826-39.

35. Hayes AM, Adams VJ, Scase TJ, Murphy S. Survival of 54 cats with oral squamous cell carcinoma in United Kingdom general practice. J Small Anim Pract. 2007;48(7):394-9.

36. Head KW, Dixon PM. Equine nasal and paranasal sinus tumours. Part 1: review of the literature and tumour classification. Vet J. 1999;157(3):261-78.

37. Hutchinson MND, Mierzwa M, D'Silva NJ. Radiation resistance in head and neck squamous cell carcinoma: dire need for an appropriate sensitizer. Oncogene. 2020;39(18):3638-49.

38. Jadhav KB, Gupta N. Clinicopathological prognostic implicators of oral squamous cell carcinoma: need to understand and revise. N Am J Med Sci. 2013;5(12):671-9.

39. Jeyamogan S, Khan NA, Siddiqui R. Application and Importance of Theranostics in the Diagnosis and Treatment of Cancer. Arch Med Res. 2021;52(2):131-42.

40. Jones DL. Squamous cell carcinoma of the larynx and pharynx in horses. Cornell Vet. 1994;84(1):15-24.

41. Kainzbauer C, Rushton J, Tober R, Scase T, Nell B, Sykora S, et al. Bovine papillomavirus type 1 and Equus caballus papillomavirus 2 in equine squamous cell carcinoma of the head and neck in a Connemara mare. Equine Vet J. 2012;44(1):112-5.

42. Khammanivong A, Saha J, Spartz AK, Sorenson BS, Bush AG, Korpela DM, et al. A novel MCT1 and MCT4 dual inhibitor reduces mitochondrial metabolism and inhibits tumour growth of feline oral squamous cell carcinoma. Vet Comp Oncol. 2020;18(3):324-41.

43. Knight CG, Dunowska M, Munday JS, Peters-Kennedy J, Rosa BV. Comparison of the levels of Equus caballus papillomavirus type 2 (EcPV-2) DNA in equine squamous cell carcinomas and non-cancerous tissues using quantitative PCR. Vet Microbiol. 2013;166(1-2):257-62.

44. Kowalczyk L, Boehler A, Brunthaler R, Rathmanner M, Rijkenhuizen A. Squamous cell carcinoma of the paranasal sinuses in two horses. Equine Vet Educ. 2011;23:435–40.

45. Lacerda S. Targeted Contrast Agents for Molecular MRI. Inorganics. 2018;6(4).

46. Laimer J, Lauinger A, Steinmassl O, Offermanns V, Grams AE, Zelger B, et al. Cervical Lymph Node Metastases in Oral Squamous Cell Carcinoma-How Much Imaging Do We Need? Diagnostics (Basel). 2020;10(4).

47. Lange CE, Vetsch E, Ackermann M, Favrot C, Tobler K. Four novel papillomavirus sequences support a broad diversity among equine papillomaviruses. J Gen Virol. 2013;94(Pt 6):1365-72.

48. Lin NC, Hsu JT, Tsai KY. Survival and clinicopathological characteristics of different histological grades of oral cavity squamous cell carcinoma: A single-center retrospective study. PLoS One. 2020;15(8):e0238103.

49. Ling Z, Cheng B, Tao X. Epithelial-to-mesenchymal transition in oral squamous cell carcinoma: Challenges and opportunities. Int J Cancer. 2021;148(7):1548-61.

50. Liptak JM. Cancer of the Gastrointestinal Tract. In: Vail DM, Thamm DH, Liptak JM, editors. Withrow & MacEven's Small Animal Clinical Oncology. Sixth ed. St. Louis, Missouri, USA: Elsevier; 2020. p. 436-7.

51. Liptak JM. Cancer of the Gastrointestinal Tract. In: Vail DM, Thamm DH, Liptak JM, editors. Withrow & MacEven's Small Animal Clinical Oncology. Sixth ed. St. Louis, Missouri, USA: Elsevier; 2020. p. 435.

52. Liu Q, Sun J, Luo Q, Ju Y, Song G. Salinomycin Suppresses Tumorigenicity of Liver Cancer Stem Cells and Wnt/Beta-catenin Signaling. Curr Stem Cell Res Ther. 2021;16(5):630-7.

53. Lundberg AP, Boudreau MW, Selting KA, Chatkewitz LE, Samuelson J, Francis JM, et al. Utilizing feline oral squamous cell carcinoma patients to develop NQO1-targeted therapy. Neoplasia. 2021;23(8):811-22.

54. MacLachlan NJ, Dubovi EJ. Papillomaviridae and polyomaviridae. In: MacLachlan NJ, Dubovi EJ, editors. Fenner's Veterinary Virology. Fourth ed. London, United Kingdom: Academic Press; 2011. p. 213–21.

55. Mahieu R, de Maar JS, Nieuwenhuis ER, Deckers R, Moonen C, Alic L, et al. New Developments in Imaging for Sentinel Lymph Node Biopsy in Early-Stage Oral Cavity Squamous Cell Carcinoma. Cancers (Basel). 2020;12(10).

56. Mai TT, Hamaï A, Hienzsch A, Cañeque T, Müller S, Wicinski J, et al. Salinomycin kills cancer stem cells by sequestering iron in lysosomes. Nature Chemistry. 2017;9(10):1025-33.

57. Marconato L, Buchholz J, Keller M, Bettini G, Valenti P, Kaser-Hotz B. Multimodal therapeutic approach and interdisciplinary challenge for the treatment of unresectable head and neck squamous cell carcinoma in six cats: a pilot study. Vet Comp Oncol. 2013;11(2):101-12.

58. Marconato L, Weyland M, Tresch N, Rossi F, Leone V, Rohrer Bley C. Toxicity and outcome in cats with oral squamous cell carcinoma after accelerated hypofractionated radiotherapy and concurrent systemic treatment. Vet Comp Oncol. 2020;18(3):362-9.

59. Martin CK, Tannehill-Gregg SH, Wolfe TD, Rosol TJ. Bone-invasive oral squamous cell carcinoma in cats: pathology and expression of parathyroid hormone-related protein. Vet Pathol. 2011;48(1):302-12.

60. Meuten DJ. Oral tumors. In: Meuten DJ, editor. Tumors in Domestic Animals. Fifth ed. Iowa, USA: John Wiley & Sons, Inc.; 2017. p. 500-3.

61. Meyer HJ, Hamerla G, Hohn AK, Surov A. CT Texture Analysis-Correlations With Histopathology Parameters in Head and Neck Squamous Cell Carcinomas. Front Oncol. 2019;9:444.

62. Morrison ML, Groover E, Schumacher J, Newton J, Pereira MM. Lingual Squamous Cell Carcinoma in Two Horses. J Equine Vet Sci. 2019;79:35-8.

63. Munday JS, French AF. Felis catus papillomavirus types 1 and 4 are rarely present in neoplastic and inflammatory oral lesions of cats. Res Vet Sci. 2015;100:220-2.

64. Munday JS, Thomson NA. Papillomaviruses in Domestic Cats. Viruses. 2021;13(8).

65. Munday JS, Thomson NA, Luff JA. Papillomaviruses in dogs and cats. Vet J. 2017;225:23-31.

66. Murphy BG, Bell CM, Soukup JW. Oral Squamous Cell Carcinoma. In: Murphy BG, Bell CM, Soukup JW, editors. Veterinary Oral and Maxillofacial Pathology. NJ, USA: John Wiley & Sons, Inc.; 2020. p. 143.

67. Murphy BG, Bell CM, Soukup JW. Oral Squamous Cell Carcinoma. In: Cabaud O, editor. Veterinary Oral and Maxillofacial Pathology. NJ, USA: John Wiley & Sons, Inc.; 2020. p. 139.

68. Murphy BG, Bell CM, Soukup JW. Oral Squamous Cell Carcinoma. In: Murphy BG, Bell CM, Soukup JW, editors. Veterinary Oral and Maxillofacial Pathology. NJ, USA: John Wiley & Sons, Inc.; 2020. p. 145.

69. Nasir L, Brandt S. Papillomavirus associated diseases of the horse. Vet Microbiol. 2013;167(1-2):159-67.

70. Nasry WHS, Wang H, Jones K, Dirksen WP, Rosol TJ, Rodriguez-Lecompte JC, et al. CD147 and Cyclooxygenase Expression in Feline Oral Squamous Cell Carcinoma. Vet Sci. 2018;5(3).

71. Nemanic S, Hollars K, Nelson NC, Bobe G. Combination of Computed Tomographic Imaging Characteristics of Medial Retropharyngeal Lymph Nodes and Nasal Passages Aids Discrimination between Rhinitis and Neoplasia in Cats. Vet Radiol Ultrasound. 2015;56(6):617-27.

72. Nemanic S, Nelson NC. Ultrasonography and noncontrast computed tomography of medial retropharyngeal lymph nodes in healthy cats. Am J Vet Res. 2012;73:1377–85.

73. Nickel R, Schummer A, Seiferle E. Lymphknoten und Lymphsammelgänge der Katze. In: Nickel R, Schummer A, Seiferle E, editors. Lehrbuch der Anatomie der

Haustiere Band III: Kreislaufsystem, Haut und Hautorgane. Fourth ed. Berlin: Parey 2005. p. 366.

74. Nickel R, Schummer A, Seiferle E. Lymphknoten und Lymphsammelgänge des Pferdes. In: Nickel R, Schummer A, Seiferle E, editors. Lehrbuch der Anatomie der Haustiere Band III: Kreislaufsystem, Haut und Hautorgane. Fourth ed. Berlin: Parey; 2005. p. 422.

75. Orsini JA, Nunamaker DM, Jones CJ, Acland HM. Excision of oral squamous cell carcinoma in a horse. Vet Surg. 1991;20(4):264–6.

76. Oshimori N. Cancer stem cells and their niche in the progression of squamous cell carcinoma. Cancer Sci. 2020;111(11):3985-92.

77. Owen LN. TNM Classification Of Tumors In Domestic Animals. 1980.

78. Palasz P, Adamski L, Gorska-Chrzastek M, Starzynska A, Studniarek M. Contemporary Diagnostic Imaging of Oral Squamous Cell Carcinoma - A Review of Literature. Pol J Radiol. 2017;82:193-202.

79. Paver EC, Currie AM, Gupta R, Dahlstrom JE. Human papilloma virus related squamous cell carcinomas of the head and neck: diagnosis, clinical implications and detection of HPV. Pathology. 2020;52(2):179-91.

80. Piegols HJ, Takada M, Parys M, Dexheimer T, Yuzbasiyan-Gurkan V. Investigation of novel chemotherapeutics for feline oral squamous cell carcinoma. Oncotarget. 2018;9(69):33098-109.

81. Poirier VJ, Kaser-Hotz B, Vail DM, Straw RC. Efficacy and toxicity of an accelerated hypofractionated radiation therapy protocol in cats with oral squamous cell carcinoma. Vet Radiol Ultrasound. 2013;54(1):81-8.

82. Restrepo MT. Anatomic and pathologic assessment of feline lymph nodes using computed tomography and ultrasonography: Universitat Autonoma de Barcelona; 2016.

83. Rossa C, Jr., D'Silva NJ. Non-murine models to investigate tumor-immune interactions in head and neck cancer. Oncogene. 2019;38(25):4902-14.

84. Sabhlok A, Ayl R. Palliative radiation therapy outcomes for cats with oral squamous cell carcinoma (1999-2005). Vet Radiol Ultrasound. 2014;55(5):565-70.

85. Scase T, Brandt S, Kainzbauer C, Sykora S, Bijmholt S, Hughes K, et al. Equus caballus papillomavirus-2 (EcPV-2): an infectious cause for equine genital cancer? Equine Vet J. 2010;42(8):738-45.

86. Schellenbacher C, Shafti-Keramat S, Huber B, Fink D, Brandt S, Kirnbauer R. Establishment of an in vitro equine papillomavirus type 2 (EcPV2) neutralization assay and a VLP-based vaccine for protection of equids against EcPV2-associated genital tumors. Virology. 2015;486:284-90.

87. Schmid D, Scholz VB, Kircher PR, Lautenschlaeger IE. Employing deep convolutional neural networks for segmenting the medial retropharyngeal lymph nodes in CT studies of dogs. Vet Radiol Ultrasound. 2022.

88. Schuh JCL. Squamous Cell Carcinoma of the Oral, Pharyngeal and Nasal Mucosa in the Horse. Vet Pathol. 1986;23(2):205-7.

89. Shiga K, Ogawa T, Katagiri K, Yoshida F, Tateda M, Matsuura K, et al. Differences between oral cancer and cancers of the pharynx and larynx on a molecular level. Oncol Lett. 2012;3(1):238-43.

90. Stebbings KE, Morse CC, Goldschmidt MH. Feline Oral Neoplasia: A Ten-Year Survey. Vet Pathol. 1989;26(2):121–8.

91. Stieger-Vanegas SM, Hanna AL. The Role of Computed Tomography in Imaging Non-neurologic Disorders of the Head in Equine Patients. Front Vet Sci. 2022;9:798216.

92. Strohmayer C, Anson A. The Role of Computed Tomography in the Oncologic Patient. Clinica Veterinaria de Pequenos Animales 2018;38(1):7-14.

93. Strohmayer C, Klang A, Kneissl S. Computed Tomographic and Histopathological Characteristics of 13 Equine and 10 Feline Oral and Sinonasal Squamous Cell Carcinomas. Front Vet Sci. 2020;7:591437.

94. Strohmayer C, Klang A, Kummer S, Walter I, Jindra C, Weissenbacher-Lang C, et al. Tumor Cell Plasticity in Equine Papillomavirus-Positive Versus-Negative Squamous Cell Carcinoma of the Head and Neck. Pathogens. 2022;11(2).

95. Supsavhad W, Dirksen WP, Martin CK, Rosol TJ. Animal models of head and neck squamous cell carcinoma. Vet J. 2016;210:7-16.

96. Sykora S, Brandt S. Papillomavirus infection and squamous cell carcinoma in horses. Vet J. 2017;223:48-54.

97. Tannehill-Gregg S, Kergosien E, Rosol TJ. Feline head and neck squamouscell carcinoma cell line: characterization, production of parathyroid hormone-related protein, and regulation by transforming growth factor-beta. In Vitro Cell Dev Biol Anim. 2001;37(10):676-83.

98. Tannehill-Gregg SH, Levine AL, Rosol TJ. Feline head and neck squamous cell carcinoma: a natural model for the human disease and development of a mouse model. Vet Comp Oncol. 2006;4(2):84-97.

99. Taylor S, Haldorson G. A review of equine mucocutaneous squamous cell carcinoma. Equine Veterinary Education. 2013;25(7):374-8.

100. Thomson NA, Dunowska M, Munday JS. The use of quantitative PCR to detect Felis catus papillomavirus type 2 DNA from a high proportion of queens and their kittens. Vet Microbiol. 2015;175(2-4):211-7.

101. Thomson NA, Howe L, Weidgraaf K, Thomas DG, Young V, Ward VK, et al. Felis catus papillomavirus type 2 virus-like particle vaccine is safe and immunogenic but does not reduce FcaPV-2 viral loads in adult cats. Vet Immunol Immunopathol. 2019;213:109888.

102. Thomson NA, Thomas DG, Weidgraaf K, Munday JS. Felis catus papillomavirus type 2 DNA loads on kittens are transient and do not reflect their susceptibility to infection. J Feline Med Surg. 2018;20(4):332-8.

103. van den Top JG, Harkema L, Lange C, Ensink JM, van de Lest CH, Barneveld A, et al. Expression of p53, Ki67, EcPV2- and EcPV3 DNA, and viral genes in relation to metastasis and outcome in equine penile and preputial squamous cell carcinoma. Equine Vet J. 2015;47(2):188-95.

104. Van den Wollenberg L, Van den Belt AJM, Van der Kolk JH. Squamous cell carcinoma of the larynx in a Shetland pony. Equine Vet Educ. 2002;14(2):60-2.

105. van Nimwegen SA, Bakker RC, Kirpensteijn J, van Es RJJ, Koole R, Lam M, et al. Intratumoral injection of radioactive holmium ( (166) Ho) microspheres for treatment of oral squamous cell carcinoma in cats. Vet Comp Oncol. 2018;16(1):114-24.

106. Waech T, Pazahr S, Guarda V, Rupp NJ, Broglie MA, Morand GB. Measurement variations of MRI and CT in the assessment of tumor depth of invasion in oral cancer: A retrospective study. Eur J Radiol. 2021;135:109480.

107. Wang G, Zhang M, Cheng M, Wang X, Li K, Chen J, et al. Tumor microenvironment in head and neck squamous cell carcinoma: Functions and regulatory mechanisms. Cancer Lett. 2021;507:55-69.

108. Wang HF, Wang SS, Tang YJ, Chen Y, Zheng M, Tang YL, et al. The Double-Edged Sword-How Human Papillomaviruses Interact With Immunity in Head and Neck Cancer. Front Immunol. 2019;10:653.

109. Wingo K. Histopathologic Diagnoses From Biopsies of the Oral Cavity in 403 Dogs and 73 Cats. J Vet Dent. 2018;35(1):7-17.

110. Witte TH, Perkins JD. Early diagnosis may hold the key to the successful treatment of nasal and paranasal sinus neoplasia in the horse. Equine Veterinary Education. 2011;23(9):441-7.

111. Wypij JM. A naturally occurring feline model of head and neck squamous cell carcinoma. Patholog Res Int. 2013;2013:502197.

112. Yamashita-Kawanishi N, Chang CY, Chambers JK, Uchida K, Sugiura K, Kukimoto I, et al. Comparison of prevalence of Felis catus papillomavirus type 2 in squamous cell carcinomas in cats between Taiwan and Japan. J Vet Med Sci. 2021;83(8):1229-33.

113. Yoshikawa H, Ehrhart EJ, Charles JB, Custis JT, LaRue SM. Assessment of predictive molecular variables in feline oral squamous cell carcinoma treated with stereotactic radiation therapy. Vet Comp Oncol. 2016;14(1):39-57.

114. Yu B, Huang C, Xu J, Liu S, Guan Y, Li T, et al. Prediction of the degree of pathological differentiation in tongue squamous cell carcinoma based on radiomics analysis of magnetic resonance images. BMC Oral Health. 2021;21(1):585.

115. Zaccone R, Renzi A, Chalfon C, Lenzi J, Bellei E, Marconato L, et al. Environmental risk factors for the development of oral squamous cell carcinoma in cats. J Vet Intern Med. 2022;36(4):1398-408.

## 5 Additional publications and scientific meeting contributions

Strohmayer, C; Klang, A; Kneissl, S (2020): Computed tomographic and histopathological characteristics of 13 equine and 10 feline oral and sinonasal squamous cell carcinomas. -ECVDI Online congress; SEP 17-18, 2020; Online, Austria.

Strohmayer, C; Hirt, RA; Gradner, GM; Högler, S; Kneissl, S. Frontal sinus squamous cell carcinoma with intracranial, extraaxial extension in a dog with chronic sinonasal aspergillosis. Vet Rec Case Reports. 2021 9 (1) e41.

Altamura G, Cuccaro B, Eleni C, Strohmayer C, Brandt S, Borzacchiello G. Investigation of multiple Felis catus papillomavirus types (-1/-2/-3/-4/-5/-6) DNAs in feline oral squamous cell carcinoma: a multicentric study. J Vet Med Sci. 2022 Apr 15. doi: 10.1292/jvms.22-0060.

Assessment of tumour cell plasticity in feline and equine papillomavirus-positive versus -negative oronasal squamous cell carcinoma. Poster MIC-Festival, Medical University Vienna, 2022.